Seasonal Land Use Planning and Evaluation System for Food Nutrition Security Using Fuzzy Expert System, GIS, and Satellite Remote Sensing

July 2021

RUBAIYA BINTE MOSTAFIZ

Seasonal Land Use Planning and Evaluation System for Food Nutrition Security Using Fuzzy Expert System, GIS, and Satellite Remote Sensing

A Dissertation Submitted to
the Graduate School of Life and Environmental Sciences,
the University of Tsukuba
in Partial Fulfillment of the Requirements
for the Degree of Doctor of Philosophy in Bioresource Engineering
(Doctoral Program in Appropriate Technology and Sciences for Sustainable Development)

RUBAIYA BINTE MOSTAFIZ

Table of Contents

ABSTRACT ..... **viii**

List of Figures ..... **ix**

List of Tables ..... **xi**

Chapter I **1**

Introduction **1**

1.1. Research Background 1

1.2. Problem Statement 2

1.3. Justification of Research 3

1.4. Research Questions 4

1.5. Objectives 4

1.6. Thesis Outline 4

Chapter II **5**

Review of Literature **5**

2.1. Food Nutrition Security 5

2.2. Crop Diversification and Land Use Pattern 5

2.3. Land Suitability 6

2.4. Geospatial Technology 7

2.5. Remote Sensing and Yield Prediction 7

Chapter III **8**

Materials and Methods **8**

3.1. Land Use plan 8

3.1.1. Calorie Requirement *8*

3.1.2. Seasonal Planting Practices/crop calendar *11*

3.2. Research Framework 11
3.3. Study Area 14
3.4. Data Sets 15
3.4.1. Statistical data *15*
3.4.2. Satellite data *15*
3.4.2.1. Image acquisition *15*
3.4.2.2. Digital image preprocessing *15*
3.5. Criteria Aggregation for Seasonal Map Preparation 15
3.5.1. Land use *16*
3.5.2. Soil-adjusted vegetation index *16*
3.5.3. Slope *17*
3.5.4. Land type *17*
3.5.5. Topsoil *18*
3.5.6. Soil pH *18*
3.5.7. Flood prone *18*
3.5.8. Temperature *19*
3.5.9. Rainfall *19*
3.6. Criteria Aggregation for Evaluation 23
3.6.1. Elevation *23*
3.6.2. Slope *23*
3.6.3. Land Surface Temperature (LST) *24*
3.6.4. Soil-Adjusted Vegetation Index (SAVI) *25*
3.6.5. Atmospherically Resistant Vegetation Index (ARVI) *26*
2.4.6. Soil Adjusted and Atmospherically Resistant Vegetation Index (SARVI) *26*
3.6.7. Modified Soil-Adjusted Vegetation Index (MSAVI) *26*
2.6.8. Optimized Soil-Adjusted Vegetation Index (OSAVI) *27*
3.7. Multi-Criteria Decision Analysis for Land Suitability 29
3.7.1. Fuzzy Rreclassification *29*
2.7.2. Overlay *36*

2.7.2.1. Fuzzy Overlay *36*

2.7.2.2. Scoring for individual suitability map preparation *36*

3.8. Seasonal land Suitability Map Preparation..... 37

3.9. Evaluation by Land Fertility Assessment..... 37

3.9.1. Data Processing for Land Fertility Analysis *37*

3.9.1.1. Pattern analysis..... *37*

3.9.1.2. Masked by Land Use/Land Cover *38*

3.9.2. Fertility Assessment..... *39*

3.9.2.1. Fertility assessment by weighted-linear combination *39*

3.9.2.2. Fertility assessment by the fuzzy membership function *39*

3.9.3. Fertility assessment using ground truth data *42*

3.9.4. Yield prediction *42*

Chapter IV 44

Results and Discussion 44

4.1. Seasonal land Use Plan..... 44

4.1.1. Crop production throughout the locality..... *44*

4.1.2. Suitability of land for a range of crops..... *45*

4.1.3. Land adaptability for multiple crops in season *49*

4.2. Land Use Plan Evaluation 53

4.2.1. Land fertility assessment *53*

4.2.2. Yield Prediction..... *54*

4.3 Discussion 60

Chapter V 63

Conclusions and Recommendations 63

5.1. Conclusions 63

5.1.1. Seasonal land use plan *63*

5.1.2. Land fertility evaluation *63*

5.2. Recommendations 64

Acknowledgements **65**

List of Abbreviations **66**

References **67**

Appendix A **85**

Table A1: Crop diversification methods in Bangladesh's northern region *85*

Table A2: SAVI, ARVI, SARVI, MSAVI and OSAVI from 2017-2020 for 36 subunits. *86*

ABSTRACT

Diet, nourishment and health are all intertwined. Food accessibility does not guarantee the consumption of a well-balanced food intake; a well-balanced diet is dependent on optimal consumption, purchasing power and local food customs. Local dietary habits are often influenced by agricultural practices. For this reason, the goal of this study is to create a seasonal land-use planning model combining varied crops for food nutrition security to assure a balanced caloric demand. The model is based on a fuzzy expert system. Furthermore, the findings were analyzed using a simple land fertility evaluation, based on satellite remote sensing-derived soil-vegetation indices. Satellite remote sensing technologies offer a significant potential for assessing land conditions and facilitating efficient agricultural planning. In this research, a multicriteria decision-making study was performed, as well as a multicrop land planning design was created using a geographic information system and fuzzy membership functions. Furthermore, vegetation index data were gathered in accordance with the seasonal crop cycle. To undertake spatial analysis, the environmental variables and restrictions were created in ArcGIS 10.4®. To select the best sites for agricultural production, a fuzzy expert system was used. The findings of the seasonal agricultural suitability evaluation were validated using data obtained from the Bangladesh Survey. The investigation found that 42 percent (3469 km^2) of the overall land was ideal for vegetable growth during the Kharif-1 season, while 55 percent (4543 km^2) was appropriate during the Kharif-2 season. Whereas current practices utilized just 12 percent and 18 percent of the area for vegetable production in the Kharif-1 and Kharif-2 seasons respectively, which is less than the regional requirement. In addition, during the Rabi season, the most suitable zones for cereals, vegetables, pulses, oilseeds and potatoes were reported as 35 percent (2891 km^2), 19 percent (1569 km^2), 15 percent (1239 km^2), 10 percent (826 km^2) and 21 percent (1734 km^2) of the total land area respectively. Moreover, the land areas suitable for farming pulses and oilseeds were found to be 15 percent (1239 km^2) and 10 percent (826 km^2) respectively. When applying the fuzzy membership function for remote sensing-based land fertility evaluation, expert knowledge was also used, along with references and field data; as a result, 48 percent of the land (2045 km^2) was identified as being highly fertile; 39 percent of the land (2045 km^2) was identified as being moderately suitable and 7 percent of the land (298 km^2) was identified as being marginally fertile. Additionally, 6 percent (256 km^2) of the land was described as not fertile. The yield estimation using SAVI (R^2 = 77.3%), ARVI (R^2=68.9%), SARVI (R^2=71.1%), MSAVI (R^2=74.5%) and OSAVI (R^2=81.2%) showed a good predictive ability. Furthermore, the combined model that used these five indices had the best accuracy (R^2 = 0.839); this model was then used to create yield forecast maps for the respective years (2017-2020). This study reveals that using satellite remote sensing methodologies in GIS platforms is an efficient and simple technique for farmed land-use designers and policymakers to identify fertile cultivable land area with the prospective for improved farmed production. Additionally, using solely distant satellite datasets to determine acceptable land conditions was a cause of worry, adding a new dimension to land fertility evaluation. The integrated model provided herein may be used to manage land allocation for varied crop production, providing policymakers with additional decision-making information to achieve regional food nutrition security in the target area along with neighboring South Asian nations.

Keywords: Caloric requirement, Food nutrition, Fuzzy membership Function, land suitability, seasonal land use plan, GIS, Remote Sensing, Vegetation indices, Land Surface Temperature, Digital Elevation Model, Yield Prediction.

List of Figures

Figure 3.1.	Recommended energy percentage from diversified food items per person/day.	10
Figure 3.2.	Crop practice calendar in the northern part of Bangladesh.	11
Figure 3.3.	Research framework for multi-cropping land use plan.	12
Figure 3.4.	land use evaluation by land fertility assessment and yield prediction.	13
Figure 3.5.	(a) Through Bangladesh, there is a predominance of malnutrition; (b) northern Bangladesh (Rangpur Division); (c) Study region: Dinajpur, Gaibandha, Rangpur, and Kurigram, four districts of Rangpur division.	14
Figure 3.6.	The criteria for determining land suitability: (a) land type; (b) precipitation (c) flood prone; (d) soil pH; (e) topsoil; (f) slope; (g) SAVI of Kharif-1 season; (h) SAVI of Kharif-2 season; (i) SAVI of Rabi Season; (j) Rabi Season temperature; (k) Kharif-1 season temperature; (l) Kharif 2 Season temperature; and (m) land use map (SOB) for 2019.	20-22
Figure 3.7.	Criteria: (a) elevation; (b) slope; (c) LST; (d) SAVI; (e) ARVI; (f) SARVI; (g) MSAVI and (h) OSAVI.	28
Figure 3.8.	Suitability range of classification by scoring based on fuzzy overlay.	37
Figure 3.9.	Variability of rice yield based on the soil-vegetation related indices across the 36 subunits	42
Figure 3.10.	Ground referenced information points in the 36 subunits.	43
Figure 4.1.	Crop production status regarding balanced nutritional requirement per year.	44
Figure 4.2.	Land suitability map: (a, b) Kharif-1 vegetables; (c, d) Kharif-1 Aus rice; (e, f) Kharif-2 vegetables; (g, h) Kharif-2 Aman rice; (i, j) Rabi vegetables; (k, l) potatoes; (m, n) pulses; (o, p) oilseeds; (q, r) Boro rice.	46-48
Figure 4.3.	Suitable zoning for seasonal crop growing: (a) Kharif-1 season land suitability map; (b) Kharif-1 present practice map; (c) Kharif-2 land suitability map; (d) Kharif-2 present practice map; (e) Rabi season land suitability map; and (f) Rabi present practice map.	51

Figure 4.4.	Suitable land fertility evaluation classes based on soil-specific satellite imagery	53
Figure 4.5.	Rice yield distributions in the 36 subunits using ground reference data.	55
Figure 4.6.	Regression analysis (a) SAVI; (b)ARVI; (c) SARVI; (d) OSAVI and (e) MSAVI for vegetation indices and ground reference time series yield information.	57
Figure 4.7.	Comparison of actual yield and predicted yield for different indices (a) SAVI; (b)ARVI; (c) SARVI; (d) OSAVI and (e) MSAVI.	58
Figure 4.8.	Yield prediction map (MT/ha) (a) 2017, (b) 2018, (c) 2019, (d) 2020.	59

List of Tables

Table 2.1.	Bangladesh's food consumption patterns (1991-2010).	5
Table 2.2.	Land suitability framework-based FAO.	6
Table 3.1.	Food items that are desired are recommended.	8
Table 3.2.	Components for crop suitability criterion.	16
Table 3.3.	list of data for land fertility evaluation	23
Table 3.4.	Suitability class for cereal crops (different varieties of rice) by fuzzy membership function.	31
Table 3.5.	Suitability class for carbohydrate-based vegetables (potatoes) by fuzzy membership.	32
Table 3.6.	Suitability class for non-carbohydrate-based vegetables by fuzzy membership.	33
Table 3.7.	Suitability class for pulses by fuzzy membership.	34
Table 3.8.	Suitability class by fuzzy membership for oilseeds.	35
Table 3.9.	Criteria reclassification of suitable class for weighted linear combination.	40
Table 3.10.	Suitable classes by fuzzy membership function for land fertility.	41
Table 4.1.	Results of land suitability analysis of diversified crops.	49
Table 4.2.	Comparison between the present practice and the suitable area of the Kharif-1 season.	52
Table 4.3.	Comparison between the present practice and the suitable area of the Kharif-2 season.	52
Table 4.4.	Comparison between the present practice and the suitable area of the Rabi season.	52
Table 4.5.	Percentage and area of each land fertility classification	54
Table 4.6.	Yield estimation based on satellite remote sensing derived soil-vegetation indices for the 36 subunits.	56
Table 4.7.	Yield prediction models based on satellite remote sensing derived soil-vegetation indices.	60
Appendix: Table A1:	Diversified crops practices in the northern part of Bangladesh.	85
Appendix: Table A2	SAVI, ARVI, SARVI, MSAVI and OSAVI from 2017-2020 for 36 subunits.	86

Chapter I

Introduction

1.1. Research Background

Increased food supply, improved food ease of access, improved crisis avoidance & supervision, and improved nutritional sufficiency are all part of the food nutrition security concept. (EI Bilali et al., 2019). Dietary intake habits are strongly linked with foods that are high in energy, protein and micronutrients as well as the variety of foods available. Cereals and starch-based staples comprised 53 percent of the world's average on a daily basis calorie consumption in overall food consumption, according the Food and Agriculture Organization (FAO) of the United Nations . In the United States, grain and grain-based staples account for about 26 percent of daily calories consumed; meanwhile, in Bangladesh, cereals and starch-based staples account for 83 percent of daily calories ingested. Cereals have dominated and limited the primary dietary groups in Bangladesh. As a result, dietary habits in this region, where rice is the dominant cereal and have remained relatively consistent over time.

Additionally, cereal crop production occupies the majority of agricultural lands in developing countries throughout the year, creating another problem; water source depletion. Rice is typically grown in irrigated areas, while maize is grown in irrigated fields or regions with sufficient and predictable rainfall (Koohafkan and Stewart, 2008). Wheat is the most widely cultivated cereal crop, and it is commonly grown in both irrigated and non-irrigated dryland areas (Koohafkan and Stewart, 2008). Agriculture consumes 80–90 percent of water in terms of consumptive use (Hamdy et al., 2003). Utilizing water for irrigation expansion is not only expensive, but it also puts circumstances in jeopardy due to soil degradation, particularly salt buildup and loss of water supplies (Cosgrove and Rijsberman 2000). According the FAO, irrigated land in developing nations would rise nearly 45 million ha by 2030 from 197 million hectares now(FAO, 2003). As a developing country, carbs (rice and wheat-based foods) outnumber vegetables, oilseeds, and pulses in terms of food consumption. For this location, land use plans that take into account climatic considerations could be a viable answer. Different climatic atmospheres characterize the climatic requirements in different seasons, which generally affect crop germination, growth, flowering and ultimately yield (Todmal et al., 2018).

Moreover, Proper land-use planning is essential for enhancing agricultural production and ecological conservation and for the protection of (Kennedy et al., 2016). Inappropriate land management practices lead to a higher rate of soil erosion, a diminished crop production, a hindered productivity and a deteriorated soil quality (Pimente and Burgess, 2013). Because of its impact on agricultural productivity, land management should be a major focus of study and policy development. Knowledge

of local land conditions is becoming more widely acknowledged as critical to long-term soil management (Nath, Lal, and Das, 2015).

In addition, together in structured farm management system; novel farming technologies integrate biology with computers and device exchange-based smart agriculture autonomously. Remote sensing, a new concept that is gaining traction, may be able to help with methodically considering difficulties related to smart agricultural technology. This review discusses remote sensing technology and demonstrates its potential to open new avenues for experts and agronomists to investigate aspects of biological facts that are not accessible through conventional processes. Remote sensing methods support the formation of growth profiles of plants and temporal evolution schema of soils over their developmental phases (Ennouri and Kallel, 2019). Remote sensing indices that incorporate environmental recovery factors are useful for tracing the development of crops, their interrelatedness and the consequences of the variables of interest for crop development.

Also, Farmers of local communities evaluate and manage soil fertility using regular observations and collective experiences (Niemeijer and Mazzucato, 2003). However, for rural communities, this knowledge is usually insufficient to understand the adequacy of soil fertility assessments, management strategies and land‐use decisions. As a result, a simple approach for assessing land condition is required in order to create an interoperable land fertility information platform that integrates science with local context and incorporates local agricultural expertise (Lobry de Bruyn and Ingram, 2019). Identification of agroecological conditions should be performed during the agroecological assessment of lands (Serio et al., 2018; Novara et al., 2017). Accordingly, the determination of agronomically meaningful parameters is essential for suitable farmland evaluation.

Following this concern, the application of smart agriculture seasonal land use planning and satellite remote sensing-based soil-vegetation index evaluations for agricultural land condition assessments is the key target of this research. Therefore, overall assessments can be performed using multicriteria decision method based on fuzzy expert system. Such evaluation provides information about specific land use potentials and constraints. Effective management along with proper land use decisions results in a higher land productivity as well as a sustained environment.

1.2. Problem Statement

Food consumption in South Asia is dictated by cereals (Mottaleb et al., 2018); the world's population of 25 percent (FAO, 2014), or nearly 23 percent of the population lacks adequate calorie intake(WDI, 2014). Rice accounts for more than 20 percent of world calorie consumption. Six Asian countries (China, Indonesia, India, Vietnam, Bangladesh, and Japan) produce and eat more than 90 percent of the

world's rice (Abdullah and Adhana, 2006). Rice is consumed by almost two billion people in Asia's developing countries (FAO, 1995). The consumption of rice is on the rise across Asia, Africa, and Latin America (Wang et al., 2005). Bangladesh, in particular, is sensitive to a lack of nutritional safety measures and has a proclivity to boost cereal crop production. Food insecurity affects one-third of Bangladeshi households with large inequities in food access (BIRDEM, 2013; HIES, 2016). Rice is also a staple diet for more than half of the world's population (FAO, 2004).

As a result, routine dietary behaviors introduce a new risk that can jeopardize a healthy lifestyle. Rice, in particular, makes up more than half of the whole diet by weight and 70% by calories (FAO, 2014). The dietary habits of each location are a natural practice. This nutritional deficiency is especially pronounced in underdeveloped countries, where cereals predominate in the diet. Nonetheless, unbalanced food intake generates a different problem in conditions of global food nutritional deficiency.

1.3. Justification of Research

Effective and accurate land fertility assessments can aid in the improvement of yield prediction models. Multiple provincial fertility signifiers (e.g., Crop growth and yield quality, the presence of earthworms, and soil qualities such as color, texture, and depth) have been reported in several studies to capture the geographical variability of soil fertility (Bajgai and Sangchyoswat, 2018; Odendo, Obare and Salasya, 2010; Buthelezi, Hughes and Modi, 2013). According to this assessment, yield prediction using vegetative indices (VIs) is the simplest method for establishing empirical correlations between ground-based harvest metrics and VIs (Tucker, 1979, Das et al.,

2020 Romano et al., 2015). Satellite remote sensing technologies and GIS applications for crop monitoring have the ability to provide rapid evaluations of changes in crop growth and development on regional scales (Campos et al., 2018; Lobell et al., 2015).

In most cases, developing location specific descriptions by soil sampling and analysis is expensive and challenging. Following this concern, advanced and affordable smart satellite remote sensing multicriteria technologies that consider climate factors are required for land fertility and accuracy assessments. When geographic references are included, the Multicriteria Decision Method (MCDM) comes to be more suitable. Geospatial recommendations utilizing MCDM-land suitability evaluations have been made possible in recent years by computing technology paired with GIS. Furthermore, the MCDM, combined with linear combination and fuzzy set theory has the potential to reduce subjectivity in the assessment of results. Several MCDM techniques, including equal-weighted linear combinations and fuzzy membership have been used to evaluate land suitability (Elsheikh et al. 2013, Kazemi et al. 2018, Ostovari et al. 2019, Habibie et al. 2019). Furthermore, the fuzzy expert system in the GIS platform can overcome these restrictions by using the required calorie ratio (FAO recommended) to produce a land use plan and convenient land fertility analyses for smart agricultural operations.

1.4. Research Questions

- How 'seasonal land planning model' can help to reduce food nutrition insecurity? Can calorie demand give aid to the land use plan?
- How to evaluate the land fertility and validate with yield prediction model from the time series vegetation indices?

1.5. Objectives

Therefore, the aim of current study is to create a seasonal multi-crop land suitability analysis model based on dietary intake to ensure nutritional food security using fuzzy-based multicriteria decision analysis as well as to evaluate the results of seasonal land use planning using a soil-vegetation intent land fertility assessment to ensure elevated productivity.

As a result, the following were the particular goals of this research:

I. To develop a seasonal land use plan of diversified crops based on caloric demand and balanced nutrition to ensure regional food security.

II. To develop a soil fertility assessment model from soil-vegetation indices with validation from yield prediction model and observed yield from time series datasets.

1.6. Thesis Outline

This dissertation is divided into four major segments, which are follows:

In Chapter 1, mainly discussed about study background, problem statement, research question and objectives. In Chapter II, review of relevant literature was discussed briefly. In Chapter III, materials and methods are described that included research framework and study area. The satellite datasets are also explained. In the Chapter IV, results of seasonal land use plan, land fertility evaluation and yield prediction by soil-vegetation indices have been described. Finally, in Chapter V, conclusions and recommendations are provided.

Chapter II

Review of Literature

2.1. Food Nutrition Security

Increased food availability, improved food accessibility, improved crisis avoidance and management, and last but not least, improved nutritional adequacy of food intake are all part of the food nutrition security concept. Due to predominantly cereal-based food production and consumption patterns that are compromising performance on nutrition outcomes in Bangladesh, cereals account for three-quarters of total calories, as opposed to the optimal 60 percent. Rice is the primary food, accounting for more than half of the total food by weight and 70% by calories (ICN2—2014: Country Nutrition Paper).

Despite major gains in cereal grain output, non-cereal food production; particularly fish, meat, oil, vegetables and fruits are insufficient to meet up the population's dietary needs, and per capita intake falls short of nutritional standards. Food insecurity affects one-third of households in the country, with considerable disparities in food access. (BBS, 2010; HIES, 2010).

Table 2.1. Bangladesh's food consumption patterns (1991-2010).

Food item (g)	1991-2	1995-6	2000	2005	2010	Desirable (g) (BIRDEM, 2013)	Difference from desirable diet (g) (consider 2010)
Rice	472.8	463.3	458.5	439.6	416.0	350	+66
Wheat	36.3	33.7	17.24	12.1	26.1	50	-24
Potato	40	49.5	55.5	63.3	70.5	100	-30
Pulses	17.9	13.9	15.8	14.2	14.30	50	-35.7
Vegetables	137.4	152.5	140.5	157.0	166.1	300	-298
Meat	8.1	11.6	13.3	15.2	19.07	40	-20.93
Eggs	4.7	3.2	5.27	5.2	7.25	30	-22.75
Fish	34.5	43.8	38.5	42.1	49.4	60	-10.6
Milk	19.1	32.6	29.7	32.4	33.7	130	-96.3
Fruits	16.9	27.6	28.4	32.5	44.8	100	-55.2

(Source: BBS- HIES, various years)

2.2. Crop Diversification and Land Use Pattern

In Bangladesh, cereal crop production has increased dramatically but land allocation and yields for minor crops have decreased. The land resource of the country is divided into two categories, i.e., agriculture lands and non-agriculture lands. The agriculture lands include croplands, homestead, forests, rivers, lake, aquaculture farms, tea gardens/estates and saltpans. While non-agriculture lands include settlements, industrial areas and accreted lands. However, a declining trend was observed for the total

agricultural lands of the country, i.e., a decrease is noted from 91.83% in 1976 to 87.69% and 83.53% over the years of 2000 and 2010, respectively. (FGG et al., 2013)

2.3. Land Suitability

The suitability of land use design has been defined as qualification for a specified form of land use of a given type of land (FAO,1976). The land evaluation framework can be used to clarify how the sustainability works. Land suitability is the method of estimating the appropriateness of a given land area for agricultural use and the suitability level. Land evaluation provides knowledge on the potential and constraints of land in terms of crop output as affected by the physical environment for a given land use classification.

There were no certain parameters concerning the requirements to be consider when evaluating the land suitability for agriculture, and that the requirements used in similar studies are generally who are available. These studies make use of land use, land cover form, topography, rainfall, stream and distance from the road. Land is classified as suitable (S) or unsuitable (N) in the FAO framework for land suitability classification (N). These suitability classifications can be further subdivided into degrees of suitability. In practice, three classes (S1, S2, S3) were also used to classify order suitable orders as highly suitable, moderately suitable and marginally suitable for a specific use. (Table 2.1). Normally there are two classes (N1 and N2) which are not suitable within the order, not suitable and permanently unsuitable. The classification of land suitability consists of determining and grouping the forms of land in order and classifying them according to their capacity

Table 2.1. Land suitability framework-based FAO.

Order	Class	Details
Suitable	S1 (Highly Suitable)	Land which has no substantial restrictions to the form of usage
	S2 (Moderately Suitable)	Land which has slight restrictions to the form of usage
	S3 (Marginally Suitable)	Land which has extreme restrictions to the form of usage
Not Suitable	N1 (Currently Not Suitable)	Land with restrictions that can be resolved in a timely manner but cannot be fixed at a reasonable cost with knowledge.
	N2 (Permanently Not Suitable)	Land with severe restrictions that preclude any possibility of use.

2.4. Geospatial Technology

Geospatial technologies are innovative tools for contributing to the geographic mapping and analysis of the world and human societies. These technologies are advancing since the maps were drawn in ancient times. With the development of times, computers able to store and transfer images together with the development of digital software, maps, data sets on socio-economic and environmental phenomena, known as Geographic Information Systems (GIS). An essential feature of the GIS is its capacity to organize the range of geospatial data into a layered series of maps that enable specific topics to be analyzed and conveyed to broader audiences. Remote Sensing (RS), Global Positioning System (GPS), Geographic Information Systems (GIS) and Internet Mapping Technologies are examples of geospatial technologies that could be useful for human rights. These geospatial technologies can also be used to establish agricultural precision technology for various crops. Precision agriculture requires site specific knowledge from a variety of information sources for preparing, planting, cultivating and harvesting of agricultural crops. Before the emergence of the idea of precision agriculture, conventional methods of agriculture were essentially unable to satisfy the in-field variability of input requirements. However, with precise positioning systems, recently developed sensors and improved vehicle controls, precision farming technology can now adapt dynamically to site-specific field needs. (Noguchi and O'Brien, 2003).

2.5. Remote Sensing and Yield Prediction

For determining the stochastic land cover change in relation to basic physical parameters such as surface radiance and reflectivity data, remote sensing is quite useful. The involvement of remote sensing and GIS in farmed drought identification, valuation and supervision is becoming increasingly important as they provide up-to-date evidence at different spatial and temporal scales, which is difficult and time consuming when done using traditional methods such as field surveys and sampling questionnaires (Arshad et al., 2008, Brian et al., 2012). Numerous scientists see the vegetation index as an essential metric for mapping agricultural areas, assessing calculating biomass, weather impacts, crop output, drought conditions and measuring vegetative vigor (Dabrowska-Zielinska et al., 2002, Chakraborthy and Sehgal 2010, Narasimhan and Srinivasan 2005). Since the 1970s, satellite-derived (for example, Landsat Thematic Mapper-TM) surface temperature data have been utilized for regional climate analyses on different scale (Tran et al., 2006). One of the most significant variables detected by satellite remote sensing is land surface temperature (LST). Data from the newly functioning Landsat-8 Thermal Infrared Sensor are now available in the public domain (TIRS). Land surface temperature (LST) is associated to surface energy and water balance at local to global scales and is responsible for a wide range of applications including climate change over, municipal climate, the hydrological sequence, and vegetation intensive care (Chapin et al., 2005; 2003, Ramanathan et al., 2001;).

Chapter III

Materials and Methods

3.1. Land Use plan

3.1.1. Calorie Requirement

Bangladesh Institute of Research and Rehabilitation in Diabetes, Endocrine, and Metabolic Disorders (BIRDEM, 2013) released a paper on Bangladesh's Desirable Dietary Pattern. The recommended meal shape was created using a variety of items (Table 3.1) contemplating adequate nutrition. That suggested diet scheme was monitored by FAO/WHO suggestions for macro and micronutrient needs. Furthermore, food products were selected based on local people's dietary habits, population, agricultural practices, accessibility, and availability (Figure 3.1). This evaluation was created for a single year. The method was followed in the following years in the same way.

Table 3.1. Food items that are desired are recommended.

Table 3.1. Food items that are desired are recommended.

Food		**Desirable intake, g**		**% Energy**
Cereal	Major	350	400	56
	Minor	50		
Pulses		50		6.5
Veg items	Carb-based	100	400	8
	Non-carb-based	300		
Oil seed		30		11
Sugar/ Molasess		20		3
Animal foods		260		10.5
Fruits		100		3
Spices		20		2
Total		1280		100

Source: BIRDEM,2013

The recommended desirable food items were computed using energy requirements, nutrition requirements, food intake patterns based on the reference, household dietary diversity score (HDDS), crop calendar and important food documentation. Furthermore, the recommended outcome was modified to reflect the most recent FAO/WHO recommendations for macro and micronutrient requirements. The current study was aided by a minorly changed chart. The desired calorie demand was determined as g/person/day. The production of various crops was translated into calorie equivalents by assuming that all crop output was consumed, and no crop output was exported or squandered. Food products used to meet energy requirements were weighted. Firstly, daily food intake was calculated in grams per day. Following that, the desired meal consumption was computed (in metric tons per year).

(a) Step 1:

Required net calorie intake (g) or total requirement of each food items,

$$TF = \sum_{i=1}^{n} R_i \times P \times 365 \qquad (1)$$

P is the total population of focus region. The computation was done based on yearly (365 days). R_i is the daily necessity of major food elements (n=8) by metric ton (Table 3.1).

(b) Step 2:

In the following step, prospective varied food crops were chosen to assess the required annual production. The Bangladesh Bureau of Statistics provided annual production data for chosen crops for the analysis (BBS, 2017). There were 78 different types of food farmed locally, which were grouped into eight classes of suggested food items (Appendix A1). Crop overall production can be stated as:

$$TP = \sum_{j=1}^{n1} CL_j + \sum_{k=1}^{n2} VN_k + \sum_{l=1}^{n3} VC_l + \sum_{m=1}^{n4} OS_m + \sum_{p=1}^{n5} PL_p + \sum_{q=1}^{n6} FR_q + \sum_{r=1}^{n7} SP_r + \sum_{s=1}^{n8} MS_s \qquad (2)$$

Where CLj describes to cereals (vector variable), in which i-th element is the consumption of nutrient of type i through the cereal of type j (j=1,2, …, $n1$); $n1$ is the number of cereals, n_1*=5;* which can be produced in the study area. Similarly, VN_k implies to non-carbohydrate vegetables, in which i-th element is the intake of nutrient of type i through non-carbohydrate vegetables of type k (j=1,2, …, $n2$); $n2$ is the number of non-carbohydrate vegetables (n_2*=31).* In a same way, VC_l implies to carbohydrate vegetables (n_3*=2;* OS_m refers to oilseeds and (n_4 *= 4);* PL_p describes to pulses (n_5 *= 7);* FR_q mentions to fruits (n_6 *= 18);* SP_r indicates to spices(n_7 *= 8),* and MS_s indicates to molasses/sugars (n_8 *= 3)(Table 1, Appendix 1). n* (n_1*……. *n_8) refers to the variation of each food group. For example, *CL* is represented as a cereal food that is generally grown-up in the target region. Here, *(*n_1=5*)* that mentions, there are

five kinds of cereal: Aus rice, Aman rice, Boro rice, wheat, and maize. Subsequent this way, the following item is *VN* that refer to non-carbohydrate vegetables, and here, $n_2 = 31$. In this cluster, there are 31 categories of vegetables, such as tomato, cauliflower, radish, eggplant, cabbage, bean, pumpkin, bitter gourd and other listed crops items (Appendix 1).

(c) Step 3:

Individual crops that needed to be grown more in order to meet up calorie or nutritional requirements were determined. Food items produced in excess of nutritional requirements were also discovered (from equations (1) and (2)) and can be stated as follows:

$TP \geq TF,\ G = TP\text{-}TF$ (3)

In which case, G: a vector variable indicating whether an element has a nutritional excess (if positive) or a nutritional deficiency (if negative). A major land use strategy for cereal food items, vegetables, oilseeds, and pulses was proposed in this study. Fruits, spices and molasses/sugars were not taken into account in contemporary land use planning (Figure 3.2). As a result, land use planning was based on 81.5 percent of total calorie consumption. As a result, equation (2) is provided by the following expression, which was employed in this study (for equation 4; indices were the same as in equation 2):

$$TP = \sum_{j=1}^{n1} CL_j + \sum_{k=1}^{n2} VN_k + \sum_{l=1}^{n3} VC_l + \sum_{m=1}^{n4} OS_m + \sum_{p=1}^{n5} PL_p \quad (4)$$

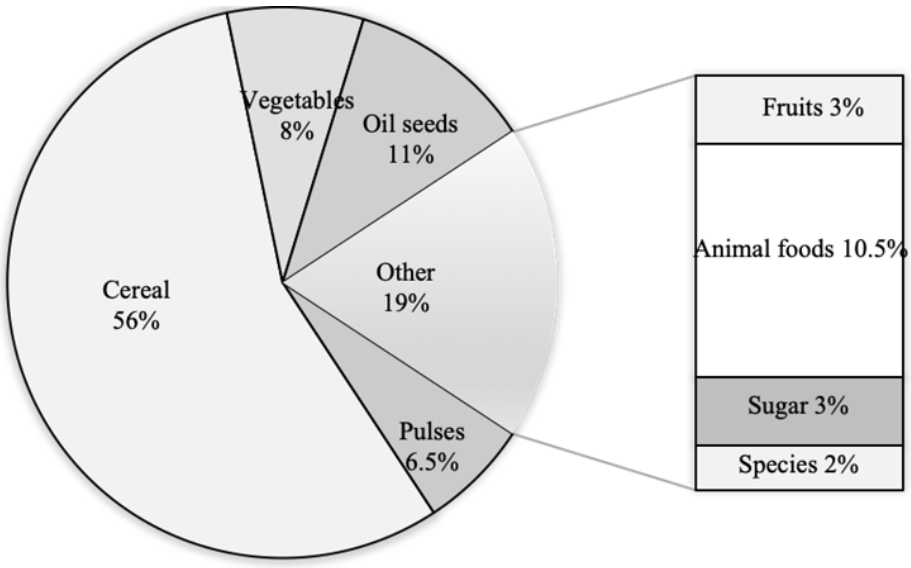

Figure 3.1. Recommended energy percentage from diversified food items per person/day.

3.1.2. Seasonal Planting Practices/crop calendar

Bangladesh rotates crops three times a year on the same plot of land. Cropping seasons are divided into 3 groups: (i) Pre-monsoon Pre-Kharif (Kharif-1) from March/April to June / July (ii) Winter or Rabi from October / November to February/March and (iii) Monsoon or Kharif (Kharif-2) from June / July to September/October. Rice is the main crop of Kharif-2, which is primarily rainfed. Several crops, including rice (known as Boro), wheat, maize, pulses (chickpea, lentil, and field peas), potatoes and oilseeds are grown during the Rabi season. Short-duration cultivars and rice (known as Aus) are planted in Kharif-1. Cropping procedures in Bangladesh are primarily rice-based (Timsina et al., 2018). Nevertheless, because tenant farmers are paid in spot products, everything is decided by established landowners, and people's nutrient intake must be limited by the cropping pattern determined by landlords. Even if there are numerous established landowners, each with their own dynamic cropping system, tenant farmers' nutrient intake must be limited to what they produce because they have essentially no monetary profits and no market access. Cropping practices also have an impact on regional food consumption trends. The triple-cropping strategy is probably the most prevalent and commonly utilized strategy in Bangladesh(Figure 3.2.) (Hassan et al., 1985, Nasim et al., 2017, Alam et al., 2010, Sarker et al., 1997).

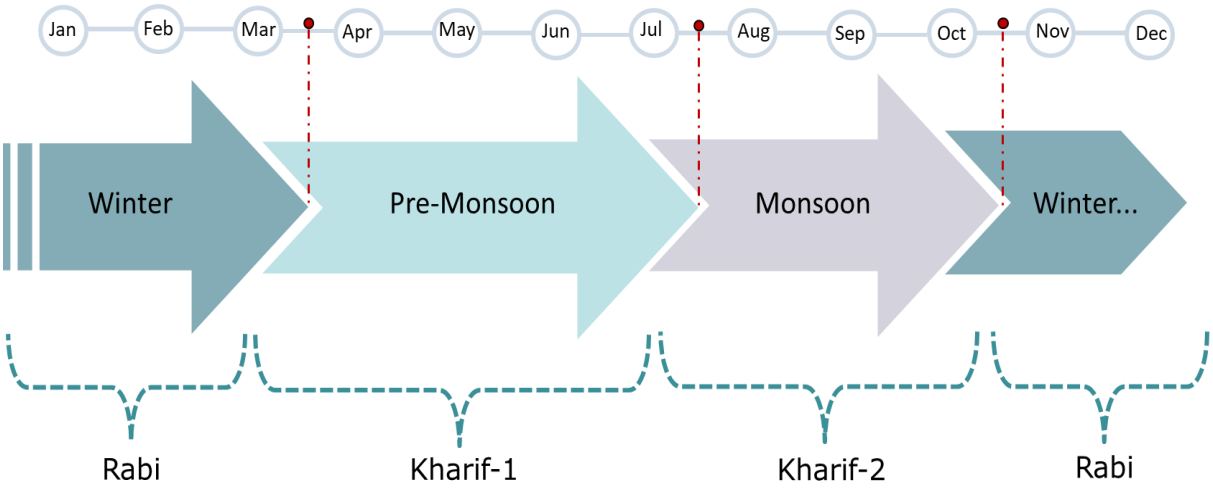

3.2. Research Framework

The implemented method for developing a seasonal map for land use planning using GIS-based multicriteria analysis consists of three major steps (Figure 3.3.); calculating the target area's calorie demand, creating fuzzy expert system-based suitability maps of diversified crops, and proposing seasonal maps.

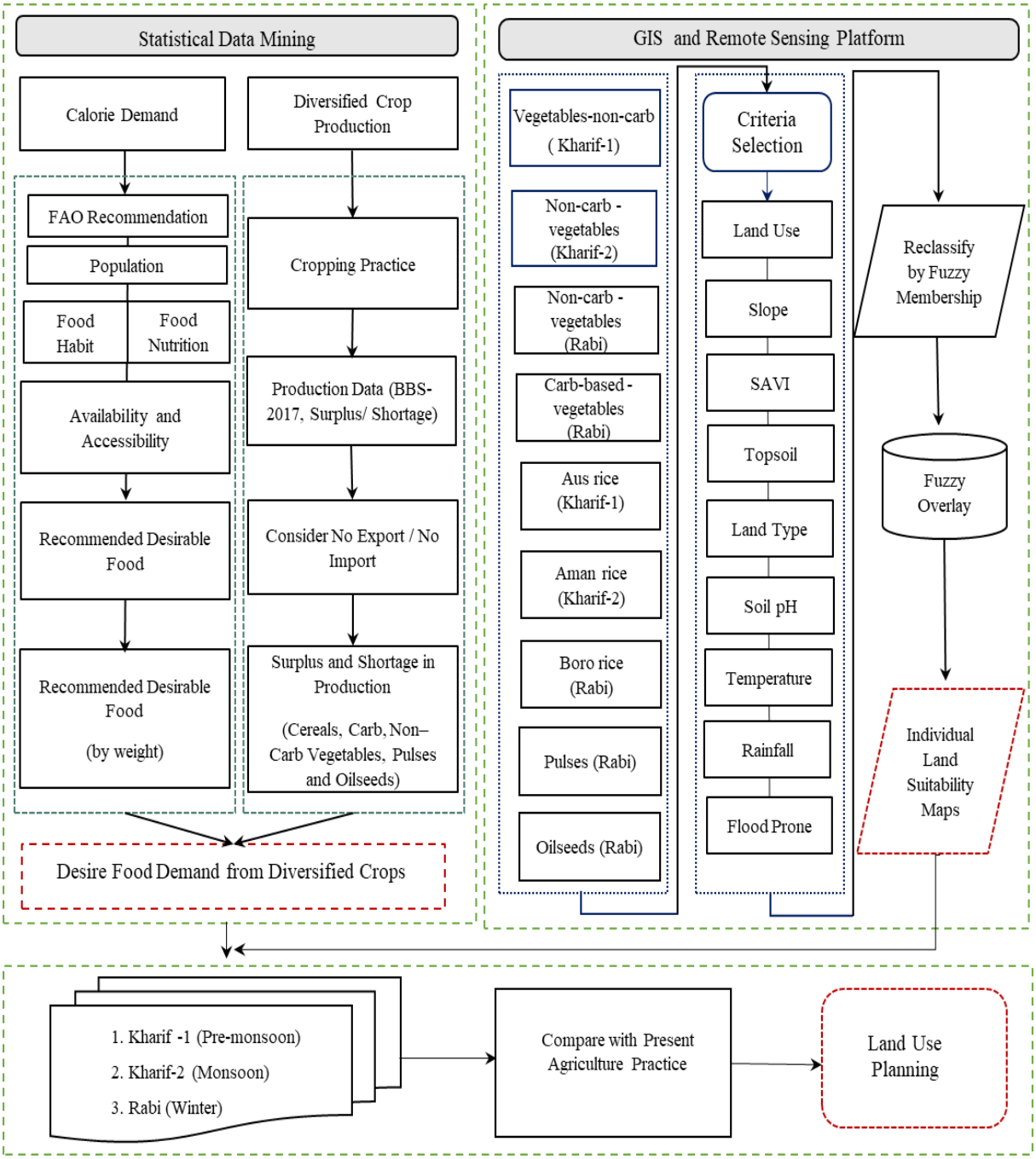

Figure 3.3. Research framework for multi-cropping land use plan.

The proposed method was validated by soil-vegetation index-associated land fertility assessment and consists of three major steps (Figure 3.4.): calculation of soil vegetation indices for land fertility mapping of diversified crops, regression analysis using ground truth yield data for validation and utilization of a yield prediction model to develop a yield map. For criterion aggregates, data pretreatment and computation standardization, weight determination via an equal-weighted overlay, raster computation, fuzzy overlay, fuzzy membership function and ArcGIS 10.4® (ESRI, CA, USA) software package.

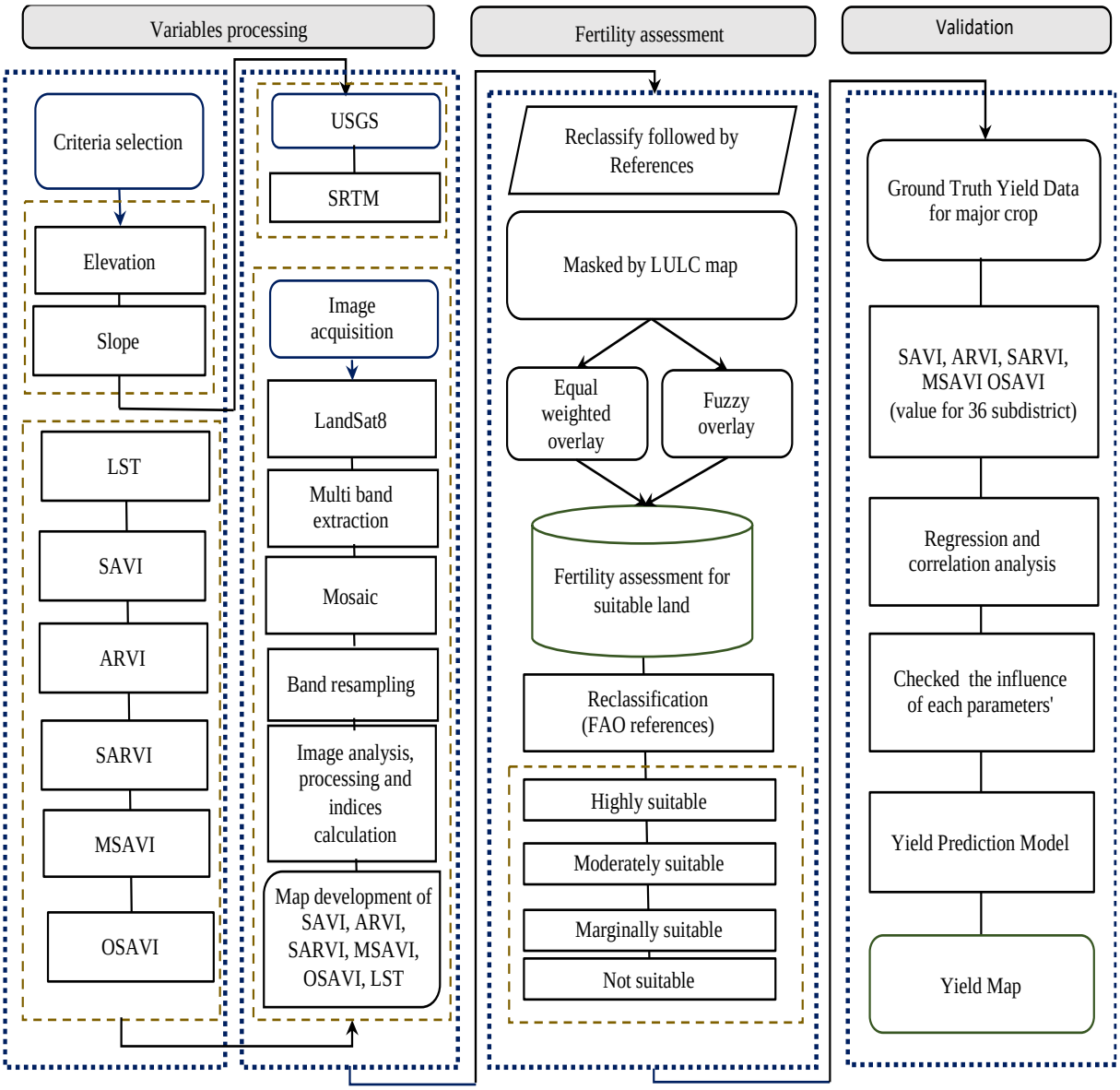

Figure 3.4. land use evaluation by land fertility assessment and yield prediction.

3.3. Study Area

The research area is 8260 square kilometers in size and is located between 25°14´ N and 26°02´ N latitudes and 88°22´ E and 89°54 E longitudes in Bangladesh's northern region. The research was carried out in the Rangpur Division's Dinajpur, Rangpur, Kurigram, and Gaibandha districts (Figure 3.5). There are 36 administrative units in the region, with a total population of 11498000 people (national census 2011; BBS, 2011).

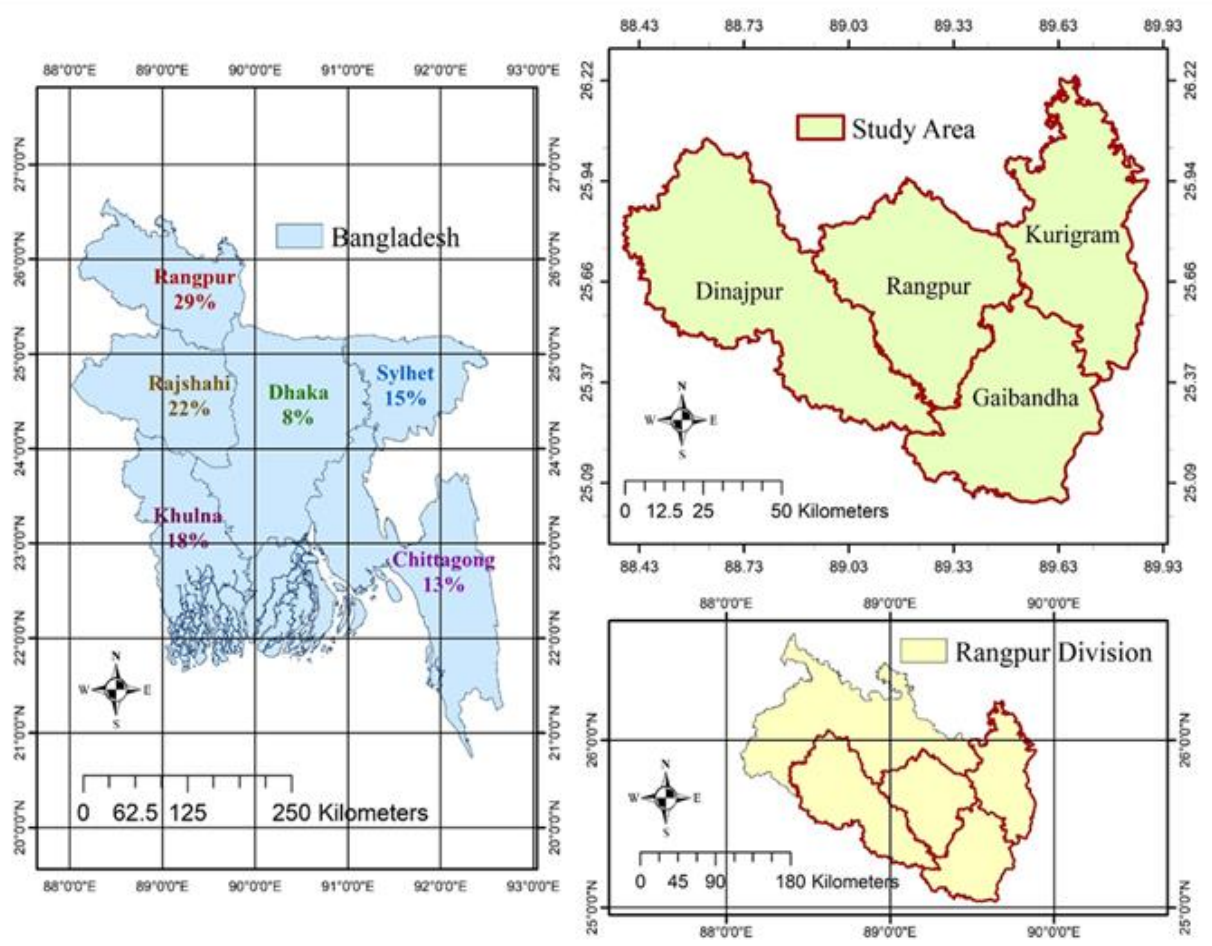

Figure 3.5. (a) Through Bangladesh, there is a predominance of malnutrition; (b) Northern Bangladesh (Rangpur Division); (c) Study region: Dinajpur, Gaibandha, Rangpur, and Kurigram, four districts of Rangpur Division.

The populace is financially engaged in agricultural activities; yet, due to climatic considerations, soil property concerns, water penetration, natural resource and local socioeconomic situations, agronomic land usage is very variable. The lowest and highest mean annual temperatures, according to meteorological data, ranges from 8.47°C to 36.3°C. The total yearly precipitation is 7650-1233 mm, with high humidity ranging from 41 to 77 percent (BBS, 2018). The altitude is between 5 and 30 meters above sea level.

3.4. Data Sets

3.4.1. Statistical data

To categorize the regional cropping pattern and yield estimation and per capital calorie intake proportion, secondary statistical database was used for target area. The data obtained from Bangladesh Bureau of Statistics (BBS-2017). In this regard statistical data mining was carried out the achieving conclusion. Recommended desirable food intake of Bangladesh was calculated based on FAO recommendation.

3.4.2. Satellite data

3.4.2.1. Image acquisition

The Operational Land Imager (OLI) and Thermal Infrared Sensor (TIRS) sensors are carried by Landsat 8, the most recently deployed Landsat satellite. OLI captures data in three spectral bands: visible, near infrared and shortwave infrared as well as a panchromatic band. Those two sensors provide seasonal coverage of the world landmass at 30 m spatial resolution (visible, NIR, and SWIR), 100 m spatial resolution (thermal), and 15 m spatial resolution (thermal) (panchromatic). To develop radiometrically, geometrically, and terrain-corrected 12-bit data products, the 100 m TIRS data are registered to the OLI dataset. Images were taken between 2017 and 2020. All satellite data for this research was obtained out from United States Geological Survey (USGS).

3.4.2.2. Digital image preprocessing

All satellite images were first processed by resampling the band resolution at 30 m and then mosaicked and masked. Subsequently, an algebraic raster operation and a radiometric calibration as well as geometric and atmospheric corrections were applied to the remote sensing images using ArcGIS 10.4®. Image acquisition was performed for each band. Afterwards when, using a resampling process, all chosen bands were transformed to a 30 m resolution to maintain a consistent cell size and data homogeneity. The average reflectance values were calculated for the study area in each band using the raster calculator tool to compensate for the spatial variability to minimize the bias. Four different blocks collected during related time periods were mosaicked to cover the large study area

3.5. Criteria Aggregation for Seasonal Map Preparation

Nine factors were used to produce a land suitability analysis for various crops. (Table 3.2.)

Table 3.2. Components for crop suitability criterion.

No	Data	Description	Source
1	Land Use Map	Scale at 1:25,000	2019, SoB, Bangladesh
2	SAVI	Derived from 30-m resolution	Landsat 8, USGS
3	Slope Map	Derived from 30-m resolution	2019, DEM STRM
4	Land type	Scale 1:50,000	2018, BCA, Bangladesh
5	Topsoil Map	Scale 1:50,000	2018, BCA, Bangladesh
6	Soil pH Map	Scale 1:50,000	2018, BCA, Bangladesh
7	Flood Prone Map	Scale 1:50,000	2018, BCA, Bangladesh
8	Temperature Map	Scale 1:50,000	2018, BCA, Bangladesh
9	Rainfall Map	Scale 1:50,000	2018, BCA, Bangladesh
10	Recommended desirable food items.	Listed in table 1	BIRDEM,2013
11	Crop production data	Locally grown 78 varies of crops	BBS, 2017, Bangladesh

3.5.1. Land use

Information collected on land use allows for the assessment of an area's vegetation, habitation, forest and water bodies. The Survey of Bangladesh (SOB), which was divided into 92 blocks, provided statistics on land usage. The data were compiled on the ArcGIS platform and utilized to create a more precise land use/land cover (LULC) map for the land suitability study. Rivers, forests, water bodies, and communities were all identified limitations in this research. Following that, only agricultural land was considered for land suitability analysis when the limits were removed. Figure 3.6.(m) shows how agricultural land was divided into cultivated land (80%), uncultivated land (0.5%) and vegetative land (19%).

3.5.2. Soil-adjusted vegetation index

Soil has a distinct spectral signature from other category of land coverage. Reflectance increases in proportion to wavelength increase in the visible and near-infrared zones. Multiple aspects, however, influence the pace of growth. Soil has a distinct spectral signature from other category of land coverage. Reflectance approximately proportional to wavelength increase in the visible and near-infrared zones.

Multiple aspects, however, influence the pace of growth. For each type of soil, this connection is quite distinct. As a result, SAVI is effective for soil and vegetation monitoring. SAVI is also a variation of NDVI (Normalized Difference Plant Index), that accounts for the effects of soil brightness when vegetation cover is limited (Jiang et al., 2006). SAVI was derived using a filter for the research region from Landsat 8 OLI images. The datasets were collected between 2015 and 2019. The triple raster for three seasons was created using these datasets. Each raster represents a different time period spanning several years (Figure 3.6. (g, h, i)). A single raster was developed in each of the seasons.

To account for first-order soil background fluctuations and achieve SAVI, updated indices were proposed utilizing the soil adjustment factor L to lessen the soil background impact (Huete, 1988). The acronym SAVI is as follows:

$$SAVI = \rho\_NIR - \rho RED \rho NIR + \rho\_RED + L\ (1+L) \quad (5)$$

where ρ_NIR is the reflectance value in the near-infrared band, ρ_RED is the reflectance value in the red band and soil brightness adjustment factor is denoted by the letter L. In reflectance space, a L value of 0.5 was found to reduce soil brightness changes and remove the need for additional soil adjustment.

3.5.3. Slope

For farmland suitability study, the slope is a critical topographic parameter. Multiple landscape processes are influenced by slope, including ground water content, erosion potential, runoff and shallow subsurface flow velocity. With rising slope, the soil layer's thickness diminishes (Ashford et al., 1997). The actual Shuttle Radar Topography Mission (SRTM) and digital elevation model (DEM) for the research region were used to create this layer. ArcGIS uses the Universal Transverse Mercator (UTM) projection and the WGS84 datum as correcting agents. The highest rate of change between each cell and its neighbors was used to compute the slope. A slope value was assigned to each cell in the output raster. Seasonal plants, in particular, prefer level terrain; just a little slope of 0 to 8% protects against erosion (Zolekar and Bhagat 2015). The slope gradient in the research region was typically under 40% (Figure 3.6 (f)), which was ideal for the majority of farming systems (Nahusenay and Kibebew 2015, Novara et al., 2019, Basche et al., 2016).

3.5.4. Land type

The government of Bangladesh has categorized the area into five groups based on seasonal flooding: highland, medium highland, medium lowland, lowland and extremely lowland (BBS, 2016).The study area comprised highland was 29.5 percent, medium highland was 17.5 percent, medium lowland was 47 percent, and lowland & very lowland was <6 percent (Figure 3.6. (a)). Medium highland and lowland were deemed extremely favorable for agricultural development, whereas high land was deemed somewhat acceptable, low land was deemed marginally acceptable and extremely low land was deemed inappropriate.

3.5.5. Topsoil

Climatic conditions and soil textural features have a big impact on vegetable cropping systems. Soil type influences crop growth patterns within a season (Schutter et al., 2001). Furthermore, averaged across cultivars and water locations, the primary cereal grain production in clay soil was 46 percent greater than that in sandy loam soil (Dou et al., 2016). The optimum soil depth is the thickness of soil above a layer that prevents root development (e.g., consolidated rock or cemented materials, such as gravel) (Zolekar and Bhagat, 2018). The chemical interactions that influence soil fertility are complicated, and they are influenced by natural vegetation and the kind of clay present; the quantities and sizes of sand, silt and clay have crucial impacts on soil formation (Dexter, 2004). There would be seven different types of topsoil in the area: majority loam 1.6%, predominant sandy loam 0.38% , predominance clay 26.4%, prominent silty clay 54.5% , predominant clay loam 0.27% , prominent silty clay loam 6.8% and prominent silty clay loam 9.9% (Figure 3.6. (e)). Such classifications had been classified as sands, loamy sands, sandy loams, sandy clay loams, and silts based on their seasonal agricultural production features and were identified as sands, loamy sands, sandy loams, sandy clay loams and silts by the United States Department of Agriculture (USDA) soil texture suitability evaluating for diversified crops.

3.5.6. Soil pH

The negative logarithm of the hydrogen ion concentration in the surface soils is used to calculate the pH of the soil. In efficient and beneficial, pH is a significant component (Guo et al., 2018). Major cereals, on the other hand, have been discovered to produce in a wide variety of pH levels, ranging from 4 to 8 (Samanta et al., 2011; Ayehu et al., 2015; Kihono and Bosco, 2015; Amin and Zhang, 2015). Furthermore, the moderate pH level is widely believed to be the best pH for crop cultivation ($6.5 < pH < 7.5$) (Huang et al., 2018). The research classified pH levels of 5.5–7.3 as extremely controlled circumstances, spanning 83 percent of the research region, based on the data available. (Figure 3.6. (d)). Likewise, regions with pH values ranging from 7.3 to 8.4 and 4.5 to 5.5 each represented 5% of the area.

3.5.7. Flood prone

Bangladesh is the sixth largest most flood-prone country (UNDP, 2004). Intense locations buried under over than 100 cm of water for 10 days to a few months, as well as places impacted by flash floods lasting more than 10 days, are examples of flood-prone habitats (BBS, 2015; Chauhan et al., 2017). The region was divided into five categories based on the availability of flood-prone data: not flood-prone 45 percent, severe river flooding 13 percent, moderate river flooding 8 percent, low river flooding 19%, low flash flooding 14%, and moderate tidal surge >1%. (Figure 3.6. (c)). Based on the current frequency

and magnitude of virtually halted, not flood-prone zones were deemed highly suitable, areas susceptible to low river flooding were deemed moderately suitable, areas susceptible to moderate river flooding were deemed marginally suitable and areas susceptible to moderate tidal surge & severe river flooding were deemed unsuitable for field crop farming. The Ministry of Education for the Future (MoEF, 2008) is a non-profit organization

3.5.8. Temperature

The most essential parameter in this study was temperature. Land surface temperature has a significant impact on seasonal conditions and agricultural productivity (Kawasaki and Uchida, 2016). Three different temperature strata were evaluated in this research for three separate seasons: Kharif-1, Kharif-2 and Rabi. The average temperature was estimated using cell statistical methods. Temperatures in the Kharif-1 and Kharif-2 seasons were from 34°C to 31°C and 32°C to 30°C respectively (Figure 5 (j, k)). The temperature varied from 23°C to 25°C throughout the Rabi season (Figure 3.6.(l)). Temperature and rainfall are meteorological elements that affect the growthand production of many crops in both direct and indirect ways

3.5.9. Rainfall

Rainfall during crucial periods of paddock development boosts crop output by allowing nutrients to dissolve quickly for seedling absorption (Amin and Zhang, 2015). The study area's four districts get yearly rainfall ranging from 1250 mm to 2000 mm. The yearly rainfall averaged among 756 and 1233 millimeters (Figure 3.6. (b)).

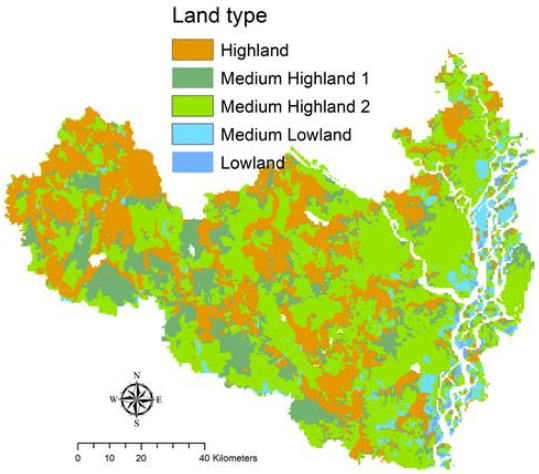
Land type
Highland
Medium Highland 1
Medium Highland 2
Medium Lowland
Lowland
0 10 20 40 Kilometers

(a)

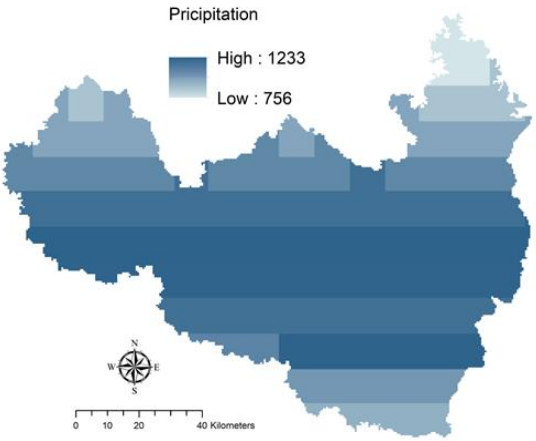
Pricipitation
High : 1233
Low : 756
0 10 20 40 Kilometers

(b)

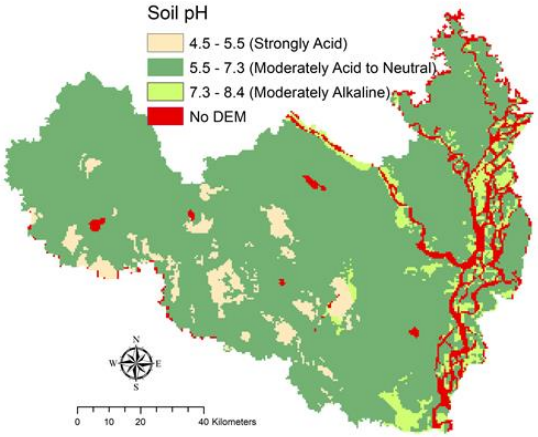
Soil pH
4.5 - 5.5 (Strongly Acid)
5.5 - 7.3 (Moderately Acid to Neutral)
7.3 - 8.4 (Moderately Alkaline)
No DEM
0 10 20 40 Kilometers

(d)

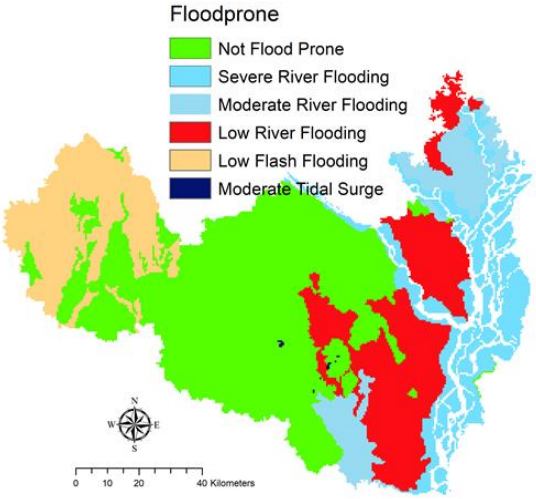
Floodprone
Not Flood Prone
Severe River Flooding
Moderate River Flooding
Low River Flooding
Low Flash Flooding
Moderate Tidal Surge
0 10 20 40 Kilometers

(c)

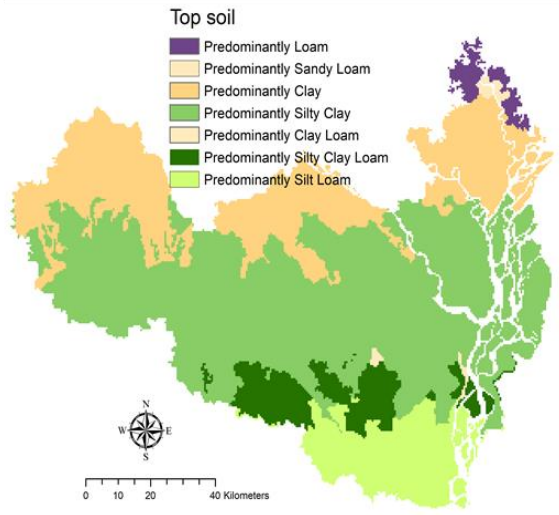
Top soil
Predominantly Loam
Predominantly Sandy Loam
Predominantly Clay
Predominantly Silty Clay
Predominantly Clay Loam
Predominantly Silty Clay Loam
Predominantly Silt Loam
0 10 20 40 Kilometers

(e)

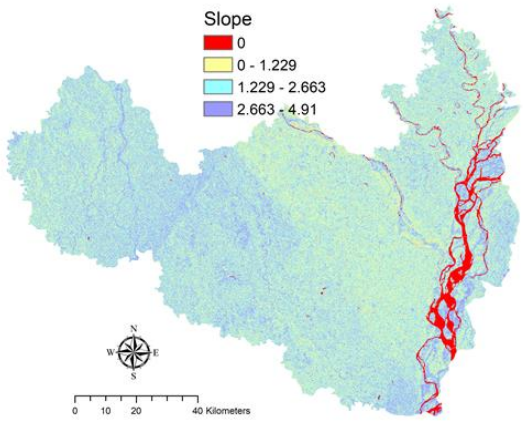
Slope
0
0 - 1.229
1.229 - 2.663
2.663 - 4.91
0 10 20 40 Kilometers

(f)

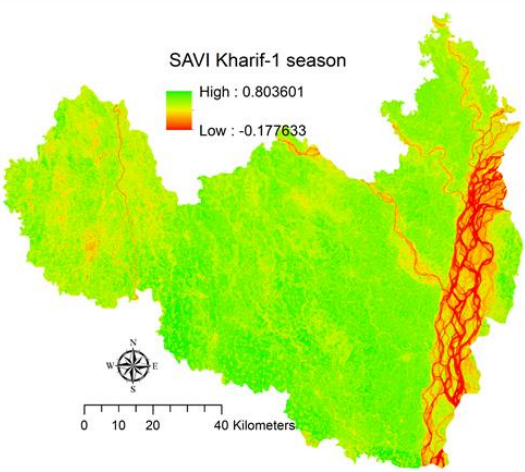
SAVI Kharif-1 season
High : 0.803601
Low : -0.177633
N
W
E
S
0 10 20 40 Kilometers

(g)

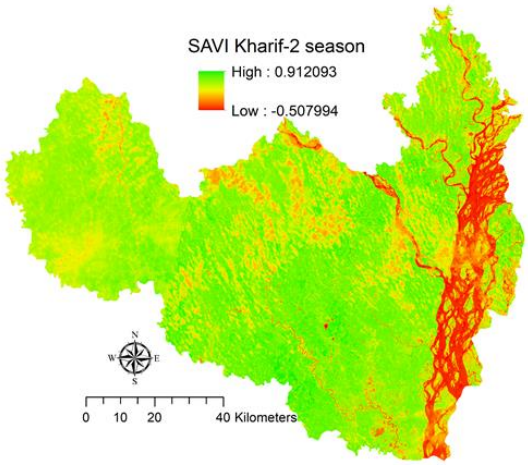
SAVI Kharif-2 season
High : 0.912093
Low : -0.507994
N
W
E
S
0 10 20 40 Kilometers

(h)

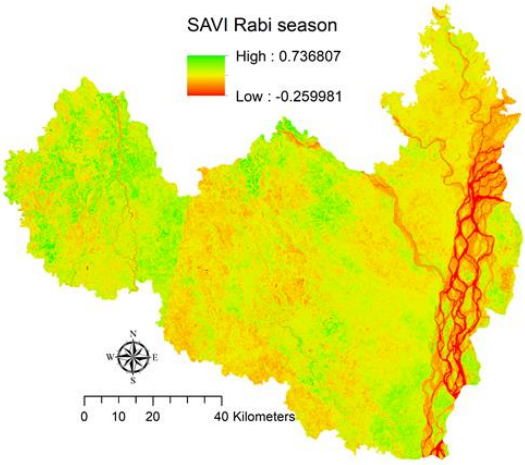
SAVI Rabi season
High : 0.736807
Low : -0.259981
N
W
E
S
0 10 20 40 Kilometers

(i)

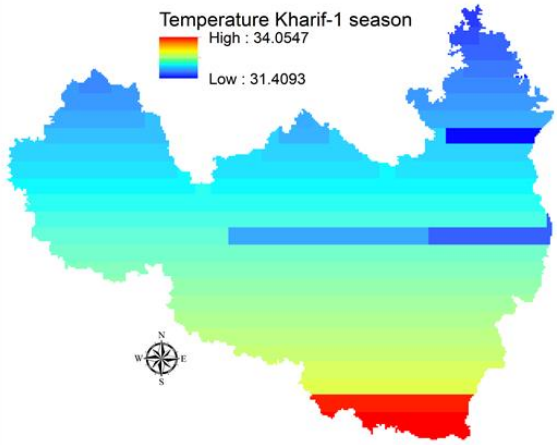
Temperature Kharif-1 season
High : 34.0547
Low : 31.4093
N
W
E
S

(j)

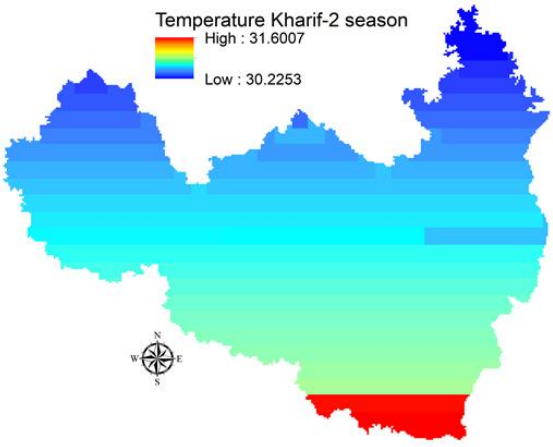
Temperature Kharif-2 season
High : 31.6007
Low : 30.2253
N
W
E
S

(k)

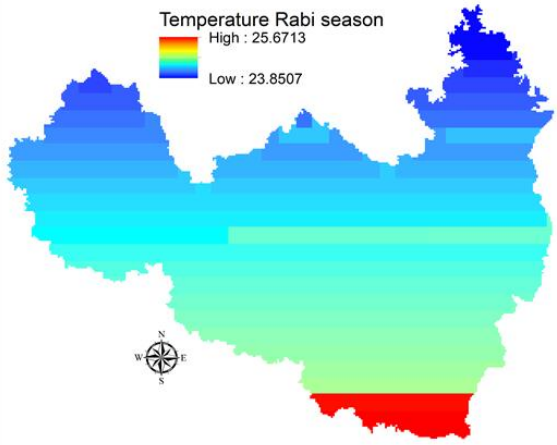
Temperature Rabi season
High : 25.6713
Low : 23.8507
N
W
E
S

(l)

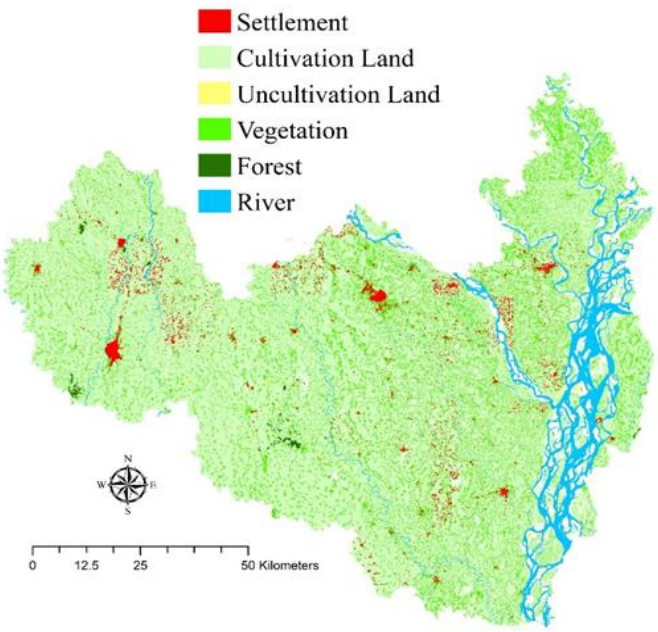

Figure 3.6. The criteria for determining land suitability: (a) land type; (b) precipitation (c) flood prone; (d) soil pH; (e) topsoil; (f) slope; (g) SAVI of Kharif-1 season; (h) SAVI of Kharif-2 season; (i) SAVI of Rabi Season; (j) Rabi Season temperature; (k) Kharif-1 season temperature; (l) Kharif 2 Season temperature; and (m) land use map (SOB) for 2019.

3.6. Criteria Aggregation for Evaluation

To evaluate the Seasonal land use planning land fertility assessment was conducted. Soil-vegetation represented eight criteria were used to determine land fertility analysis (Table 3.3).

Table 3.3. For land fertility evaluation, a list of data and original data sources are provided.

No	Data	Native Format	Description	Source
1	Land Use Map	92 small vector blocks (point, line, polygon and tabular)	Scale at 1:25,000m	2019, SoB, Bangladesh
2	Elevation Map	raster	Extracted from 30 m resolution	2020, STRM
3	Slope Map	raster	Derived from 30-m resolution	2020, STRM
4	Land Surface Temperature (LST)	raster	Derived from 30-m resolution	2020, Landsat 8
5	SAVI Map	raster	Derived from 30-m resolution	2020, Landsat 8, USGS
6	ARVI Map	raster	Derived from 30-m resolution	2020, Landsat 8, USGS
7	SARVI Map	raster	Derived from 30-m resolution	2020, Landsat 8, USGS
8	MSAVI Map	raster	Derived from 30-m resolution	2020, Landsat 8, USGS
9	OSAVI Map	raster	Derived from 30-m resolution	2020, Landsat 8, USGS

3.6.1. Elevation

Elevation is a significant component that influences plant cover variations and causes temperature fluctuations, particularly in highland environments. Rainfall is more intense in areas with greater topographic heights (Bozdağ et al., 2016). The research area is flat land with a maximum elevation of less than 131 meters (Figure 3.6 (a)). A data elevation model (DEM) was used to extract the elevation data, which was then downscaled to a resolution of 30 meters.

3.6.2. Slope

Slope is a significant topography feature in determining whether a piece of land is suited for farming or not. Many landscape phenomena, including soil water content, runoff, erosion potential and shallow

subsurface flow velocity are all indicated by slope. With rising slope, the topsoil layer's density diminishes (Ashford et al., 1997). Data from the original Shuttle Radar Topography Mission (SRTM) and a digital elevation model were used to create the slope (DEM). The DEM was downscaled to a resolution of 30 meters. ArcGIS uses the Universal Transverse Mercator (UTM) projection system and the WGS84 datum as correcting agents. The highest rate of change between each cell and its neighbors was used to compute the slope. A slope value was assigned to each cell in the output raster. Field crops require level terrain; only a little slope of 0% to 8% is resistant to erosion (Zolekar & Bhagat, 2015). Because slope gradient is the key element governing soil erosion, soil sediment losses remain substantial after crop cessation when the slope gradient is quite steep (40 percent) (Koulouri and Giourga, 2007). The slope gradient in the research region was less than 10% (Figure 3.7 (b)), which is ideal for most farming operations (Novara et al., 2019, Nahusenay and Kibebew, 2015, Basche et al., 2016).

3.6.3. Land Surface Temperature (LST)

When there was reduced cloud covering, the LST (Figure 3.7. (c)) was estimated using temporal data from Landsat 8 OLI pictures (Jeevalakshmi et al., 2017). The LST values from the acquired photos varied from 17°C to 33°C from 2017 to 2020. Using the moving average approach, the LST was calculated. Multiple years of raster datasets were merged into a single raster. The LST was calculated using the moving average approach. As the multiple prediction's raster, a single raster was created from various years of raster information.

For the farmland, LST was computed using temporal data from Landsat 8 OLI, which was picked at a time with low cloud coverage. The LST was determined in two steps: firstly, the NDVI for the specific time period was determined.

$$NDVI = \frac{\rho_{NIR} - \rho_{RED}}{\rho_{NIR} + \rho_{RED}} \qquad (6)$$

The NDVI value obtained was then used to calculate the percent vegetation (PV), which may be represented as follows:

$$PV = \left(\frac{NDVI - NDVI_{min}}{NDVI_{max} - NDVI_{min}}\right)^2 \qquad (7)$$

The land surface emissivity (ε_λ) may be described as follows after computing the PV (Jesus and Santana, 2017)

$$\varepsilon_\lambda = 0.004 * PV + 0.986 \qquad (8)$$

Secondly, the thermal bands from Landsat 8 images are shown in bands 10 and 11. To calculate the radiance, the thermal bands were replaced by digital data. The following is an example of spectral radiance:

$$L\lambda = ML + Q_{CAL} + AL \qquad (9)$$

$$L\lambda = 0.0003342 * Band10 + 0.1 \; and \; L\lambda = 0.0003342 * Band11 + 0.1$$
$$L\lambda = 0.0003342 * Band10 + 0.1 \; and \; L\lambda = 0.0003342 * Band11 + 0.1$$

QCAL is the quantized and calibrated standard product pixel value (DN), and AL is the band-specific multiplicative rescaling factor first from metadata, where L is the TOA spectral radiance at the sensor aperture, ML is the band-specific multiplicative rescaling factor from the metadata, and AL is the band-specific additive different spreading factor from the metadata. The brightness temperature (BT) might thus be stated in the following way: (Jesus and Santana, 2017):

$$BT = \frac{K2}{\ln\left[\left(K1/_{L\lambda}\right)+1\right]} - 273.15 \qquad (10)$$

wherein BT is the satellite brightness temperature [Celsius], K2 is the calibration constant 2 [Kelvin], and K1 is the calibration constant 1 [Kelvin], where the band-specific thermal conversion constant is retrieved from the metadata. LST was finally determined and represented as follows: (Jesus and Santana, 2017):

$$LST = \frac{BT}{1+\left(\frac{\lambda * BT}{\rho}\right) * ln\,\varepsilon_{\lambda}} \qquad (11)$$

Where, λ is the average wavelength of band 10; ε_{λ} is the obtained from equation (8); and ρ is ($h*\frac{c}{\sigma}$), which is equal to 1.438 x 10^{-2} mK, where σ is the Boltzmann constant (1.38 x 10^{-23} J/K), h is Plank's constant (6.626 x 10^{-34} *J.s*) and *c* is the velocity of light (3 x 10^{8} m/s).

3.6.4. Soil-Adjusted Vegetation Index (SAVI)

At each soil types, this connection is quite distinct. As a result, SAVI is effective for soil monitoring. SAVI is also a variant of the normalized difference vegetation index (NDVI), which accounts for the effects of soil brightness when vegetation cover is modest (Jiang et al., 2006). A filter for research area was used to extract SAVI (Figure 3.7. (d)) from Landsat 8 OLI images. From 2017 through 2020, data was collected. Using map algebra on the ArcGIS platform, these datasets were combined to create a single raster. For the research region, the SAVI exposure to a variety from 0.798 to -0.302. (Figure 3.7 (d)).

3.6.5. Atmospherically Resistant Vegetation Index (ARVI)

Because of the ARVI's high atmospheric resistance, it's conceivable to get the ARVI (Figure 3.7.(e)) by using a consciousness technique for the atmospheric influence on the red channel, which utilizes the brightness discrepancy between the blue and red channels to adjust the red channel's brightness. (Somvanshi et al., 2020).

$$ARVI = \frac{\rho_{NIR} - (\rho_{RED} - \gamma(\rho_{BlUE} - \rho_{RED}))}{\rho_{NIR} + (\rho_{RED} - \gamma(\rho_{BlUE} - \rho_{RED}))} \qquad (12)$$

where γ depends on the aerosol type. A good default value is γ = 1 when the aerosol model is not available. ARVI's self-correction method makes it immune to atmospheric impacts. To adjust the brightness in the red band, that index considers the variance in brightness between the blue and red bands. ARVI has a comparable frequency range to SAVI, but it is four times less sensitive to atmospheric factors than NDVI, according to models. (Kaufman et al., 1992). The ARVI value fluctuated between 0.886 and -0.662 (Figure 3.7. (e)).

2.4.6. Soil Adjusted and Atmospherically Resistant Vegetation Index (SARVI)

SARVI has a dynamic range equivalent to NDVI, however it is 4 times less susceptible to atmospheric factors. For moderate to small aerosol particles (e.g., continental, urban or smoking aerosol), SARVI works significantly better than for big particles. As a result, in ARVI calculations, a single combination of blue and red channels may be employed in just about all distant optoelectronic devices (Kaufman & Tanre, 1992).

$$SARVI = (1 + L)(\rho_{NIR} - (\rho_{RED} - \gamma(\rho_{BlUE} - \rho_{RED}))/(\rho_{NIR} + (\rho_{RED} - \gamma(\rho_{BlUE} - \rho_{RED})) + L) \qquad (13)$$

where L is a correction factor identical to that used in the SAVI assessment and is a correction factor similar to that used in the ARVI calculation. Relational canopy backdrop and ambient impacts can be reduced using SARVI (Haboudane et al., 2004; Kim et al., 1994). The SARVI performance was found to vary from 0.679 to -0.397 in this research. (Figure 3.7 (f)).

3.6.7. Modified Soil-Adjusted Vegetation Index (MSAVI)

A modified secondary soil-adjusted vegetation index (MSAVI) was suggested by Richardson and Wiegand (1977), which may be written as follows:

$$\text{MSAVI} = 0.5 * \left[(2\rho_{NIR} + 1) - \sqrt{(2\rho_{NIR} + 1)^2 - 8\rho_{NIR} - \rho_{RED}} \right] \qquad (14)$$

MSAVI is primarily utilized in soil organic matter analysis, drought assessment and soil erosion analyzation since it does not rely on the soil line concept and has a simpler methodology. It may also be used for plant development analysis, desertification research, yield of grassland calculations, and leaf area index (LAI) evaluations. The MSAVI value in the research region was found to range between +1 and -1. (Figure 3.6(g)).

2.6.8. Optimized Soil-Adjusted Vegetation Index (OSAVI)

The Optimized Soil Adjusted Vegetation Index (OSAVI) is a novel option which may well account for more variability owing to high soil background values (Melillos et al., 2020). OSAVI is not responsible for soil line and can adequately eliminate the effects of the soil backdrop. Nonetheless, the implications of OSAVI are limited; it is primarily used to calculate aboveground biomass, leaf nitrogen content, chlorophyll content, and so forth (Mwinuka et al., 2020).

$$OSAVI = \frac{\rho_{NIR} - \rho_{RED}}{\rho_{NIR} + \rho_{RED} + X} \qquad (15)$$

where X = 1.6. OSAVI is primarily used to calculate aboveground biomass, leaf nitrogen content, chlorophyll content and other parameters. The measured value ranged within 0.531 and -0.201. (Figure 3.6(h)).

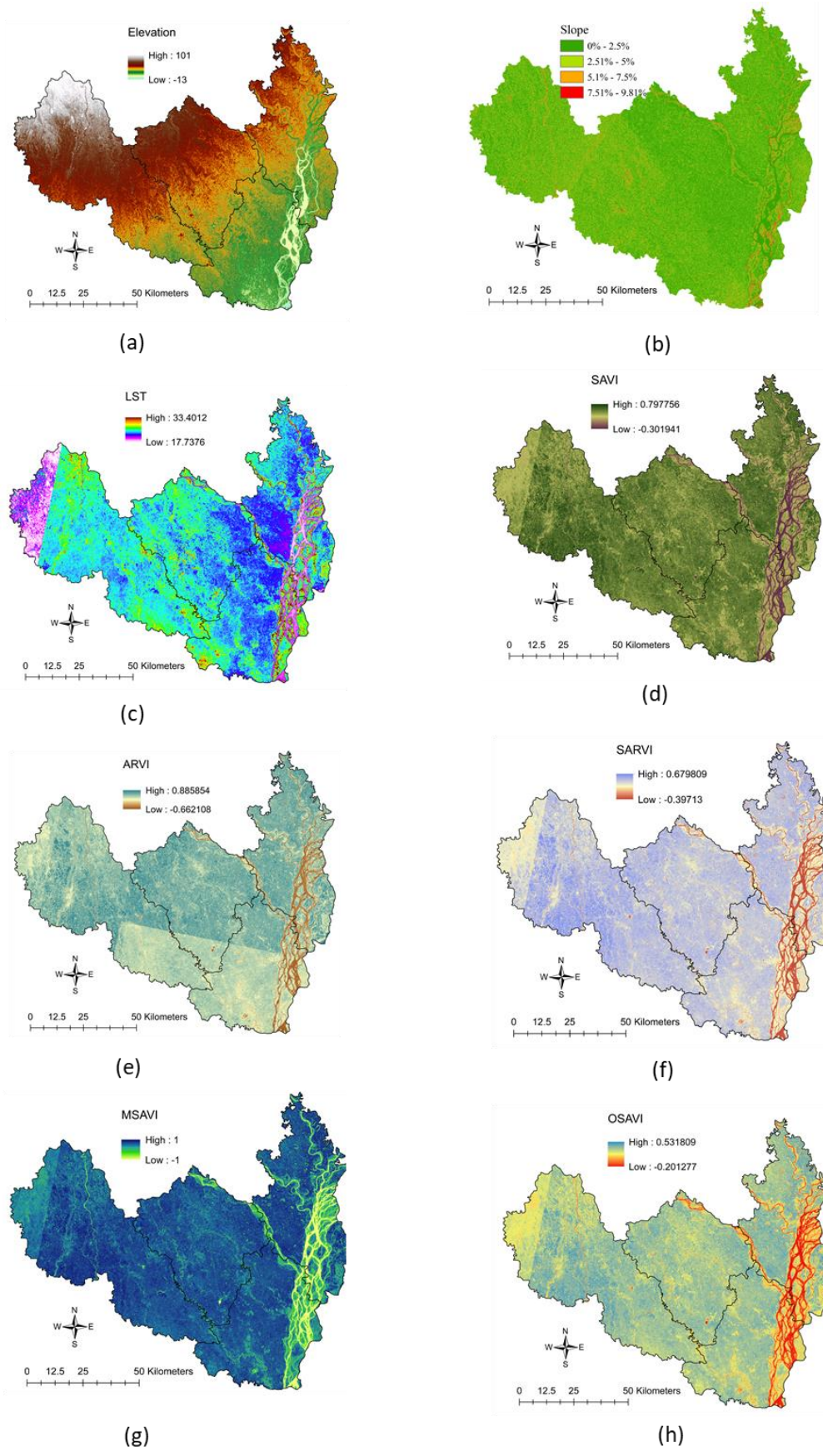

Figure 3.6. Criteria: (a) elevation; (b) slope; (c) LST; (d) SAVI; (e) ARVI; (f) SARVI; (g) MSAVI and (h) OSAVI.

3.7. Multi-Criteria Decision Analysis for Land Suitability

Land suitability analysis (LSA) is a difficult work involving several domains, including climatic conditions, environmental factors, and geography, all of which are involved and influence the production processes. Furthermore, local rules and site characteristics influence the usability of land. When regions with diverse land uses and heavily inhabited regions are addressed, the complexity of LSA grows. Multicriteria decision making is a method for combining and transforming a variety of spatial information (Table 2) into a judgement consequence (Malczewski, 2006). A vast number of viable choices are presented as well as several contradictory and unbalanced criteria. As a result, multicriteria decision making (MCDM) centered on geographic information systems is used to solve numerous actual spatial challenges (GIS). Nine criteria were chosen to perform MCDM with many stages in the spatial environment, according to the research aims in this study (Beinat and Nijkamp, 1998). Each criterion for each crop was assigned a weight in MCDM to signify its significance in the occurrence (Chow and Sadler, 2010). Even though multiple factors of production may be evaluated and weighted independently that according to their relative relevance in the best growing circumstances for crops, the current study employed a multicriteria evaluation (MCE) technique (measured by fuzzy membership function in ArcGIS platform).

3.7.1. Fuzzy Rreclassification

Various fuzzy membership functions were employed to normalize factors using fuzzy set theory. The membership was between 0 and 1. The notion of these continual aspects might be described using fuzzy set theory in a suitability assessment inside GIS or a geographic domain. In a traditional method, membership in a class was specifically articulated as either being in the class or not being in the category (Bellman and Zadeh, 1970). In the present study, fuzzy membership classification was employed to account for the significant uncertainty of scoring systems when assigning appropriateness classes; numerous fuzzy membership functions were employed for normalization in ArcGIS 10.4® (ESRI, CA, USA). Fuzzy functions were chosen for this study based on references and a survey of the literature (Table 3.4.-3.8).

The big, small, Gaussian and linear fuzzy membership functions were employed in this study considering ecological requirements, out of seven variations of fuzzy membership functions in ArcGIS10.4®. Continuous fuzzy classifications of standardized criteria are generated by these routines. ArcGIS's reclassification tool converts categorical data to a scale of 0 to 10, then divides the modified data by 10 to provide a 0 to 1 scale. The equations for the fuzzy large (Equation (16)), small (Equation (17)), linear (Equation (18)), and Gaussian functions (Equation (19)) below (ESRI, CA, USA).

$$\mu(x) = \frac{1}{1+\left(\frac{x}{f_2}\right)^{-f_1}} \qquad (16)$$

When large input values were more likely to be members of the set, the fuzzy large transformation function was utilized. After the rainfall layer, there was a fuzzy large membership function.

$$\mu(x) = \frac{1}{1+\left(\frac{x}{f_2}\right)^{f_1}} \qquad (17)$$

When sufficiently small values were more likely to be members of the set, the fuzzy small transformation function was utilized. In this study, the criterion slope, topsoil and flood prone strata were each followed by a fuzzy small function.

$$\mu(x) = e^{(-f1*(x-f2)^2)} \qquad (18)$$

The SAVI criteria used a fuzzy linear transformation function to connect a linear function between the user-specified minimum and maximum reclassification values.

$$\mu(x) = f(x) = \begin{cases} 0 & x \le a \\ \frac{x-a}{b-a} & a < x < b \\ 1 & x \ge b \end{cases} \qquad (19)$$

The fuzzy Gaussian function generates a normal distribution from primal values. When the membership of the input values decreases, they move away from the midpoint (Purnamasari et al., 2019) set the fuzzy Gaussian function's midpoint to 1. The fuzzy Gaussian membership function was used to analyze the land type, soil pH, temperature and land use layers.

The control point in the fuzzy small, Large and Gaussian membership functions contained a midpoint (f2) and a spread (f1). A midway was a particular location with a membership in the large and small functions of 0.5. The user determined Gaussian functions based on recommendations (ESRI, CA, USA). In practice, the spread was assigned a value between 1 and 10. With increasing spread value, the fuzzy membership curve grew steeper. A linear function between the lowest and maximum values was used by the fuzzy linear transformation function. Any value less than the minimum was considered to be 0 (not a member)and any value more than the maximum was found to be 1 (a member) (Barbosa, 2015; Bahrani et al., 2016).

Table 3.4. Suitability class for cereal crops (different varieties of rice) by fuzzy membership function

Criteria	**Most suitable condition**	**Maximum expectable condition**	**Minimum acceptable condition**	**Not Fuzzy Member**	**Reference**	**Fuzzy Membership Function**
Slope	x<4°	20°	0°	20^{o} <x	Ayehu et al., 2015	Fuzzy small
Land Type	Medium High/lowland	High Land	Lowland	Very Lowland	Paul and Rashid, 2016; BBS, 2016	Fuzzy Gaussian
Topsoil	Predominant Clay Predominant Silt Clay Predominant Silt Clay Loam	Predominant Silt Loam Predominant Clay Loam	Predominant Loam	Predominant Sandy Loam	Dou et al., 2016; USDA; Asai et al., 2009	Fuzzy Small
Soil pH	5.6<x<7.3	8.4	4	x<4 or x>8	Ayehu et al., 2015; Kihoro et al., 2013	Fuzzy Gaussian
Flood Prone	Not Flood Prone	Moderate River Flooding	Moderate Tidal Surge	Low River Flooding, Severe River Flooding	Datta et. al., 2017; BBS, 2016	Fuzzy Small
Temperature	20°C <x<30°C (Aus, Aman) 10 °C <x<20°C (Boro)	Aus & Aman up to 45°C Boro rice up to 35°C	10°C	x>35 °C or x<20°C	Samanta et al., 2011; Kihoro et al., 2013	Fuzzy Gaussian
Rainfall	x>1400mm	2000mm	800mm	<800	Ayehu & Besufekad, 2015	Fuzzy Large
SAVI	0.80301 (Aus), 0.912093 (Aman), 0.736807 (Boro)	+1	-1	-0.178<x x<0.803 (Aus), -0.508<x<0.912 (Aman), -0.26<x< 0.737 (Boro)	Purnamasari et al., 2019; Habibie et al., 2019; Venancio et al., 2019; Rondeaux et al., 1996	Fuzzy Linear
Land Use	Agriculture land	Vacant land	Used land	Settlements, Rivers, Waterbodies, Forests		

Table 3.5. Suitability class for carbohydrate-based vegetables (potatoes) by fuzzy membership.

Criteria	**Most suitable condition**	**Maximum expectable condition**	**Minimum acceptable condition**	**Not Fuzzy Member**	**Reference**	**Fuzzy Membership Function**
Slope	x<3°	3°<x<5°	5°<x<8°	x>8	Gitari et al, 2019; Shimoda et al., 2018	Fuzzy small
Land Type	Medium High/lowland	High Land	Lowland	Very Lowland	BBS, 2016	Fuzzy Gaussian
Topsoil	Loam Sandy loam Sandy clay loam Silt loam	Predominant Sandy Loam	Sandy clay	Gravel Sand Silty clay loam Clay loam Silty clay Silt Clay	Shimoda et al., 2018	Fuzzy Small
Soil pH	5<x<6.5	6.6<x<8.2	5.0<x<5.4	x>8.2 or, x<5.0	Saini et al., 1980	Fuzzy Gaussian
Flood Prone	Not Flood Prone	Moderate Tidal Surge	Moderate River Flooding	Low River Flooding, Severe River Flooding	BBS, 2016	Fuzzy Small
Temperature	15°C <x<18°C	30°C	10°C	x>35°C x<2.5°C	Zhao et al., 2012	Fuzzy Gaussian
Rainfall	700<x<1000 mm	2000 mm	Less than 700 mm	x<300	Xing et al., 2011; Qin et al., 2013	Fuzzy Large
SAVI	0.736807	+1	-1	x<0.736680 or, x> -0.29981	Purnamasari et al., 2019; Habibie et al., 2019; Venancio et al., 2019; Rondeaux et al., 1996	Fuzzy Linear
Land Use	Agriculture land	Vacant land	Used land	Settlements, Rivers, Waterbodies, Forests	2018; Bahrani et al., 2016; Zhu et al. 2020	Fuzzy Gaussian

Table 3.6. Suitability class for non-carbohydrate-based vegetables by fuzzy membership.

Criteria	**Most suitable condition**	**Maximum expectable condition**	**Minimum acceptable condition**	**Not Fuzzy Member**	**Reference**	**Fuzzy Membership Function**
Slope	0^0 <x<7^0	15°<x<25°	7°<x<15°	x< 25^0	Yalew et al., 2016	Fuzzy small
Land Type	Medium High/lowland	High Land	Lowland	Very Lowland	BBS, 2016	Fuzzy Gaussian
Topsoil	Loam soils with moderate to gentle slope	Clay loam, Loam soils on steep slope also acceptable condition			Zolekar & Bhagat, 2015.	Fuzzy Small
Soil pH	5.3<x<6.6	8.2	5	x>8.3, x<5	Mapanda et al., 2005; Yang 2014	Fuzzy Gaussian
Flood Prone	Not Flood Prone	Moderate Tidal Surge	Moderate River Flooding	Low River Flooding, Severe River Flooding	BBS, 2017	Fuzzy Small
Temperature	14°C <x<15°C	30°C <x<32 °C (summer) 26°C <x<28°C (winter)	13°C<x<15 °C (summer) 4°C <x<7°C (winter)	x>38°C x<3°C	Meng et al., 1997; Marklein et al., 2020; Ngoy & Shebitz 2020	Fuzzy Gaussian
Rainfall	1000<x<2000 mm	700<x<1000 mm	Less than 700 mm		Richards et al., 2014;	Fuzzy Large
SAVI	0.80301 (Kharif-1) 0.912093 (Kharif-2) 0.736807 (Rabi)	+1	-1	(Kharif -1) - 0.178<x <0.803, -0.508<x<0.912 Kharif- 2, -0.26<x< 0.737 (Rabi)	Purnamasari et al., 2019; Habibie et al., 2019; Venancio et al., 2019; Rondeaux et al. ,1996	Fuzzy Linear
Land Use	Agriculture and Fallow land	Sparse forest, Scrub land , Barren land, Dense forest also acceptable condition		Water body, Settlement	Zolekar, & Bhagat, 2015 Akinci et al., 2013	Fuzzy Gaussian

Table 3.7. Suitability class for pulses by fuzzy membership.

Criteria	**Most suitable condition**	**Maximum expectable condition**	**Minimum acceptable condition**	**Not Fuzzy Member**	**Reference**	**Fuzzy Membership Function**
Slope	<2°	8°	3°<x<5°	>8	Kladivko et al., 1986;	Fuzzy small
Land Type	Medium High/lowland	High Land	Lowland	Very Lowland	BBS, 2016	Fuzzy Gaussian
TopSoil	Loam Sandy loam Sandy clay loam Silt loam	Predominant Sandy Loam	Sandy clay	Gravel Sand	Nguyen et al., 2015	Fuzzy Small
Soil pH	5.8<x<6	8.5	x> 5.5	x> 8.5 and x< 5.5	FAO, 2016c; Egamberdieva et al., 2016	Fuzzy Gaussian
Flood Prone	Not Flood Prone	Moderate Tidal Surge	Moderate River Flooding	Low River Flooding, Severe River Flooding	BBS, 2016	Fuzzy Small
Temperature	17°C <x< 20°C	26°C <x< 30°C	10°C <x< 12°C	x>32°C x<10°C	Yallew et al., 2016; Kladivko et al., 1986	Fuzzy Gaussian
Rainfall	700 <x<1000 mm	1000 <x< 2000 mm	Less than 360 mm		Miller et al., 2002	Fuzzy Large
SAVI	0.736807	+1	-1	x<-.0259981 or, x>0.736807	Purnamasari et al., 2019; Habibie et al., 2019; Venancio et al., 2019; Rondeaux et al., 1996	Fuzzy Linear
Land Use	Agriculture land	Vacant land	Used land	Settlements, Rivers, Waterbodies, Forests	Bahrani et al., 2016; Zhu et al., 2020	Fuzzy Gaussian

Table 3.8. Suitability class by fuzzy membership for oilseeds

Criteria	**Most suitable condition**	**Maximum expectable condition**	**Minimum acceptable condition**	**Not Fuzzy Member**	**Reference**	**Fuzzy Membership Function**
Slope	$0° < x < 4.5^0$	0^0	16.7^0	$x > 16.7^0$	Arief & Nafi 2018	Fuzzy small
Land Type	Medium High/lowland	High Land	Lowland	Very Lowland	BBS, 2016; Kamkar et al., 2014	Fuzzy Gaussian
Topsoil	Silty loam, silty clay loam				Petosi et al., 2020	Fuzzy Small
Soil pH	5.8<x<7.3	8.7	4.3	x<4.3, x> 9	Petosi et al., 2020; Chaignon et al., 2002	Fuzzy Gaussian
Flood Prone	Not Flood Prone	Moderate Tidal Surge	Moderate River Flooding	Low River Flooding, Severe River Flooding	BBS, 2016	Fuzzy Small
Temperature	20°C	35°C	10°C <x< 15°C	x>35°C, <10°C	Petosi et al., 2020, Johnston et al., 2002.	Fuzzy Gaussian
Rainfall	400 <x< 600 mm	3500 mm	325 mm	x>500 mm	Arief & Nafi, 2018; McCormick et al., 2012; Kamkar et al., 2014	Fuzzy Large
SAVI	0.736807	+1	-1	x<-.0259981 or, x >0.736807	Purnamasari et al., 2019; Habibie et al., 2019; Venancio et al., 2019; Rondeaux et al. ,1996	Fuzzy linear
Land Use	Agriculture land	Vacant land	Used land	Settlements, Rivers, Waterbodies, Forests	Islam et al., 2018; Bahrani et al., 2016; Zhu et al., 2020	Fuzzy Gaussian

2.7.2. Overlay

2.7.2.1. Fuzzy Overlay

In ArcGIS, the fuzzy overlay analysis accepts the potential of a phenomena belonging to many sets and analyzes the connection between the memberships of the numerous sets. Each fuzzy overlay approach enables the examination of each cell's membership in numerous input criteria. Fuzzy overlay techniques were utilized to investigate the linkages and interactions between all of the sets for the 9 criteria in the overlay model. The overlay approaches illustrate the interplay of the errors in the small, big, linear and Gaussian memberships of the sets, because the fuzzification process is dependent on the degree of membership to a set. Based on set theory, the fuzzy overlay approach was applied (ESRI, CA, USA). Set theory is a mathematical subject that quantifies individual member's relationship to specified sets.

Fuzzy or, Fuzzy Product, Fuzzy Sum, and Fuzzy Gamma are the available fuzzy set overlay algorithms in ArcGIS. Each of these methods specifies the membership of the cell in relation to the input sets. Fuzzy Gamma overlay was used in this work to help produce 9 different agricultural suitability maps for three different seasons, which were calculated using references and a literature review. (ESRI, CA, USA).

2.7.2.2. Scoring for individual suitability map preparation

The final map was displayed as stretched values after fuzzy overlay, requiring score for visual understanding and extensive justification. The FAO's multiple categorization categories were used to conduct the land suitability study for diverse crops. According to the FAO's land appraisal framework, the first class was designated as suitable (S) or not suitable (N). The purpose of the suitability categorization was to illustrate how suitable each land unit was for agricultural production. In reality, Three grades are typically used to define land that is extremely appropriate, moderately appropriate and marginally acceptable, respectively: (S1), (S2), and (S3) (Figure 3.8).

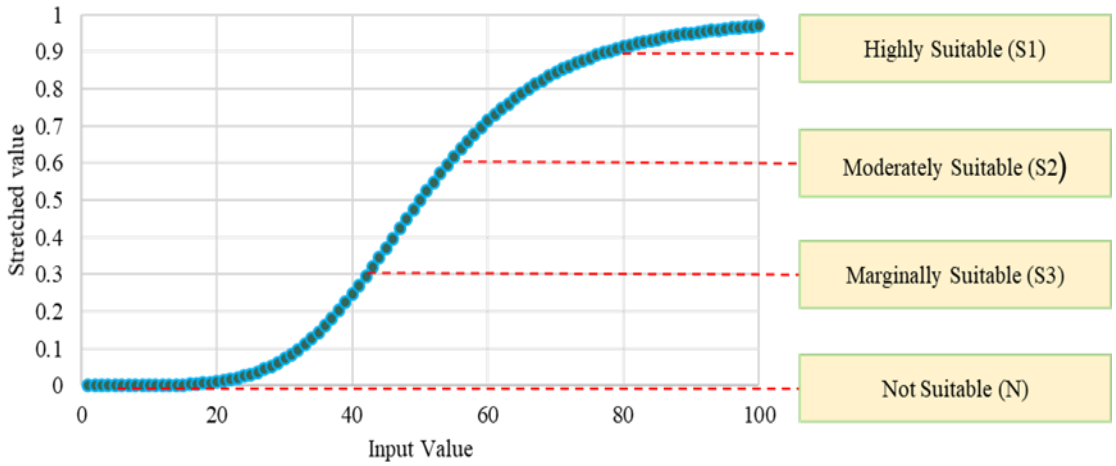

Figure 3.8. Suitability range of classification by scoring based on fuzzy overlay.

3.8. Seasonal land Suitability Map Preparation

The purpose of the suitability assessment was to illustrate how suitable each land unit was for agricultural production. In reality, Three grades are typically used to define land that is extremely appropriate, moderately appropriate and marginally acceptable, respectively: (S1), (S2), and (S3). At this step, ArcGIS® (ESRI, CA, USA) was used to conduct spatial and statistical analysis in order to create seasonal crop suitability maps based on regional food need. The predicted outcomes were then related to the existing farming practices in the research region.

3.9. Evaluation by Land Fertility Assessment

To create a land fertility assessment map, the weighted overlay was utilized to maximize the weights of each criterion. In ArcGIS®, the weighted overlay was blended with the classed raster data layers. The combining criteria were first entered as linear combinations with equal weights. Second, a fuzzy membership function, fuzzy reclassification and fuzzy overlay were used to analyze the uniformity of the two results in the fertility evaluation

3.9.1. Data Processing for Land Fertility Analysis

3.9.1.1. Pattern analysis

Pattern analysis needed pattern analyses from several years or months of data to generate a projected raster for reclassification, that needed pattern analyses from several years or months of data. The individual raster-based computation proved unreliable, and there were insufficient datasets. The pattern analysis for multitemporal datasets into a single raster is discussed in the next section.

(a) Moving Average

Once finishing the digital image processing stages, the moving average was calculated. For single year, the moving average was determined and represented as follows:

$$MA_n = \frac{\sum_{i=1}^{n} Di}{n} \quad (20)$$

here D is the raster cell's number of data points and n is the quantity of data to average.

(b) Multiple predicted raster

A single predicted raster was created as part of the point pattern analysis. From 2017 to 2020, LST, SAVI, ARVI, SARVI, MSAVI, and OSAVI were calculated. The general density pattern was included in the fundamental scope. The multiple predicted rasters are defined as the ratio of the observed number of single predicted raster of points (r) to the study area located (a) (MPR). The MPR was used as a criterion for determining land suitability. MPR can be expressed as follows:

$$MPR = \frac{r}{a} \quad (21)$$

where r is the ratio of the observed number of single predicted raster points and a is the area of the study region.

3.9.1.2. Masked by Land Use/Land Cover

The occupancy of an area with vegetative areas, communities, forests and water bodies may be estimated using land use data. The Survey of Bangladesh (SOB), which was divided into 92 blocks, provided statistics on land usage. The data were utilized to produce a more accurate land use/land cover (LULC) map for the land fertility evaluation after being aggregated on the ArcGIS platform. Rivers, forest, aquatic bodies and communities were all considered limitations in this research. Following that, only agricultural property was considered for land appraisal when the limits were removed. Farmland was divided into three categories: cultivated land (80%), uncultivated land (0.5%), and vegetated land (19%). (Figure 2).

3.9.2. Fertility Assessment

3.9.2.1. Fertility assessment by weighted-linear combination

To analyze the raster data, first reclassification was performed by substituting a single value as the new value or classifying the frequencies into a single value. Every input map was classed into one of four categories (Table 3.9). The FAO proposed different classifications groups for land suitability classes for the land fertility evaluation. The first class was categorized as suitable (S) or not suitable (N) according to the FAO's criteria for land appraisal (N). The purpose of the suitability categorization was to illustrate how suitable each land unit was for agricultural production. In reality, Three grades are commonly used to define highly appropriate, moderately appropriate, and marginally acceptable land, respectively: (S1), (S2), and (S3). The analysis was categorized into four classes based on the aforementioned criteria. Ultimately, the weighted linear combination was used to determine the classes.

$$Weighted\ Overlay = \sum_{i=1}^{n} C_i * W_n \qquad (22)$$

where C_i is each criterion (i) that has been reclassified and W_n is the number of data (n) that were weighted.

3.9.2.2. Fertility assessment by the fuzzy membership function

Each of the SAVI, ARVI, SARVI, MSAVI, and OSAVI layers was followed by a fuzzy linear transformation function that connected a linear function between the user-specified minimum and maximum reclassification values. (Table 3.10).

The primordial values are converted into a normal distribution using the fuzzy Gaussian function. When the membership of the input values decreases, they move away from the midway. Purnamasari et al. (2019) adjusted the fuzzy Gaussian function's midpoint to 1. The fuzzy Gaussian membership function was used to examine the elevation and LST layers.

Table 3.9. Criteria reclassification of suitable class for weighted linear combination.

Criteria	**Suitability class**	**Sub criteria**	**Reference**
Slope	S1	0 – 8%	Zolekar and Bhagat 2015; Gitari et al, 2019; Shimoda et al., 2018
	S2	8 – 15%	
	S3	15 – 25%	
	N	>25%	
Elevation	S1	0-25	Bozdağ et al., 2016; GriSP, 2013; Yalew et al., 2016
	S2	25-125	
	S3	125-250	
	N	>250	
LST	S1	20 – 25	Jeevalakshmi et al. 2017 Ceglar et al., 2018; Samanta et al., 2011,
	S2	18 – 20	
	S3	15 – 18	
	N	9 – 15, < 25	
SAVI	S1	0.372483-0.797756	Huete,1988; Ren et al., 2018; Venancio at al., 2019
	S2	0.217838-0.372483	
	S3	0- 0.217838	
	N	-0.301941- 0	
ARVI	S1	0.293275 – 0.885854	Somvanshi et al. 2020; Kaufman et. Al,1992; Sonobe et al., 2018
	S2	0.1542-0.293275	
	S3	0-0.1542	
	N	-0.662108-0	
SARVI	S1	0.301197-0.671395	Kaufman & Tanre ; 1992, Svinurai et al., 2018; Cho & Skidmore 2009;
	S2	0.301197-0.16658	
	S3	0.16658-0	
	N	-0.39713-0	
MSAVI	S1	0.752112-1	Richardson and Wiegand 1977; Ren, et al., 2018; Ren& Feng, 2015
	S2	0.752112-0.443157	
	S3	0.443157-0	
	N	-1-0	
OSAVI	S1	0.245221-0.526082	Melillos et al. 2020; Gilabert et al.,2002; Ren & Feng, 2015
	S2	0.145221-0.248311	
	S3	0-0.145221	
	N	-0.201272-0	

Table 3.10 Suitable classes by fuzzy membership function for land fertility assessment.

Criteria	**Most suitable condition**	**Maximum expectable condition**	**Minimum acceptable condition**	**Not Fuzzy Member**	**Reference**	**Fuzzy Membership Function**
Slope	<4°	20°	0°	<20	Ayehu et al., 2015; Yalew et al., 2016	F small
Elevation	0	0-25	250	>250	Gerpacio and Pingali 2007; Bozdağ et al. 2016	F Gaussian
LST	10 °C –20°C	up to 35°C	10°C	>35 °C or <20°C	Samanta et al., 2011; Kihoro et al., 2013	F Gaussian
SAVI	0.7978	+1	-1	-0.3019< SAVI <0.7978	Purnamasari et al., 2019; Habibie et al., 2019; Venancio et al., 2019; Rondeaux et al., 1996	F Linear
ARVI	0.8859	+1	-1	-0.3971< ARVI <0.8859	Somvanshi et al. 2020; Kaufman et. Al,1992; Sonobe et al., 2018	F Linear
SARVI	0.6713	+1	-1	-0.3971< SARVI <0.6713	Kaufman & Tanre ; 1992, Svinurai et al., 2018; Cho & Skidmore 2009;	F Linear
MSAVI	1	+1	-1	-0.1 < MSAVI <1	Richardson and Wiegand 1977; Ren, et al., 2018; Ren& Feng, 2015	F Linear
OSAVI	0.5261	+1	-1	-0.2013< OSAVI <0.5261	Melillos et al. 2020; Gilabert et al.,2002; Fern et al.,2018	F Linear

3.9.3. Fertility assessment using ground truth data

Ground reference data confirmed the presence of a fruitful zone. The yield prediction models were developed and validated using time - series data information. Rice agriculture takes up approximately 80% of the entire land area in Bangladesh (Mottaleb et al., 2018). Furthermore, nearly 70% of the land in the northwestern region of the nation is grown with dry season irrigated rice (Zinat et al., 2020; Acharjee et al., 2017, Alamgir et al., 2020). (boro rice). To facilitate further analysis, the major rice crop was carefully chosen for approval. Ground truth yielding data was used to confirm the appropriate location. To examine the reliability of the soil fertility evaluation, yield data of dry season irrigated rice were obtained from the Department of Agricultural Extension (DAE), Ministry of Agriculture, Bangladesh, for the 36 subdistricts in 2017-2020 (Figures 3.9 and 3.10). The correlations among the five specified indices were assessed once the data was prepared in Microsoft Excel.

3.9.4. Yield prediction

Field data was used to evaluate the yield prediction models' performance. The yield map was created once the relationships between the 5 different vegetation metrics were determined. To establish the best-fitted models for rice production, simple and multiple regression analyses were performed between the mean values of the vegetation indicators and the ground referenced data of the dry season irrigated rice. These statistics were categorized in order to assess output between 2017 and 2020. The values for SAVI, ARVI, SARVI, MSAVI and OSAVI were combined into a time series pattern (Figure 3.9.). Regression was used to compare the yield data. The five vegetation index data were obtained from 36 subdistrict reference stations (Figure 3.10.). The yield was given in metric tons per hector (MT/ha) and pixel - level data was acquired from the 36 subdistricts.

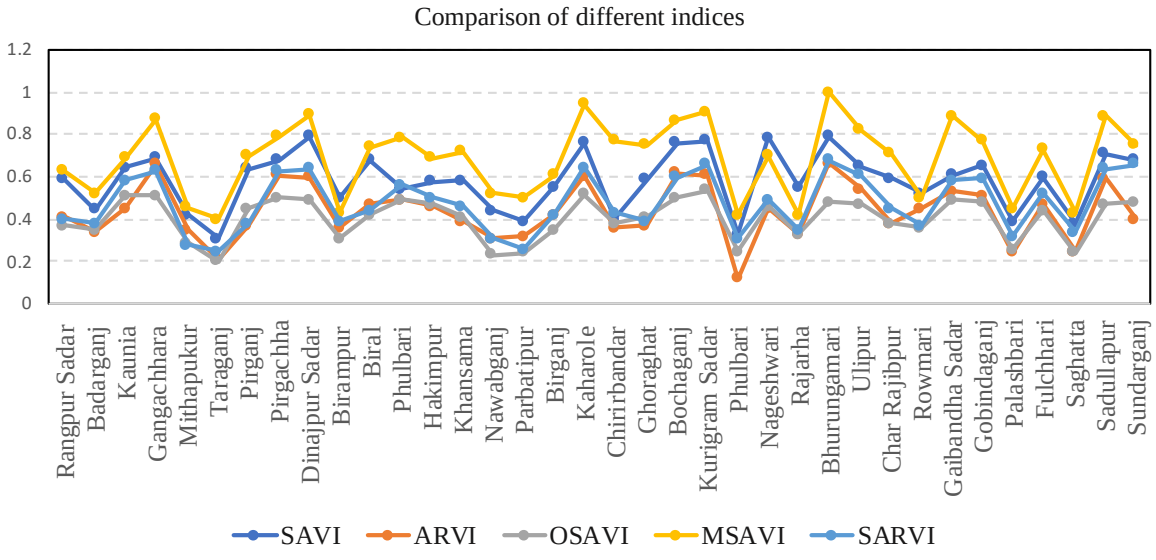

Figure 3.9. Variability of rice yield based on the soil-vegetation related indices across the 36 subunits.

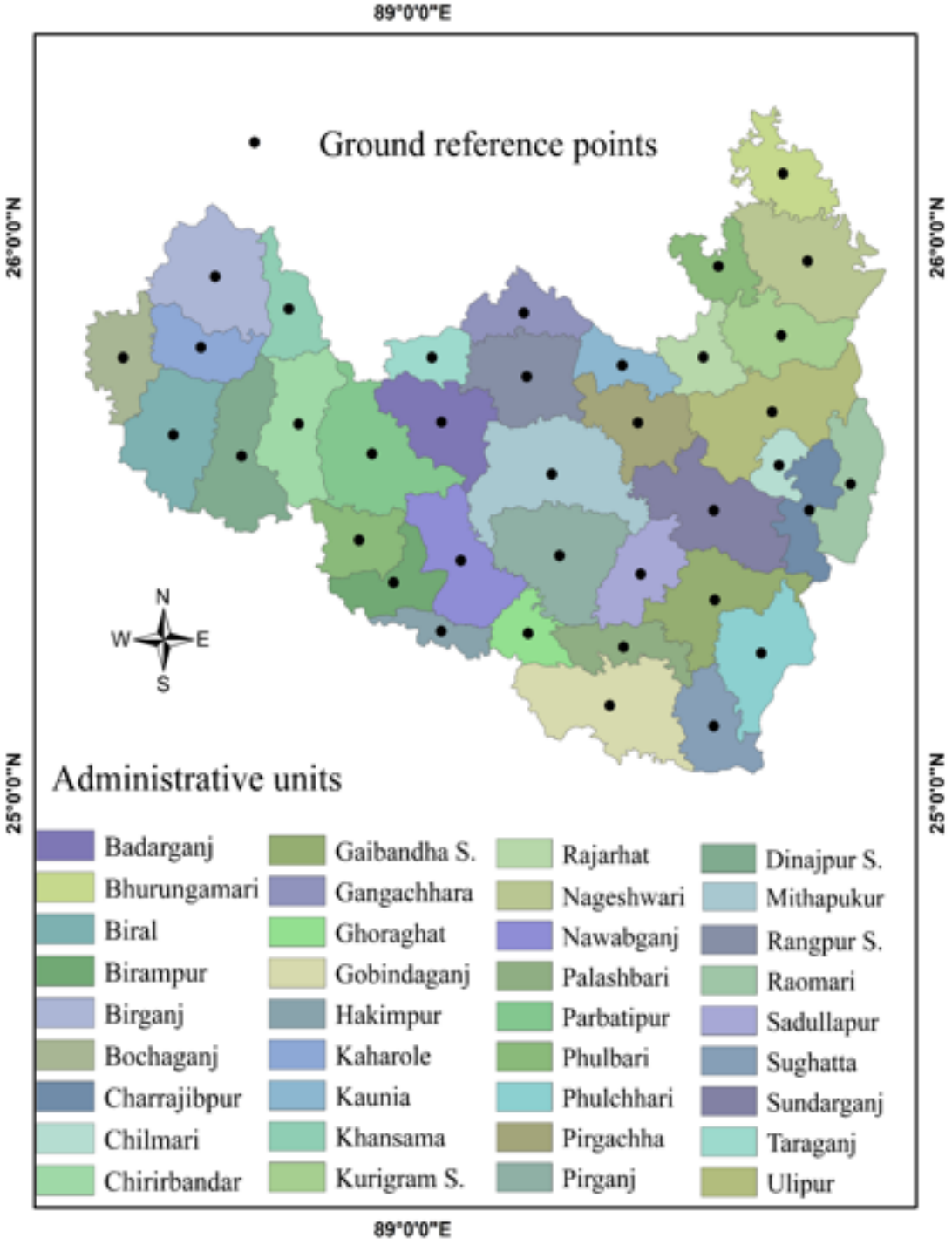

Figure 3.10. Ground referenced information points in the 36 subunits.

Chapter IV

Results and Discussion

4.1. Seasonal land Use Plan

4.1.1. Crop production throughout the locality

Crop production data revealed that some crops produced more than needed, while others produced less than needed in the study region when nutritional balance was taken into account (Figure 4.1). Rice, minor cereals and carbohydrate-based vegetables were grown with greater yields of 2396992 metric tons, 750366 metric tons and 3104403 metric tons, accordingly. Productivity of non-carbohydrate-based vegetables, oilseeds and pulses,, on the other hand, was lower than the required at 1009120 metric tons, 204293 metric tons, and 89550 metric tons, correspondingly

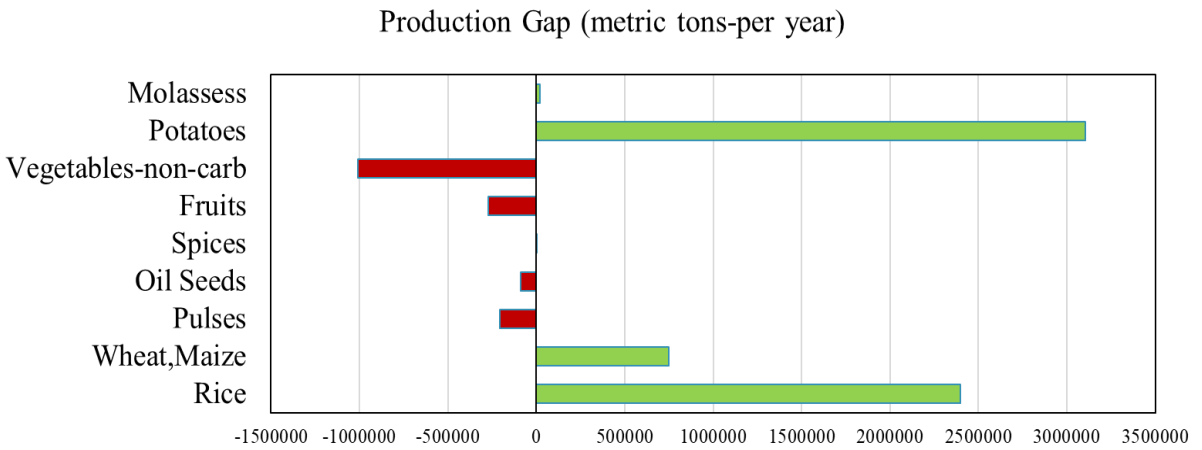

	Rice	Wheat,Maize	Pulses	Oil Seeds	Spices	Fruits	Vegetables-non-carb	Potatoes	Molassess
metric-tons/ year	2396992	750366	-204293	-89550	1945	-271813	-1009120	3104403	19289

Figure 4.1. Crop production status regarding balanced nutritional requirement per year.

4.1.2. Suitability of land for a range of crops

In different locales, the F-MCDM model identified viable locations for different crops in the Kharif-1, Kharif-2 and Rabi seasons (Figure 4.2 (a-r)). The extremely favorable region for Aus rice was determined to be 30.9 percent in the Kharif-1 season (Figure 4.2.(d)), whereas the acceptable area for vegetables was 50 percent (Figure 4.2. (b)). For grains and vegetables, the unsuitable area was determined to be 25.5 percent and 17 percent, respectively (Table 4.1). The very appropriate region for the local variety of Aman rice (Figure 4.2. (h)) was roughly 5% smaller than the highly appropriate region for vegetables (Figure 4.2(f)) according to the Kharif-2 season's data. In the Kharif-2 season, a fairly appropriate region was identified as 34.6 percent for rice and 22 percent for vegetables. For Aman rice, the unsuitable area appeared to be 46.5 percent.

Similarly, outcomes for the five types of crops cultivated in the Rabi season varied depending on whether the location was extremely (S1), moderately (S2), marginally (S3) or not appropriate (N). Boro rice grew in 47 percent of the very appropriate region (Figure 4.2 (r)). In the Rabi cropping season, the extremely favorable zone for winter vegetables was determined to be 40% (Figure 4.2. (j)), while the not appropriate zone was found to be 16.5 percent. Throughout the northeastern portion of the research area seemed to be a favorable zone for pulse (Figure 4.2.(n)) cultivation; the extremely favorable area in this region encompassed 43 percent. Furthermore, 20 percent of the time, marginal and unsuitable regions were discovered. The percentage of very appropriate places for producing carbohydrate-based vegetables (potatoes) (Figure 4.2 (l)) was determined to be 19 percent, with the majority of them being in the research area's northern half. Furthermore, a scattered suitable area for oilseed cultivation was discovered, which covered parts of the northern and western regions; highly, moderately, marginally and not suitable areas for growing oilseeds were found at 16 percent, 17 percent, 9 percent and 58 percent, respectively (Figure 4.2. (p)).

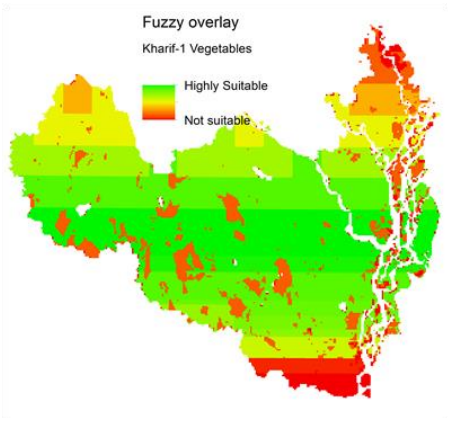
Fuzzy overlay
Kharif-1 Vegetables
Highly Suitable
Not suitable

(a)

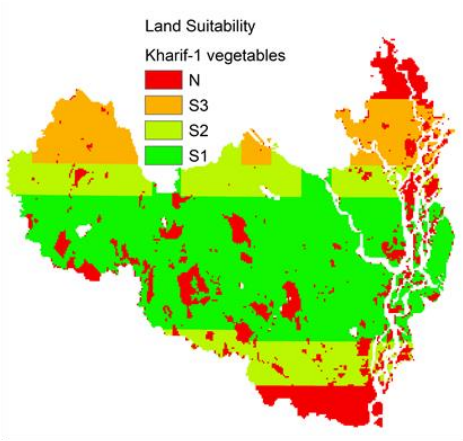
Land Suitability
Kharif-1 vegetables
N
S3
S2
S1

(b)

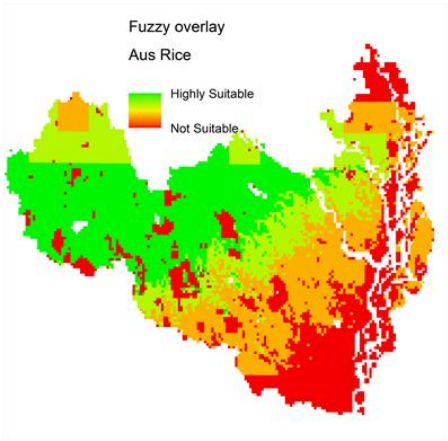
Fuzzy overlay
Aus Rice
Highly Suitable
Not Suitable

(c)

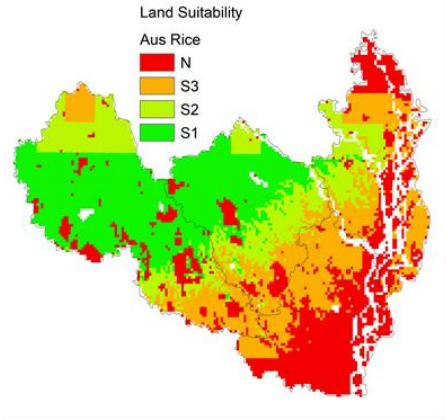
Land Suitability
Aus Rice
N
S3
S2
S1

(d)

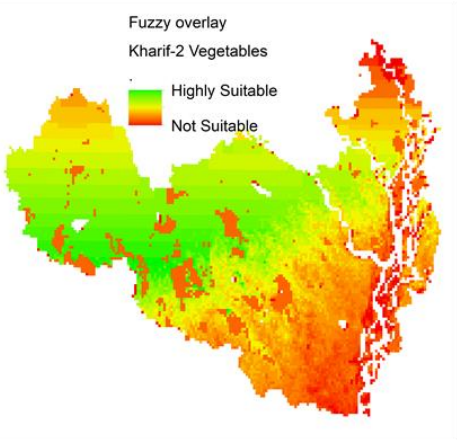
Fuzzy overlay
Kharif-2 Vegetables
Highly Suitable
Not Suitable

(e)

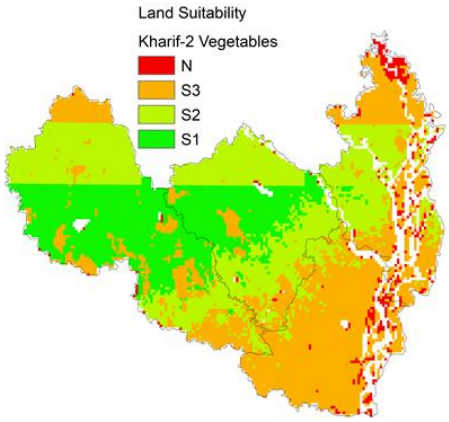
Land Suitability
Kharif-2 Vegetables
N
S3
S2
S1

(f)


N
W
E


0
10
20
40 Kilometers

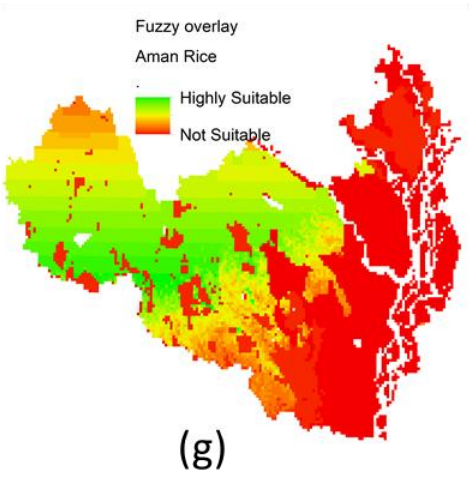
Fuzzy overlay
Aman Rice
Highly Suitable
Not Suitable

(g)

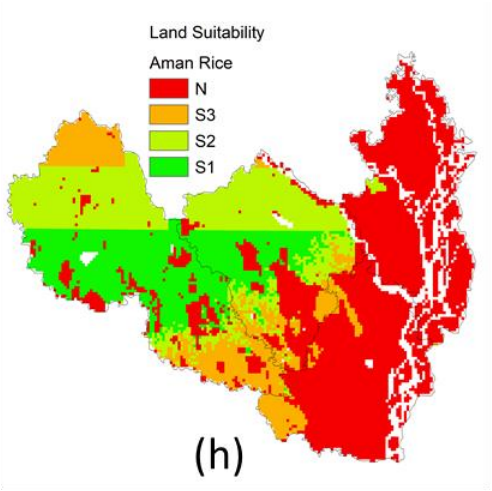
Land Suitability
Aman Rice
N
S3
S2
S1

(h)

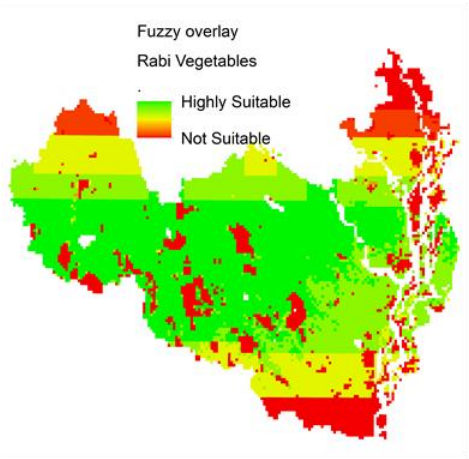
Fuzzy overlay
Rabi Vegetables
Highly Suitable
Not Suitable

(i)

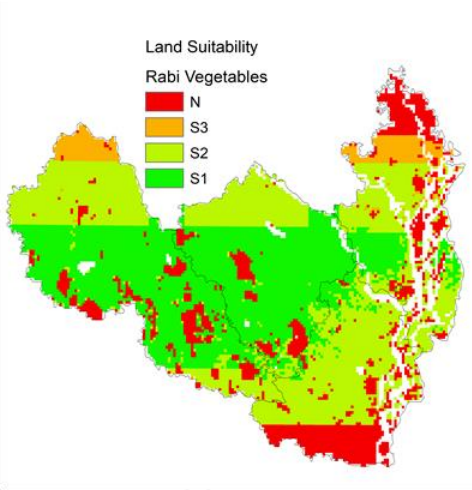
Land Suitability
Rabi Vegetables
N
S3
S2
S1

(j)

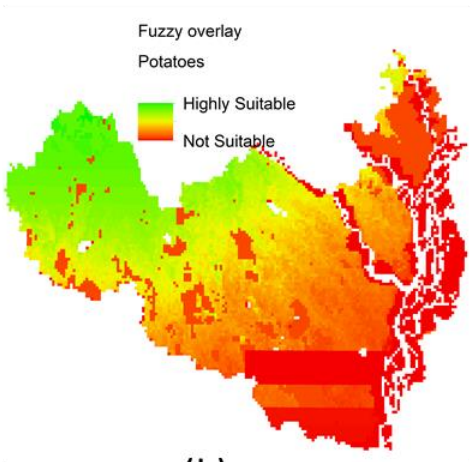
Fuzzy overlay
Potatoes
Highly Suitable
Not Suitable

(k)

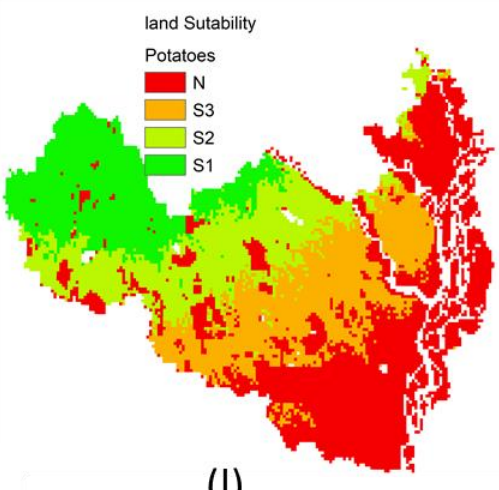
land Sutability
Potatoes
N
S3
S2
S1

(l)


N
W
E


0
10
20
40 Kilometers

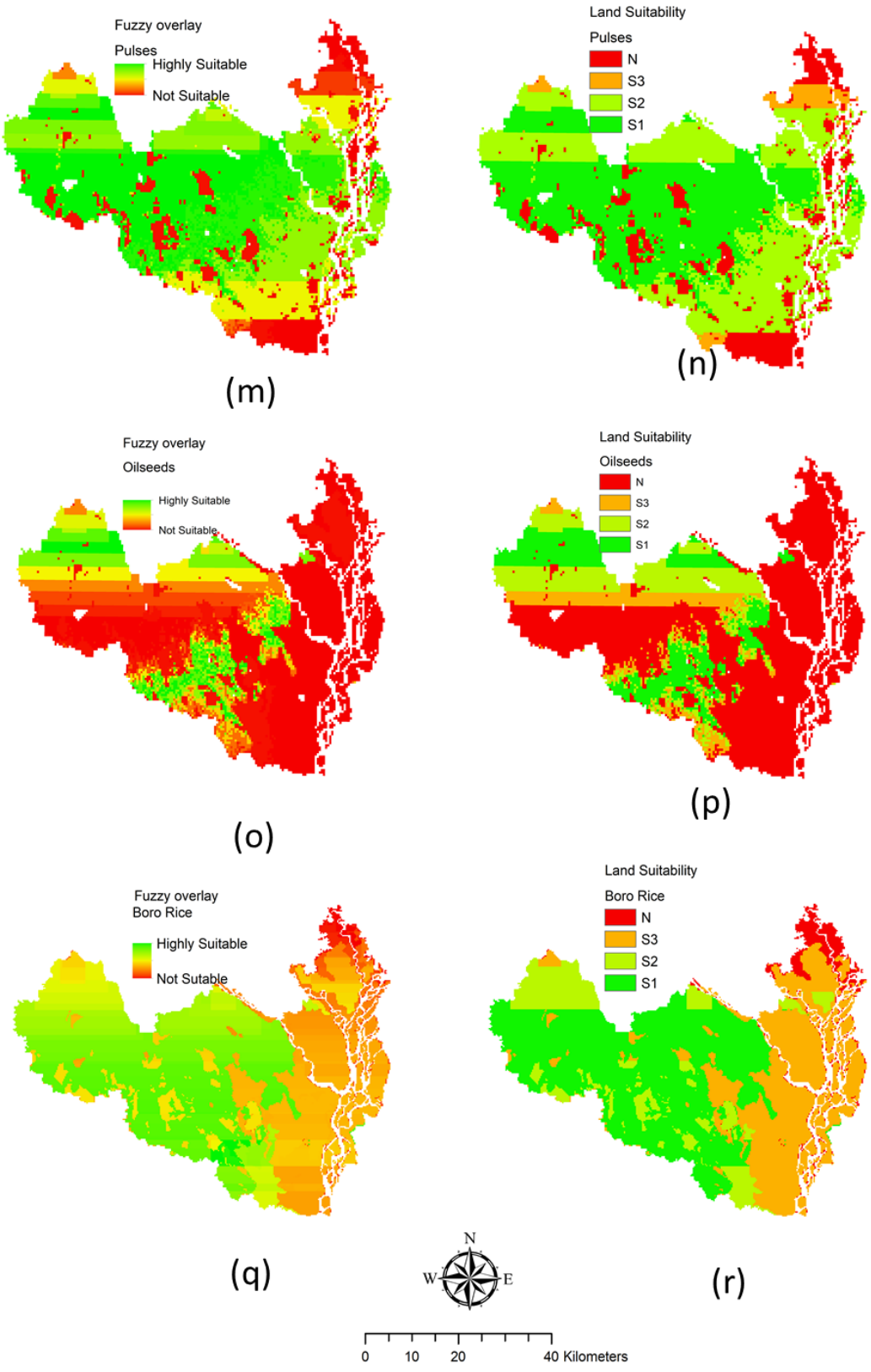

Figure 4.2. Land suitability map: (a, b) Kharif-1 vegetables; (c, d) Kharif-1 Aus rice; (e, f) Kharif-2 vegetables; (g, h) Kharif-2 Aman rice; (i, j) Rabi vegetables; (k, l) potatoes; (m, n) pulses; (o, p) oilseeds; (q, r) Boro rice.

Table 4.1. Results of land suitability analysis of diversified crops.

Suitability classes	K1 rice Areas (km²)	K1 vegetables Areas (km²)	K2 rice Areas (km²)	K2 Vegetables Areas (km²)	Rabi rice Areas (km²)	Rabi vegetables Areas (km²)	Pulses Areas (km²)	Potatoes Areas (km²)	Oilseeds Areas (km²)
Highly Suitable (S1)	3745 (30.9%)	4130 (50 %)	1569 (19%)	1999 (24.2%)	3887.9 (47%)	3304 (40%)	3551 (43%)	3279 (19%)	1321 (16%)
Moderately Suitable (S2)	2298 (19%)	1555 (20.6 %))	1817 (22%)	2458 (34.6%)	11564 (14%)	3221 (39%)	3056 (37%)	1784.2 (19.7%)	1404 (17%)
Marginally suitable (S3)	2979 (24.6%)	1024 (12.4%)	1032 (12.5%)	3138 (38%)	2849.7 (34.5%)	371 (4.5%)	330 (4%)	1627.2 (21.6%)	743 (9%)
Not Suitable (N)	3094 (25.5%)	1404 (17%)	3840 (46.5%)	264 (3.2%)	364.3 (4.5%)	1362 (16.5%)	1321 (16%)	15694 (39.7%)	4790 (58%)

4.1.3. Land adaptability for multiple crops in season

Triple-cropping suitability maps depict separate appropriate zones by combining the individual crops of each season. The calorie ratio was used with seasonal appropriateness studies to create three distinct Kharif-1, Kharif-2 and Rabi season appropriate maps. The research region was obscured by the SOB's land use maps, which were created using agricultural land practices to create three seasonal maps. Restricted regions, such as rivers, villages and woods were not aggregated for the final output or area computation and displayed on the maps as a white hue. (Figure 4.3).

The Kharif-1 calorie-based distribution map reveals that the most appropriate region for vegetable production makes up 42 percent (3469 km2) of the land area (Figure 4.3 (a)). When it came to rice, 20 percent (1652 km2) of the land area was ideal. Furthermore, 21% of the area was identified as appropriate for cultivating both crops. Rice-growing regions were largely found in the northern sections of Dinajpur and Rangpur districts as well as some western sections of Kurigram. Vegetable-growing regions were largely found in the research area's center section, which includes the Gaibandha and Kurigram districts. Summer vegetable production was also advocated in the southern portions of two districts, Dinajpur and Rangpur. Rice and vegetables may both be grown in this typical appropriate region. This area, however, can be utilized for rice and certain cereal crop production, as per the balanced calorie suggestion. The rice growing zone was largely the northern sections and certain distinct sections of the four districts, according to the local agricultural practices of the Kharif-1 season map. However, a highly encouraging result was discovered, with just 12 percent (991 km2) of the land suitable for vegetable production (Figure 4.3. (b)). In the Kharif-1 season, fallow land accounted for 45 percent of the total area utilized (Table 4.2.).

In the following season, Kharif-2, mostly two types of crops, Aman rice and vegetables, are planted. According to the Kharif-2 map, 55 percent of the land and 35 percent of the land are best suited for vegetables and rice respectively (Figure 4.3.(c)). 6 percent (495 km2) of the land was reasonably suited for rice and vegetables. Four percent of the total land area was unsuitable for rice and vegetables. Kurigram and Gaibandha districts have the most appropriate vegetable-growing land. Rice-growing areas were mostly found in the districts of Dinajpur and Rangpur. Figure 4.3.(d) shows that now, 57 percent of the land is used for rice growing and 18 percent for vegetable production. During the Kharif-2 season, 21% of the land was declared barren (Table 4.4).

In the Rabi season, Boro rice and cereals, winter vegetables, carbohydrate-based vegetables (potatoes), pulses and oilseeds were among the crops grown on the site (Figure 4.3 (e)). The seasonal suitability map revealed that the most favorable locations for cereal crops, vegetables, pulses, oilseeds, and potatoes were 35% (2891 km²), 19% (1569 km²), 15% (1239 km²), 10% (826 km²), and 21% (1734 km²) of the land respectively. The Kurigram and Gaibandha districts have the most favorable areas for carbohydrate-based and non-carbohydrate-based veggies. In the four districts of the research region, land suitable for cereal crops was clearly visible. The oilseed growing region was mostly found in the Dinajpur and Rangpur districts' northern areas. Figure 4.3 (f) depicts the farming practices during the Rabi season, which revealed that grain crops were grown on 45 percent of the farmland (3717 km²). In addition, pulses and oilseeds were planted on 21% of the land. Only 4% (330 km²) of the land was utilized for non-carbohydrate vegetable production, whereas 18% of the land was utilized for potato production (Table 4.5).

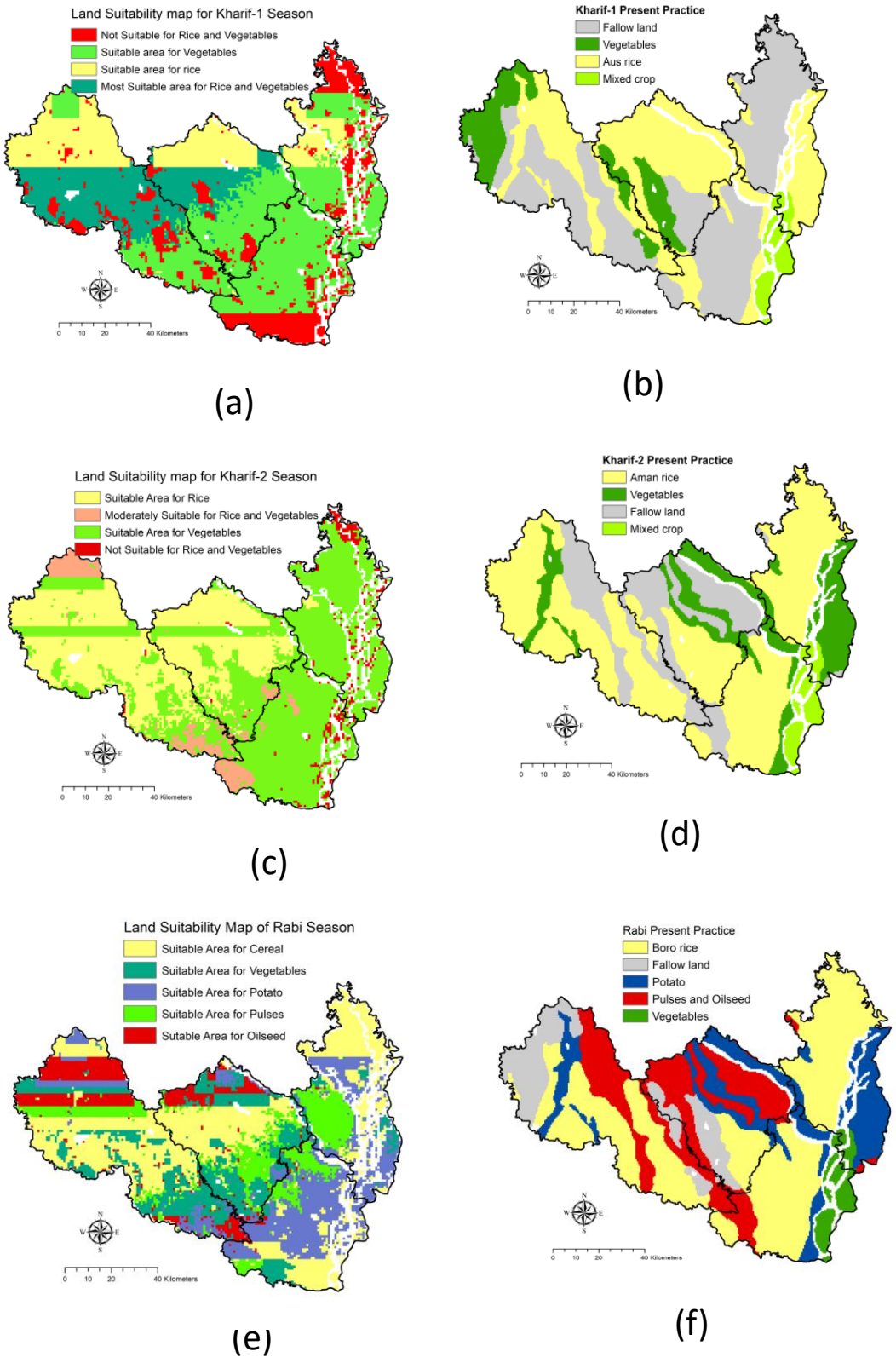

Figure 4.3. Suitable zoning for seasonal crop growing: (a) Kharif-1 season land suitability map; (b) Kharif-1 present practice map; (c) Kharif-2 land suitability map; (d) Kharif-2 present practice map; (e) Rabi season land suitability map; and (f) Rabi present practice map.

Table 4.2. Comparison between the present practice and the suitable area of the Kharif-1 season.

Criteria.	**Present practice**		**Suitability zoning**	
	Area (%)	Areas (km²)	Area (%)	Areas (km²)
Cereal	39	3221	20	1652
Vegetables	12	991	42	3469
Mixed crops	4	330	21	1734

Table 4.3. Comparison between the present practice and the suitable area of the Kharif-2 season.

Criteria	**Present practice**		**Suitability zoning**	
	Area (%)	Areas (km²)	Area (%)	Areas (km²)
Cereal	57	4708	35	2891
Vegetables	18	1487	55	4543
Mixed crops	4	330	6	495

Table 4.4. Comparison between the present practice and the suitable area of the Rabi season

Criteria	**Present practice**		**Suitable zoning**	
	Area (%)	Areas (km²)	Area (%)	Areas (km²)
Cereal	45	3717	35	2891
Vegetables	4	330	19	1569
Pulses & Oilseed	21	1735	15+10	1239+826
Potatoes	18	1486	21	1734

4.2. Land Use Plan Evaluation

4.2.1. Land fertility assessment

To construct the land fertility evaluation, the weighted linear model was utilized to evaluate the weights of each criterion. First, the variables were analyzed as equally weighted linear combinations. Second, the fertility assessment was carried out by a fuzzy membership function to verify the consistency of the two procedure results (Table 4.5). The land fertility analysis (Figure 4.4 (a)) with equal weights showed that 43% of the land (1832 km^2) was highly suitable, 41% of the land (1747 km^2) was moderately suitable and 10% of the land (426 km^2) was marginally suitable. In addition, the restricted zone was defined as an unsuitable area. In this research, the unsuitable area was found to cover 6% (256 km^2). Nevertheless, using the fuzzy membership method to analyze land suitability (Figure 4.4 (b)), it was discovered that 48% (2045 km^2) of the land area consisted of the most suitable area, 39% of the land (1661 km^2) was moderately suitable and 7% of the land (298 km^2) was marginally suitable. In addition, restricted areas accounted for 6% of the land area. In fuzzy overlay analysis, 256 km^2 of the area was classified as fallow land that is not suitable for cultivation.

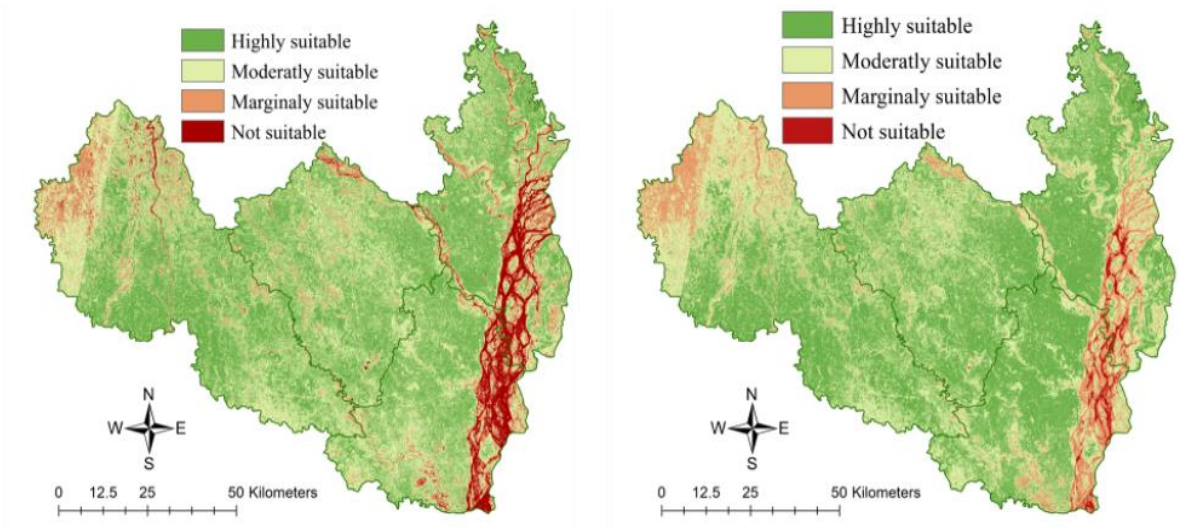

(**a**) Equal weighted overlay. (**b**) Fuzzy overlay.

Figure 4.4. Suitable land fertility evaluation classes based on soil-specific satellite imagery

Table 4.5. Percentage and area of each land fertility classification.

Classification	Fertility assessment by Equal-weighted linear combination		Fertility assessment by Fuzzy	
	Percentage Area (%)	Area (km^2)	Percentage Area (%)	Area (km^2)
Highly Suitable (S1)	43	1832	48	2045
Moderately Suitable (S2)	41	1747	39	1661
Marginally Suitable (S3)	10	426	7	298
Not Suitable (N)	6	256	6	256

4.2.2. Yield Prediction

The most efficient spectral parameters for forecasting rice yield were those generated from satellite imaging in the form of spectral bands or vegetation indices (SAVI, SAVI, ARVI, SARVI, MSAVI and OSAVI). Furthermore, the individual index values for the subdistricts were derived from the ground truth data (Figure 4.5.) that were in the highly suitable areas. The index impacts were verified using a trend line methodology at several research points. The vegetation indicators and the measured yield were put through a regression analysis. Satellite imagery from 2017 to 2020 was used to calculate the SAVI, SARVI, ARVI, MSAVI and OSAVI values (Table 4.6.). The results showed good accuracy in the regression analysis using SAVI (R^2 = 77.3%), ARVI (R^2=68.9%), SARVI (R^2=71.1%), MSAVI (R^2=74.5%) and OSAVI (R^2=81.2%) (Figure 4.6. and Figure 4.7.). Using more than one variable for yield prediction improves model accuracy by increasing the R^2 value, according to the multiple regression model. The SAVI-ARVI-SARVI-MSAVI-OSAVI composite vegetation index, on the other hand, yielded the best-fitting models. The yield prediction model with the composite index had a goodness of fit of R^2 = 0.839. The model was used to estimate the yield in the time series dataset (Table 4.7.).

The developed yield map indicated that, in 2017, the maximum yield was 4.59 MT/ha. Furthermore, in 2018 and in 2019, it was 4.9 MT/ha and 5.08 MT/ha respectively. For 2020, the predicted yield range appeared to be between 0.269 MT/ha and 4.537 MT/ha (Figure 4.8).

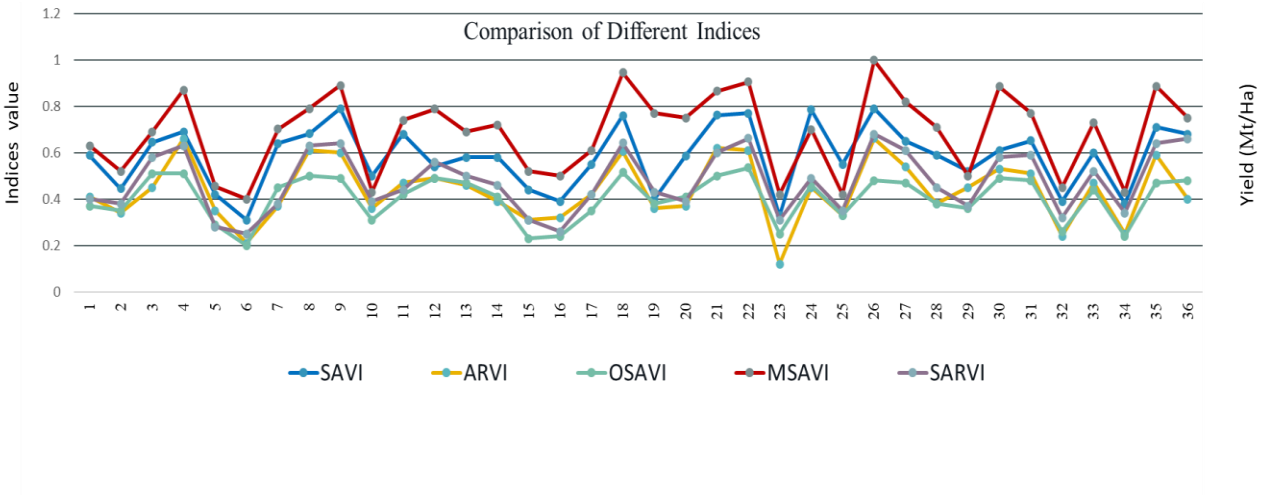

Figure 4.5. Rice yield distributions in the 36 subunits using ground reference data.

Table 4.6. Yield estimation based on satellite remote sensing derived soil-vegetation indices for the 36 subunits.

No	Name	Longitude	Latitude	SAVI	ARVI	SARVI	MSAVI	OSAVI	Yield
1	Rangpur Sadar	89°12’38.681” E	25°45’19.004” N	0.588	0.41	0.37	0.63	0.40	4.03
2	Badarganj	89°3’3.041” E	25°40’31.185” N	0.445	0.34	0.35	0.52	0.38	3.96
3	Kaunia	89°23’36.554” E	25°46’41.239” N	0.644	0.45	0.51	0.69	0.58	4.26
4	Gangachhara	89°12’52.386” E	25°51’42.764” N	0.69	0.66	0.51	0.87	0.63	4.37
5	Mithapukur	89°15’9.443” E	25°35’2.248” N	0.42	0.35	0.29	0.45	0.28	3.38
6	Taraganj	89°1’54.513” E	25°46’54.944” N	0.31	0.21	0.20	0.40	0.25	2.89
7	Pirganj	89°16’17.972” E	25°25’40.315” N	0.64	0.37	0.45	0.701	0.38	4.19
8	Pirgachha	89°24’58.788” E	25°40’31.185” N	0.681	0.61	0.50	0.79	0.63	4.34
9	Dinajpur Sadar	88°40’39.883” E	25°36’38.188” N	0.79	0.60	0.49	0.89	0.64	4.40
10	Birampur	88°58’15.222” E	25°22’55.846” N	0.50	0.36	0.31	0.43	0.39	3.94
11	Biral	88°32’53.89” E	25°38’55.245” N	0.68	0.47	0.42	0.74	0.44	4.20
12	Phulbari	88°53’27.402” E	25°27’2.549” N	0.54	0.49	0.49	0.78	0.56	4.25
13	Hakimpur	89°2’49.336” E	25°17’13.204” N	0.579	0.46	0.47	0.69	0.50	4.23
14	Khansama	88°45’55.114” E	25°52’51.292” N	0.58	0.39	0.41	0.72	0.46	4.16
15	Nawabganj	89°5’33.804” E	25°25’12.903” N	0.44	0.31	0.23	0.52	0.31	3.69
16	Parbatipur	88°55’44.459” E	25°37’19.305” N	0.39	0.32	0.24	0.50	0.26	3.60
17	Birganj	88°37’28.004” E	25°56’3.172” N	0.55	0.42	0.35	0.61	0.42	4.08
18	Kaharole	88°35’38.358” E	25°48’17.178” N	0.76	0.60	0.51	0.94	0.64	4.50
19	Chirirbandar	88°47’3.643” E	25°40’31.185” N	0.40	0.36	0.38	0.77	0.43	4.10
20	Ghoraghat	89°12’52.386” E	25°17’26.91” N	0.59	0.37	0.41	0.75	0.39	4.16
21	Bochaganj	88°26’43.836” E	25°47’22.356” N	0.761	0.62	0.50	0.86	0.60	4.35
22	Kurigram Sadar	89°41’39.304” E	25°49’39.413” N	0.77	0.61	0.54	0.91	0.66	4.50
23	Phulbari	88°53’27.402” E	25°27’2.549” N	0.33	0.12	0.25	0.42	0.31	3.06
24	Nageshwari	89°44’37.478” E	25°58’6.523” N	0.79	0.45	0.46	0.70	0.49	4.20
25	Rajarha	89°32’44.782” E	25°47’8.65” N	0.55	0.33	0.33	0.42	0.35	3.90
26	Bhurungamari	89°41’39.304” E	26°7’1.045” N	0.79	0.66	0.48	0.99	0.67	4.50
27	Ulipur	89°40’3.364” E	25°40’58.596” N	0.65	0.54	0.47	0.82	0.61	4.30
28	Char Rajibpur	89°45’4.889” E	25°30’55.546” N	0.59	0.38	0.38	0.71	0.45	4.10
29	Rowmari	89°49’11.592” E	25°33’53.72” N	0.52	0.45	0.36	0.50	0.37	4.02
30	Gaibandha Sadar	89°34’48.133” E	25°57’11.701” N	0.61	0.53	0.49	0.88	0.58	4.30
31	Gobindaganj	89°22’0.614” E	25°10’8.327” N	0.65	0.51	0.48	0.77	0.59	4.28
32	Palashbari	89°23’22.848” E	25°16’18.381” N	0.39	0.24	0.26	0.45	0.32	4.34
33	Fulchhari	89°39’35.953” E	25°15’37.264” N	0.60	0.47	0.44	0.73	0.52	4.24
34	Saghatta	89°34’34.427” E	25°7’37.565” N	0.38	0.25	0.24	0.43	0.34	3.27
35	Sadullapur	89°25’12.494” E	25°24’4.375” N	0.71	0.59	0.47	0.88	0.64	3.34
36	Sundarganj	89°33’39.605” E	25°30’28.134” N	0.68	0.4	0.48	0.75	0.66	4.31

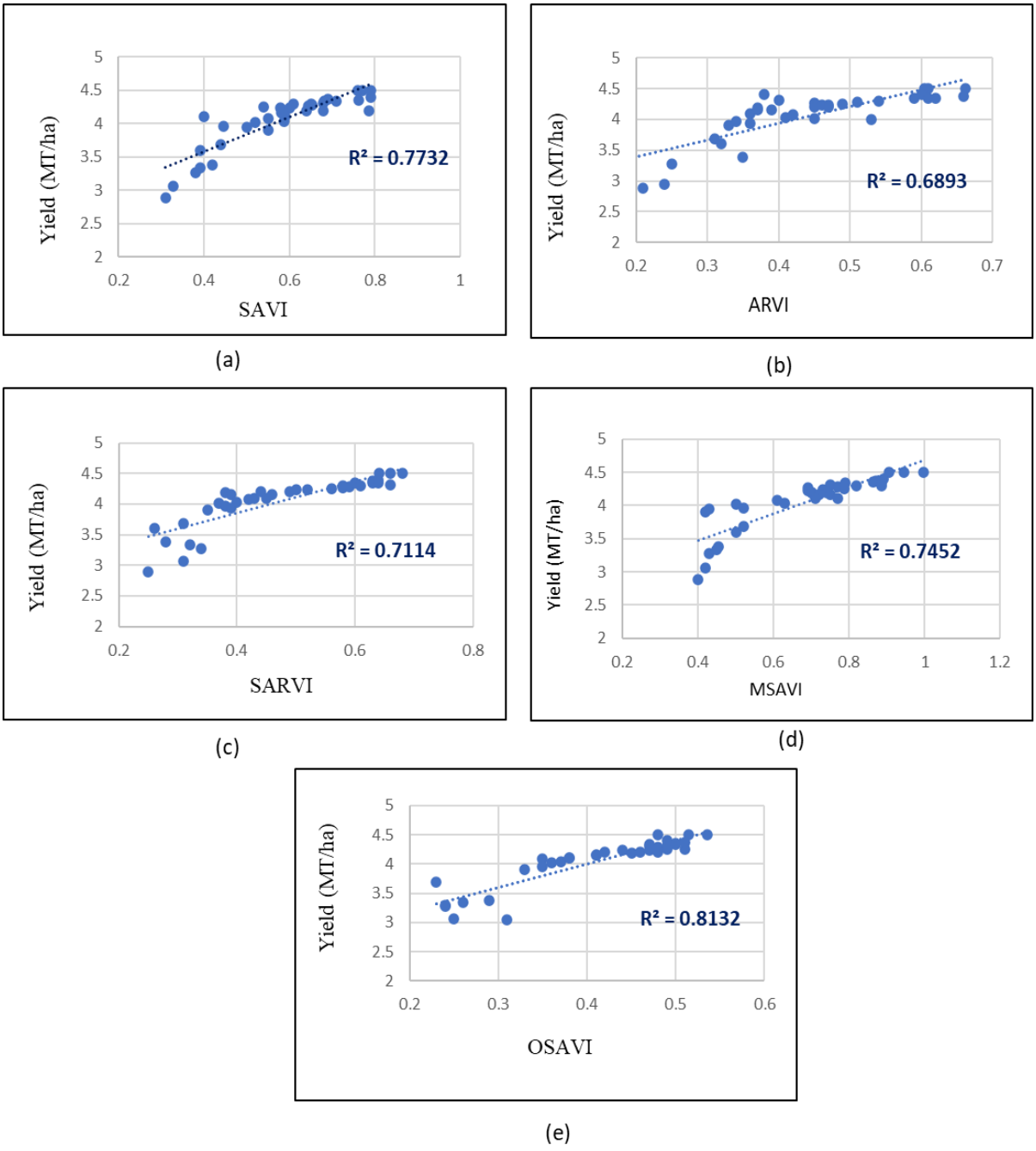

Figure 4.6. Regression analysis (a) SAVI; (b)ARVI; (c) SARVI; (d) OSAVI and (e) MSAVI for vegetation indices and ground reference time series yield information.

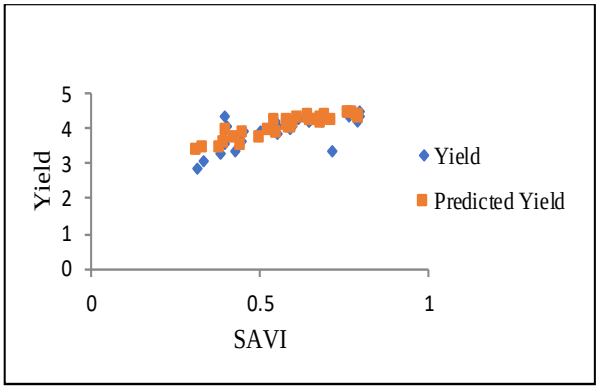

(a)

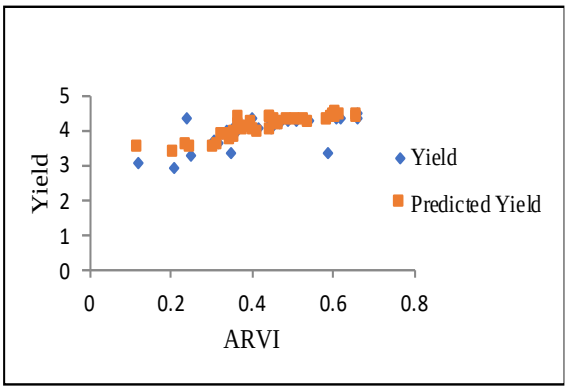

(b)

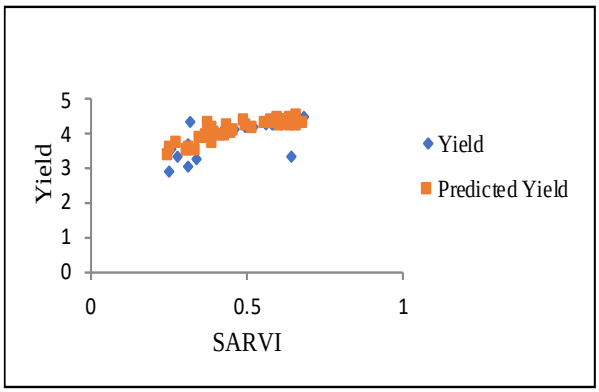

(c)

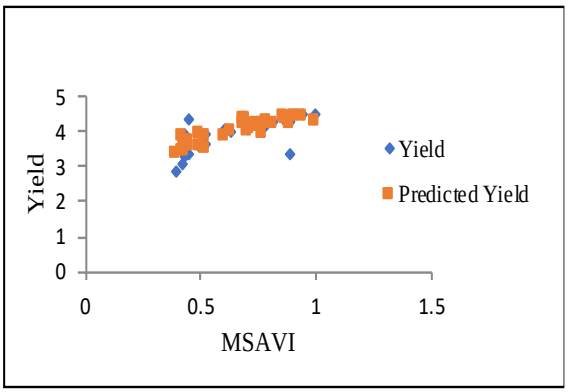

(d)

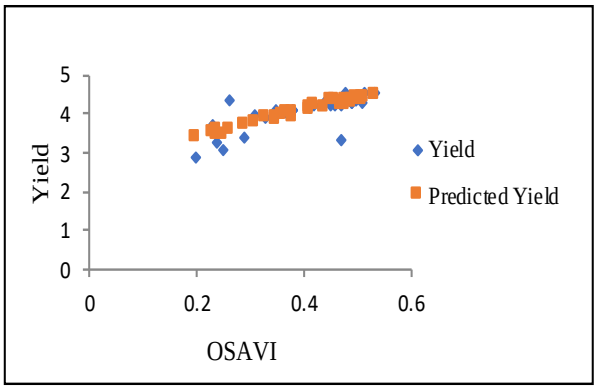

(e)

Figure 4.7. Comparison of actual yield and predicted yield for different indices (a) SAVI; (b)ARVI; (c) SARVI; (d) OSAVI and (e) MSAVI.

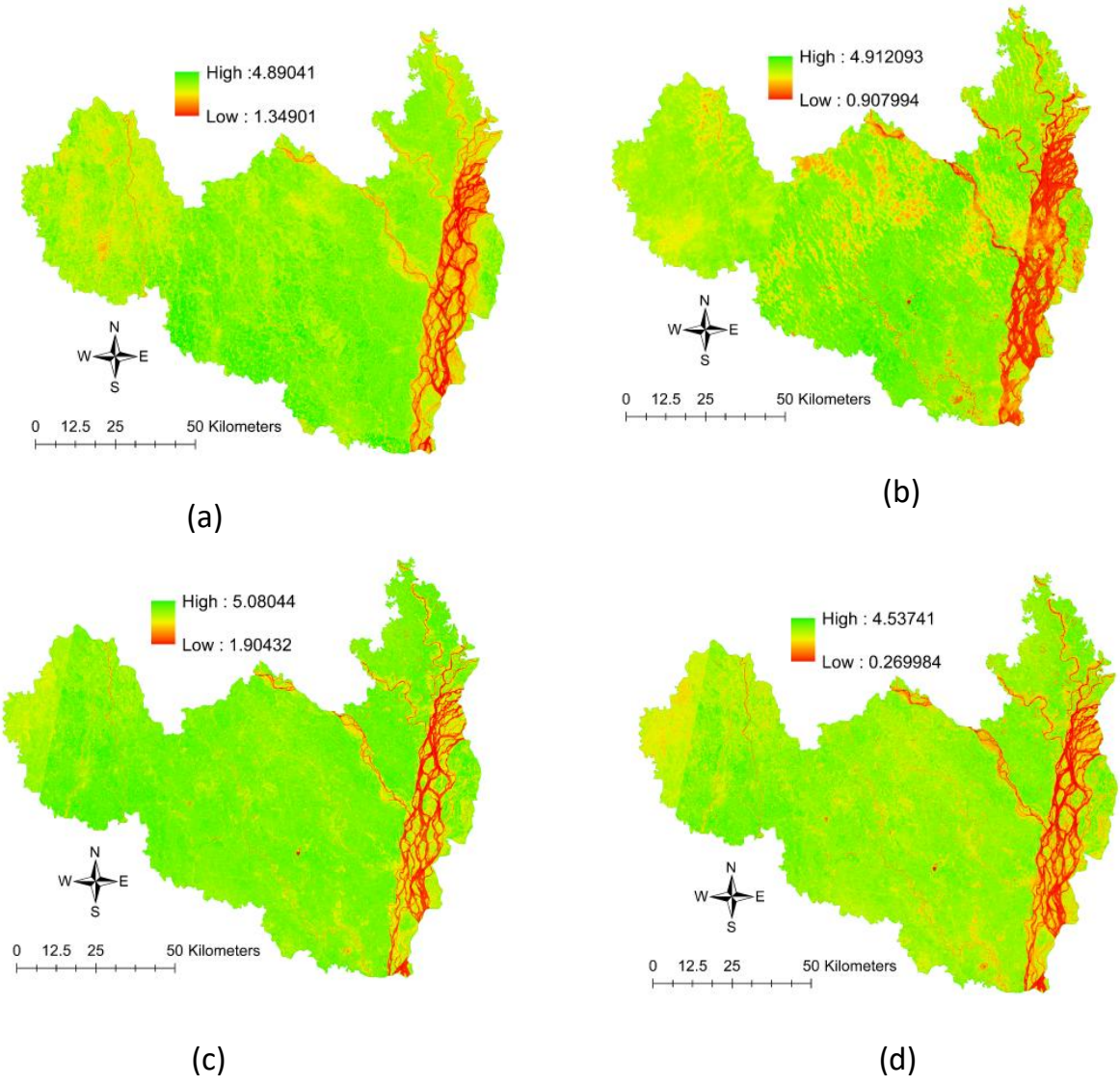

Figure 4.8. Yield prediction map (MT/ha) (a) 2017; (b) 2018; (c) 2019 and (d) 2020.

Table 4.7. Yield prediction models based on satellite remote sensing derived soil-vegetation indices.

Forecasting factors	R^2	Simple regression
SAVI	0.773	Y= 2.6021* SAVI+ 2.5319
ARVI	0.689	Y= 2.726 *ARVI + 2.8479
SARVI	0.711	Y= 2.5832* SARVI + 2.8184
MSAVI	0.745	Y= 2.024* MSAVI + 2.6627
OSAVI	0.812	Y= 4.0094 *OSAVI + 2.4039
All Combination	0.839	Y= 0.534* SAVI + 0.226 *ARVI - 0.907 *SARVI + 0.0922 * MSAVI + 3.264 * OSAVI

4.3 Discussion

This study has produced a thorough technique for developing agricultural land use plans for a variety of seasonal crops while taking calorie demand into account. Previously, much of the study focused on the suitability of land for site-specific or single-cropping programs (Noorollahi et al., 2016, Sulaiman et al., 2019). This study, on the other hand, tried to create season-based multicrop land suitability maps. Another challenge that necessitated a new level of land suitability study was preparing a seasonal map utilizing balanced, calorie-rich crops. Throughout this research, statistical data mining was utilized to assess regional calorie demand and balanced nutrition circumstances, and the results were utilized as a weight for land use map development, resulting in higher performance in land use planning. This finding added to the evidence that the advice to promote food nutrition security is sound.

Most studies use either the AHP-based weighted overlay or the equal-overlay technique (Islam et al., 2018, Seyedmohammadi et al., 2019, Pilevar et al., 2020, Tashayo et al., 2020); few studies using fuzzy membership methods in the GIS platform use the AHP technique (Seyedmohammadi et al., 2019, Pilevar et al., 2020, Tashayo, 2018), However, employing the F-MCDM technique to create seasonal, varied crop suitability maps is a new development in this study. Individual suitability maps, on the other hand, were created to assess the same appropriate zones of several crops. To decrease biases in land suitability evaluation, a multicriteria decision-making approach was used. Seasonal temperature variation was one of the most important aspects in this area, influencing the best places for agricultural development. Remote sensing data are essential for land suitability analysis since they help to classify the growth regions of each crop as suitable or not appropriate.

Crop production statistics compared to nutritional requirements indicated the rice-based prevalent farming method in the research area. With the recently created patterns, such departures from "ideal

crop production patterns" were identified. As a result, the people of the nation feel that if they can cultivate enough rice, the country would not experience food insecurity; nevertheless, this thought has generated a new challenge in terms of food nutritional adequacy. Now, the study's major focus is not just food security, but also ensuring Bangladesh's food nutrition security.

In terms of seasonal land planning, a diversified production plan was devised, which included current techniques and a crop calendar based on locally grown crops. Kharif-1, Kharif-2 and Rabi were the three seasons studied. In the Kharif-1 season, 42 percent (3469 km^2) of land was suggested for vegetable production, up from 12 percent (991 km^2) prior. The vegetable-growing area was identified to be 55 percent (4543 km^2) in the Kharif-2 season, compared to 18 percent in the previous season. The land area suitable for growing vegetables in the next season was 4%, while this study found 19% (1569 km^2) as appropriate of land as suitable for cultivating vegetables. Additionally, this recommendation was also shown in the Rabi season; 25% (2065 km^2) of suitable land was detected for pulse and oilseed cultivation, although this area was only 21% earlier. This study only looked at agricultural land, which is a constraint for constructing a planning model. Furthermore, the suggested seasonal maps do not include spices, fruits, or molasses/sugars. Furthermore, dairy products were not taken into account in current study. This planning technique contributes to a food security rate of 81.5 percent.

Furthermore, this study offered a complete technique for developing agricultural land use plans for cultivation that took into account fertility conditions generated from satellite remote sensing data. However, this research attempted to develop an overall land fertility assessment using soil-vegetation representative variables that extracted only satellite remote sensing data when field soil sampling is inconvenient and expensive. Applying only remote satellite datasets to assess suitable land conditions was a source of concern that added a new dimension to land fertility analyses. In this study, the reliability of five vegetation indices was verified by a regression analysis that incorporated ground truth yield data, and the results were used for yield map preparation. Vegetation phenology analyses have potential (Das et al., 2020; Habibie et al., 2019) in estimating yield prediction with good accuracy in highly suitable areas. In addition, two main topological factors (slope and elevation) and one main environmental parameter, land surface temperature were extracted from the USGS which ensured better performance of the results in land use planning. The combined model represented the batter result.

Variation in the land surface temperature was a dominant factor in this area and influenced the locations considered most suitable for crop cultivation. Moreover, atmospherically restricted vegetation indices (ARVI) and soil adjusted atmospherically restricted vegetation indices (SARVI) were used to reduce the biases associated with atmospheric effects.

The fertility evaluation shows Most of the suitable lands were located in the northern part, and marginally suitable lands were mostly located in the northwestern part; this result was likely due to the influence of high elevation. In addition, unsuitable zones were found mostly in the eastern part due to

the presence of water bodies that are not arable for cultivation along with other adverse edaphic factors. Previous studies had the limitation of obtaining inappropriate validation results due to inadequate ground reference information. In this research, validation of the results was accomplished by physical verification with the corresponding time series yield data of the most cultivated crop, dry season irrigated rice, which usually grows over 70% (Zinat et al., 2020) of the agricultural land area. The suitable conditions were not verified by the other crop yield data, which was the main limitation of this research.

Furthermore, the goal of this study was to construct a nutritionally diverse crop production system that included vegetables, cereals, pulses and oilseeds. The research area was at risk due to imbalance food consumption habits. As a result, the research hypothesis was to develop a technique to promote varied food (nutritive) cultivation while also increasing consumption. In this case, land suitability study identified a good place for the suggestion of locally suited produced crops. Unfortunately, the research was limited by its financial evaluation, which was insignificant in view of food nutrition security. To distribute economic analysis, further study is required. Furthermore, the farmers and residents in the research region are unaware of the existence of chain stores. The majority of agricultural goods are usually sold on the local market. Due to a shortage of transportation, post-harvest losses are considerably higher. In the current planning model, the production values of different crops were translated into equivalent units by assuming that all agricultural produced was consumed without being traded or abused.

Chapter V

Conclusions and Recommendations

5.1. Conclusions

This study focused not only on food security in Southeast Asia, but also on guaranteeing food nutrition security. Bangladesh has the most nutritionally deficient diets in all of Southeast Asia. As a result, the purpose of this study was to undertake a seasonal land suitability analysis for land use planning utilizing nutritious proportions from cereals, vegetables and pulses. Land suitability maps for the Kharif-1, Kharif-2 and Rabi seasons were developed using high-resolution vector and satellite remote sensing datasets that took into account the geographical expanse. Furthermore, using a GIS platform to create seasonal land suitability maps with a balanced food demand ratio yielded more accurate results. The geographic distributions of different crops were clearly exposed using remote sensing data in combination with the assessment of biophysical soil factors in this study. In the context of a GIS, topographic data might be useful for crop management decisions such as intensification or diversification.

5.1.1. Seasonal land use plan

The outcomes of the seasonal maps were compared to current agricultural practices: appropriate land for vegetable cultivation was discovered in the Kharif-1 (42%), Kharif-2 (55%) and Rabi (19%) seasons. In terms of calorie-based land use planning, an additional 30% of land can be used in the Kharif-1 season, an additional 37% of land can be used in the Kharif-2 season and an additional 15% of land can be used in the Rabi season; vegetable crops have the potential to expand agricultural land use beyond current practices. Furthermore, 25 percent of eligible land for pulses and oilseeds was identified, which might be employed for cultivation based on the research area's local need. To aid in the accuracy evaluation, the land use layer from the SOB was used to uncover the agricultural land. The F-MCDM techniques and the proposed seasonal land suitability maps based on the nutrition demand validated the good outcomes of land use planning. Finally, a nutrition assessment will aid in the formulation of policy recommendations for land use planning in the next years, which is a critical problem in terms of food nutrition security in developing nations.

5.1.2. Land fertility evaluation

This research established a method to identify the land fertility evaluation by using the potentiality of satellite remote sensing data integrated fuzzy expert system. The multicriteria decision analysis was performed for fertility assessment using eight criteria: elevation, slope and LST vegetation indices

(SAVI, ARVI, SARVI, MSAVI and OSAVI). To derive a more accurate result, a land use/land cover layer was also used to mask restricted zones. The land suitability analysis with equal weights showed that 43% of the land (1832 km^2) was highly suitable, 41% of the land (1747 km^2) was moderately suitable and 10% of the land (426 km^2) was marginally suitable. Conversely, expert knowledge was also considered, along with consistent assessments when using the fuzzy membership function; 48% of the land (2045 km^2) was highly suitable, 39% of the land (2045 km^2) was moderately suitable and 7% of the land (298 km^2) was marginally suitable. The yield estimation using SAVI (R^2 = 77.3%), ARVI (R^2=68.9%), SARVI (R^2=71.1%), MSAVI (R^2=74.5%) and OSAVI (R^2=81.2%) showed a good accuracy. In addition, every combination of these five indices represented the best accuracy (R^2 = 0.839), which was used to develop the yield maps for the corresponding years (2017-2020). The results of the land fertility evaluation method for land crops will be very useful in the decision-making process to boost production as well as for the sustainable management of agricultural lands. Thus, the influence of vegetation index evaluations, fertility assessments and yield prediction models is essential for understanding future land use and production trends in the agricultural crop sector in Bangladesh as well as other applications.

The proposed seasonal planning strategy contributes to a food nutrition security rate of 81.5 percent. Our future plan is to present a machine learning method-based inventory planning model to ensure overall regional self-sufficiency to overcome the limitation of this research.

5.2. Recommendations

From the viewpoint of this research, the following suggestions have been made:

- The calorie-distributed seasonal land-use plan could be helpful to diminish food nutrition insecurity for Bangladesh and as well as south Asian countries.
- Satellite data especially Landsat 8 OLI datasets could be a helpful and convenient method for land fertility evaluation for the policymaker.
- SAVI, ARVI, SARVI, MSAVI, MSAVI based combined yield prediction model shows the more accurate result for crop yield estimation.

Acknowledgements

First, I am grateful to The Almighty God for helping me to complete my Doctoral research at the University of Tsukuba. In this extend, I would like to express the deepest appreciation to the University of Tsukuba for cordial support and education system.

My deepest gratitude goes his Doctoral Research Supervisor Dr. Tofael Ahamed, Associate Professor, University of Tsukuba, and his family, who expertly guided me through my graduate education. His unwavering enthusiasm for physics kept me constantly engaged with my research, and his personal generosity helped make my time at University of Tsukuba enjoyable.

I am grateful to the Supervisory and Examination Committee, Associate Professor Dr. Ryozo Noguchi, Professor Matsushita Shusuke and Professor Enomae Toshiharu for their great inspirational ideas and comments during studies. I also want to acknowledge all the peer students at the Laboratory of Bioproduction and Machinery, Academic Staff in the Doctoral Program for their informative conversations, supporting research and assistance.

I am thankful to the Department of Agriculture Extension, the Ministry of Agriculture, Bangladesh and Bangladesh Bureau of Statistics and Survey of Bangladesh for providing the data.

I also expense my gratitude to the United States Geological Survey (USGS) and SRTM for providing geological, geospatial and atmospheric data free of cost. I also thankful to JITCAS for technical support.

Finally, I am indebted to my parents for their support and valuable prayers. I am also very thankful to my family for understanding, prayer, and continuing support to complete this research work.

With Thanks

Rubaiya Binte Mostafiz

List of Abbreviations

AHP	Analytical Hierarchy Process
ARVI	Atmospherically resistant vegetation index
BBS	Bangladesh Bureau of Statistics
DAE	Department of Agricultural Extension
DEM	Data Elevation Model
FAO	Food and Agriculture Organization
GIS	Geographic Information Systems
GOB	Government of Bangladesh
GPS	Global Positioning System
Ha	Hectare
LSA	Land Suitability Analysis
LST	Land Surface Temperature
LULC	Land Use Land Cover
MCDM	Multicriteria Decision Method
MPR	Multiple Predicted Raster
MSAVI	Modified Soil-Adjusted Vegetation Index
MT	Metric ton
NDVI	Normalized Difference Vegetation Index
NIR	Near-infrared
OLI	Operational Land Imager
OSAVI	Optimized Soil-Adjusted Vegetation Index
SARVI	Soil adjusted and atmospherically resistant vegetation index
SAVI	Soil-adjusted Vegetation Index
SRTM	Shuttle Radar Topography Mission
SWIR	Short Wavelength Infrared
TIRS	Thermal Infrared Sensor
UNDP	United Nations Development Program
USDA	United States department of Agriculture
USGS	United States Geological Survey
UTM	Universal Transverse Mercator
WHO	World Health Organization

References

Abdullah, A. B., Ito, S., & Adhana, K. (2006, March). Estimate of rice consumption in Asian countries and the world towards 2050. In *Proceedings for Workshop and Conference on Rice in the World at Stake* (Vol. 2, pp. 28-43).

Acharjee, T. K., van Halsema, G., Ludwig, F., & Hellegers, P. (2017). Declining trends of water requirements of dry season Boro rice in the north-west Bangladesh. *Agricultural Water Management*, *180*, 148-159. https://doi.org/10.1016/j.agwat.2016.11.014. Aguilar-Rivera, N., Algara-Siller, M., Olvera-Vargas, L. A., & Michel-Cuello, C. (2018).

Akinci, H., Özalp, A. Y., & Turgut, B. (2013). Agricultural land use suitability analysis using GIS and AHP technique. Computers and Electronics in Agriculture, 97, 71–82. doi: 10.1016/j.compag.2013.07.006.

Alam, M. S., Quayum, M. A., & Islam, M. A. (2010). Crop production in the Haor areas of Bangladesh: insights from farm level survey. *The Agriculturists*, *8*(2), 88-97. https://doi.org/10.3329/agric.v8i2.7582.

Alamgir, M., Mohsenipour, M., Homsi, R., Wang, X., Shahid, S., Shiru, M. S., ... & Yuzir, A. (2019). Parametric assessment of seasonal drought risk to crop production in Bangladesh. *Sustainability*, *11*(5), 1442. https://doi.org/10.3390/su11051442.

Alamgir, M.S., Furuya, J., Kobayashi, S. *et al.* Farm income, inequality, and poverty among farm families of a flood-prone area in Bangladesh: climate change vulnerability assessment. *GeoJournal* (2020). https://doi.org/10.1007/s10708-020-10231-2.

Amin, M., Zhang, J., & Yang, M. (2015). Effects of climate change on the yield and cropping area of major food crops: A case of Bangladesh. *Sustainability*, *7*(1), 898-915. https://doi.org/10.3390/su7010898.

Amini, S., Rohani, A., Aghkhani, M. H., Abbaspour-Fard, M. H., & Asgharipour, M. R. (2019). Assessment of land suitability and agricultural production sustainability using a combined approach (Fuzzy-AHP-GIS): A case study of Mazandaran province, Iran. *Information Processing in Agriculture*. https://doi.org/10.1016/j.inpa.2019.10.001

Arief, U. M., & Nafi, A. Y. (2018). An accurate assessment tool based on intelligent technique for

suitability of soybean cropland: case study in Kebumen Regency, Indonesia. *Heliyon*, *4*(7), e00684. https://doi.org/10.1016/j.heliyon.2018.e00684.

Arshad S, Morid S, Reza Mobasheri.M., and Agha Alikhani.M., (2008). Development of Agricultural Drought Risk Assessment Model for Kermanshah Province (Iran), using satellite data and intelligence methods. Option Mediterrianeennes, Series A, No:80.

Asai, H., Samson, B. K., Stephan, H. M., Songyikhangsuthor, K., Homma, K., Kiyono, Y., ... & Horie, T. (2009). Biochar amendment techniques for upland rice production in Northern Laos: 1. Soil physical properties, leaf SPAD and grain yield. *Field crops research*, *111*(1-2), 81-84. https://doi.org/10.1016/j.fcr.2008.10.008.

Ashford, S. A., Sitar, N., Lysmer, J., & Deng, N. (1997). Topographic effects on the seismic response of steep slopes. *Bulletin of the seismological society of America*, *87*(3), 701-709.

Aydi, A., Abichou, T., Nasr, I. H., Louati, M., & Zairi, M. (2016). Assessment of land suitability for olive mill wastewater disposal site selection by integrating fuzzy logic, AHP, and WLC in a GIS. *Environmental monitoring and assessment*, *188*(1), 59. https://doi.org/10.1007/s10661015-5076-3.

Ayehu, G. T., & Besufekad, S. A. (2015). Land suitability analysis for rice production: A GIS based multi-criteria decision approach. *American Journal of Geographic Information System*, *4*(3), 95-104. DOI: 10.5923/j.ajgis.20150403.02

Bahrani, S., Ebadi, T., Ehsani, H., Yousefi, H., & Maknoon, R. (2016). Modeling landfill site selection by multi-criteria decision making and fuzzy functions in GIS, case study: Shabestar, Iran. *Environmental Earth Sciences*, *75*(4), 337. DOI 10.1007/s12665-015-5146-4.

Bajgai, Y., & Sangchyoswat, C. (2018). Farmers' knowledge of soil fertility in West-Central Bhutan. Geoderma Regional, 14, e00188. https://doi.org/10.1016/j.geodrs.2018.e00188.

Bangladesh Bureau of Statistics (BBS), (2011) Statistics and Informatics Division (SID) Ministry of Planning: Population and housing census 2011.

Bangladesh Bureau of Statistics (BBS). *Small Area Atlas of Bangladesh*; Ministry of Planning: Dhaka, Bangladesh, 2014.

Bangladesh Bureau of Statistics (BBS). Statistical Pocket Book Bangladesh 2016; Ministry of Planning:

Dhaka, Bangladesh, 2018.

Bangladesh Bureau of Statistics (BBS). *Yearbook of Agricultural Statistics-2015*; Ministry of Planning: Dhaka, Bangladesh, 2016.

Bangladesh Bureau of Statistics (BBS).; *Bangladesh Agricultural Statistics Yearbook 2017.* Ministry of Planning: Dhaka, Bangladesh, 2018.

Bangladesh Institute of Research and Rehabilitation in Diabetes, Endocrine and Metabolic Disorders (BIRDEM). *Desirable Dietary Pattern for Bangladesh;* National Food Policy Capacity Strengthening Programme,2013

Barbosa, A. M. (2015). fuzzySim: applying fuzzy logic to binary similarity indices in ecology. *Methods in Ecology and Evolution*, *6*(7), 853-858. https://doi.org/10.1111/2041-210X.12372.

Basche, A. D., Archontoulis, S. V., Kaspar, T. C., Jaynes, D. B., Parkin, T. B., & Miguez, F. E. (2016). Simulating long-term impacts of cover crops and climate change on crop production and environmental outcomes in the Midwestern United States. *Agriculture, Ecosystems & Environment*, *218*, 95-106. https://doi.org/10.1016/j.agee.2015.11.011.

Beinat, E., & Nijkamp, P. (Eds.). (1998). *Multicriteria analysis for land-use management* (Vol. 9). Springer Science & Business Media.

Bellman, R. E., & Zadeh, L. A. (1970). Decision-making in a fuzzy environment. *Management science*, *17*(4), B-141. https://doi.org/10.1287/mnsc.17.4.B141.

Bozdağ, A., Yavuz, F., & Günay, A. S. (2016). AHP and GIS based land suitability analysis for Cihanbeyli (Turkey) County. *Environmental Earth Sciences*, *75*(9), 813. https://doi.org/10.1007/s12665-016-5558-9.

Brian D., Wardlow, Martha C., Anderson J. and Verdin P. (2012). Remote Sensing of Drought, Taylor & Francis Group.

Buthelezi, N. N., Hughes, J. C., & Modi, A. (2013). The use of scientific and indigenous knowledge in agricultural land evaluation and soil fertility studies of two villages in KwaZulu-Natal, South Africa. African Journal of Agricultural Research, 8, 507–518.

Buthelezi-Dube, N. N., Hughes, J. C., Muchaonyerwa, P., Caister, K. F., & Modi, A. T. (2020). Soil

fertility assessment and management from the perspective of farmers in four villages of eastern South Africa. *Soil Use and Management*, *36*(2), 250-260. https://doi.org/10.1111/sum.12551.

Campos, I., Gonzalez-Gomez, L., Villodre, J., Gonzalez-Piqueras, J., Suyker, A. E., & Calera, A. (2018). Remote sensing-based crop biomass with water or light-driven crop growth models in wheat commercial fields. *Field Crops Research*, *216*, 175-188. https://doi.org/10.1016/j.fcr.2017.11.025.

Ceglar, A., Toreti, A., Prodhomme, C., Zampieri, M., Turco, M., & Doblas-Reyes, F. J. (2018). Land-surface initialisation improves seasonal climate prediction skill for maize yield forecast. *Scientific reports*, *8*(1), 1-9. https://doi.org/10.1038/s41598-018-19586-6.

Chaignon, V., Bedin, F. & Hinsinger (2002). P. Copper bioavailability and rhizosphere pH changes as affected by nitrogen supply for tomato and oilseed rape cropped on an acidic and a calcareous soil. *Plant and Soil*243, 219–228. https://doi.org/10.1023/A:1019942924985.

Chakraborthy A., Sehgal V. K., (2010), Assessment of Agricultural Drought Using MODIS Derived Normalized Difference Water Index, Journal of Agricultural Physics, Vol. 10, pp. 28-36.

Chapin F.; Sturm M.; Serreze M.; McFadden J.; Key J.; Lloyd A.; McGuire A.; Rupp T.; Lynch A.; Schimel J. (2005). Role of Land-Surface Changes in Arctic Summer Warming. Science, 310, 657–660.

Chauhan, B. S., Jabran, K., & Mahajan, G. (Eds.). (2017). *Rice production worldwide* (Vol. 247). Springer International Publishing. Basel, Switzerland, 2017; pp. 255–277. DOI: 10.1007/978-3-319-47516-5.

Cho, M. A., & Skidmore, A. K. (2009). Hyperspectral predictors for monitoring biomass production in Mediterranean mountain grasslands: Majella National Park, Italy. *International Journal of Remote Sensing*, *30*(2), 499-515. https://doi.org/10.1080/01431160802392596.

Chow, T. E., & Sadler, R. (2010). The consensus of local stakeholders and outside experts in suitability modeling for future camp development. *Landscape and urban planning*, *94*(1), 9-19. https://doi.org/10.1016/j.landurbplan.2009.07.013

Cosgrove, W. J., Rijsberman, F. R., & Rijsberman, F. (2000a). *World water vision: making water everybody's business*. World Water Council, Publications, London, UK (2000).

Dabrowska-Zielinska K., Kogan F., Ciolkosz A., Gruszczynska M. & Kowalik W. (2002): Modelling of crop growth conditions and crop yield in Poland using AVHRR based indices, International Journal of Remote Sensing, 23:6, 1109-1123.

Das, A. C., Noguchi, R., & Ahamed, T. (2020). Integrating an Expert System, GIS, and Satellite Remote Sensing to Evaluate Land Suitability for Sustainable Tea Production in Bangladesh. *Remote Sensing*, *12*(24), 4136. https://doi.org/10.3390/rs12244136.

Datta A., Ullah H., Ferdous Z. (2017) Water Management in Rice. In: Chauhan B., Jabran K., Mahajan G. (eds) Rice Production Worldwide. (pp. 255-277). Springer, Cham.

de Lima, T. M., Weindorf, D. C., Curi, N., Guilherme, L. R., Lana, R. M., & Ribeiro, B. T. (2019). Elemental analysis of Cerrado agricultural soils via portable X-ray fluorescence spectrometry: Inferences for soil fertility assessment. *Geoderma*, *353*, 264-272. https://doi.org/10.1016/j.geoderma.2019.06.045.

Dexter, A. R. (2004). Soil physical quality: Part I. Theory, effects of soil texture, density, and organic matter, and effects on root growth. *Geoderma*, *120*(3-4), 201-214. https://doi.org/10.1016/j.geoderma.2003.09.004.

Dharumarajan, S., & Singh, S. K. (2014). GIS based soil site suitability analysis for potato-a case study in lower indogangetic alluvial plain. *Potato Journal*, *41*(2), 113-121.

Dou, F.; Soriano, J.; Tabien, R.E.; Chen, 2016 K. Soil Texture and Cultivar Effects on Rice (*Oryza Sativa, L.*) Grain Yield, Yield Components and Water Productivity in Three Water Regimes. *PLoS ONE* **2016**, *11*, e0150549.https://doi.org/10.1007/978-3-319-47516-5_11.

Egamberdieva, D., Jabborova, D. & Berg, G (2016). Synergistic interactions between *Bradyrhizobium japonicum* and the endophyte *Stenotrophomonas rhizophila* and their effects on growth, and nodulation of soybean under salt stress. *Plant Soil* 405, 35–45. https://doi.org/10.1007/s11104-015-2661-8.

El Bilali, H., Callenius, C., Strassner, C., & Probst, L. (2019). Food and nutrition security and sustainability transitions in food systems. *Food and Energy Security*, *8*(2), e00154. https://doi.org/10.1002/fes3.154.

Elsheikh, R., Shariff, A. R. B. M., Amiri, F., Ahmad, N. B., Balasundram, S. K., & Soom, M. A. M.

(2013). Agriculture Land Suitability Evaluator (ALSE): A decision and planning support tool for tropical and subtropical crops. *Computers and electronics in agriculture*, *93*, 98-110. https://doi.org/10.1016/j.compag.2013.02.003.

Ennouri, K., & Kallel, A. (2019). Remote sensing: an advanced technique for crop condition assessment. *Mathematical Problems in Engineering*, *2019*. https://doi.org/10.1155/2019/9404565.

Feizizadeh, B., Blaschke, T., (2013). GIS-multicriteria decision analysis for landslide susceptibility mapping: comparing three methods for the Urmia lake basin, Iran. Nat. Hazards 65 (3), 2105–2128. https://doi.org/10.1007/s11069-012-0463-3.

Feizizadeh, B., Blaschke, T., Nazmfar, H., & Rezaei Moghaddam, M. H. (2013). Landslide susceptibility mapping for the Urmia Lake basin, Iran: a multi-criteria evaluation approach using GIS. *International Journal of Environmental Research*, *7*(2), 319-336. https://doi.org/10.1007/s11069-012-0463-3.

Fern, R. R., Foxley, E. A., Bruno, A., & Morrison, M. L. (2018). Suitability of NDVI and OSAVI as estimators of green biomass and coverage in a semi-arid rangeland. *Ecological Indicators*, *94*, 16-21. https://doi.org/10.1016/j.ecolind.2018.06.029.

Food and Agriculture Organization of the United Nations (FAO) (2016c). *Soils and pulses: symbiosis for life*. FAO, Rome.

Food and Agriculture Organization of the United Nations (FAO) (2003). Bruinsma, Jelle, ed. *World agriculture: towards 2015/2030: an FAO perspective*. Earthscan, 2003

Food and Agriculture Organization of the United Nations (FAO) (2004). Cereals and other starch-based staples: are consumption patterns changing? FAO 2004 Rome, Italy, 10-11 February 2004. Joint meeting of the intergovernmental group on grains (30th session) and the intergovernmental group on rice (41st session) Rome, Italy, 10-11 February 2004**.**

Food and Agriculture Organization of the United Nations (FAO), 1976. A framework for land evaluation. Food and Agriculture Organization of the United Nations, Soils Bulletin 32. FAO, Rome.

Food and Agriculture Organization of the United Nations (FAO), 2014. W. Country nutrition paper Bangladesh. In *Joint FAO/WHO International Conference on Nutrition* (Vol. 21, p. 47).

Food and Agriculture Organization of the United Nations (FAO), 2001. *The State of Food and Agriculture 2001*. No. 33. Food & Agriculture Org., 2001.

Food and Agriculture Organization of the United Nations (FAO). (1995). FAO Quarterly Bulletin of Statistics. 18: 1-2.

Food and Agriculture Organization of the United Nations (FAO). (2004). The State of Food Security in The World. pp. 30-31.

Food and Agriculture Organization. A Framework for Land Evaluation; FAO: Rome, Italy, 1976.

Gerpacio, R. V., & Pingali, P. L. (2007). Tropical and Subtropical Maize in Asia: Production Systems, Constraints, and Research Priorities. *CIMMYT*.

Gilabert, M. A., González-Piqueras, J., Garcıa-Haro, F. J., & Meliá, J. (2002). A generalized soil-adjusted vegetation index. *Remote Sensing of environment*, *82*(2-3), 303-310. https://doi.org/10.1016/S0034-4257(02)00048-2.

Gitari, H.I., Gachene, C.K.K., Karanja, N.N. *et al.* (2019). Potato-legume intercropping on a sloping terrain and its effects on soil physico-chemical properties. *Plant Soil* 438**,** 447–460. https://doi.org/10.1007/s11104-019-04036-7.

GRiSP, G. R. S. P. (2013). Rice Almanac (4th editio). *Los Baños, Philippines: Global Rice Science Partnership*.

Guo, Xi, Hongyi Li, Huimin Yu, Weifeng Li, Yingcong Ye, and Asim Biswas. "Drivers of spatio-temporal changes in paddy soil pH in Jiangxi Province, China from 1980 to 2010." *Scientific reports* 8, no. 1 (2018): 1-11. https://doi.org/10.1038/s41598-018-20873-5.

Habibie, M. I., Noguchi, R., Shusuke, M., & Ahamed, T. (2019). Land suitability analysis for maize production in Indonesia using satellite remote sensing and GIS-based multicriteria decision support system. *GeoJournal*, 1-31. https://doi.org/10.1007/s10708-019-10091-5.

Haboudane, D., Miller, J. R., Pattey, E., Zarco-Tejada, P. J., & Strachan, I. B. (2004). Hyperspectral vegetation indices and novel algorithms for predicting green LAI of crop canopies: Modeling and validation in the context of precision agriculture. *Remote sensing of environment*, *90*(3), 337-352. https://doi.org/10.1016/j.rse.2003.12.013.

Hamdy, A., Ragab, R., & Scarascia-Mugnozza, E. (2003). Coping with water scarcity: water saving and increasing water productivity. *Irrigation and Drainage: The Journal of the International Commission on Irrigation and Drainage*, *52*(1), 3-20. https://doi.org/10.1002/ird.73.

Hassan, N., Huda, N., & Ahmad, K. (1985). Seasonal patterns of food intake in rural Bangladesh: its impact on nutritional status. *Ecology of Food and Nutrition*, *17*(2), 175-186. https://doi.org/10.1080/03670244.1985.9990891.

HIES. *Preliminary Report on Household Income and Expenditure Survey 2016*; Bangladesh Bureau of Statistics (BBS), Statistics and Informatics Division (SID), Ministry of Planning: Dhaka, Bangladesh, 2016.https://doi.org/10.5897/AJAR2014.9248.

Hu, W., Huang, B., Borggaard, O. K., Ye, M., Tian, K., Zhang, H., & Holm, P. E. (2018). Soil threshold values for cadmium based on paired soil-vegetable content analyses of greenhouse vegetable production systems in China: implications for safe food production. *Environmental Pollution*, *241*, 922-929. https://doi.org/10.1016/j.envpol.2018.06.034.

Huete, A. (1988). Huete, AR A soil-adjusted vegetation index (SAVI). Remote Sensing of Environment. *Remote sensing of environment*, *25*, 295-309. https://doi.org/10.1016/0034-4257(88)90106-X.

Jeevalakshmi, D., Narayana Reddy, S., & Manikiam, B. (2017). Land surface temperature retrieval from LANDSAT data using emissivity estimation. *International Journal of Applied Engineering Research*.12, 9679-9687. Retrieved from https://www.ripublication.com/ijaer17/ijaerv12n20_57.pdf.

Jesus, J. B. De, & Santana, I. D. M. (2017). Estimation of land surface temperature in caatinga area using Landsat 8 data. Journal of Hyperspectral Remote Sensing. *7*(3), 150–157. Retrieved from https://periodicos.ufpe.br/revistas/jhrs/article/viewFile/22766/pdf.

Jhariya, D. C., Kumar, T., Dewangan, R., Pal, D., & Dewangan, P. K. (2017). Assessment of groundwater quality index for drinking purpose in the Durg district, Chhattisgarh using geographical information system (GIS) and multi-criteria decision analysis (MCDA) techniques. *Journal of the Geological Society of India*, *89*(4), 453-459. https://doi.org/10.1007/s12594-017-0628-5.

Jiang, Z., Huete, A. R., Chen, J., Chen, Y., Li, J., Yan, G., & Zhang, X. (2006). Analysis of NDVI and scaled difference vegetation index retrievals of vegetation fraction. *Remote sensing of*

environment, *101*(3), 366-378. https://doi.org/10.1016/j.rse.2006.01.003.

Johnston, A. M., Tanaka, D. L., Miller, P. R., Brandt, S. A., Nielsen, D. C., Lafond, G. P., & Riveland, N. R. (2002). Oilseed crops for semiarid cropping systems in the northern Great Plains. *Agronomy Journal*, *94*(2), 231-240. https://doi.org/10.2134/agronj2002.2310.

Kamkar, B., Dorri, M. A., & da Silva, J. A. T. (2014). Assessment of land suitability and the possibility and performance of a canola (Brassica napus L.)–soybean (Glycine max L.) rotation in four basins of Golestan province, Iran. *The Egyptian Journal of Remote Sensing and Space Science*, *17*(1), 95-104. https://doi.org/10.1016/j.ejrs.2013.12.001.

Kaufman, Y. J., & Tanre, D. (1992). Atmospherically resistant vegetation index (ARVI) for EOS-MODIS. *IEEE transactions on Geoscience and Remote Sensing*, *30*(2), 261-270. https://doi.org/10.1109/36.134076.

Kawasaki, K., & Uchida, S. (2016). Quality Matters more than quantity: asymmetric temperature effects on crop yield and quality grade. *American Journal of Agricultural Economics*, *98*(4), 1195-1209. https://doi.org/10.1093/ajae/aaw036.

Kazemi, H., & Akinci, H. (2018). A land use suitability model for rainfed farming by Multi-criteria Decision-making Analysis (MCDA) and Geographic Information System (GIS). *Ecological Engineering*, *116*, 1-6. https://doi.org/10.1016/j.ecoleng.2018.02.021.

Kenfack Essougong, U.P., Slingerland, M., Mathé, S. *et al.* Farmers' Perceptions as a Driver of Agricultural Practices: Understanding Soil Fertility Management Practices in Cocoa Agroforestry Systems in Cameroon. *Hum Ecol* **48,** 709–720 (2020). https://doi.org/10.1007/s10745-020-00190-0.

Kennedy, C. M., Hawthorne, P. L., Miteva, D. A., Baumgarten, L., Sochi, K., Matsumoto, M., ... & Kiesecker, J. (2016). Optimizing land use decision-making to sustain Brazilian agricultural profits, biodiversity and ecosystem services. *Biological Conservation*, *204*, 221-230. https://doi.org/10.1016/j.biocon.2016.10.039.

Kihoro, J., Bosco, N. J., & Murage, H. (2013). Suitability analysis for rice growing sites using a multicriteria evaluation and GIS approach in great Mwea region, Kenya. *SpringerPlus*, *2*(1), 265. https://doi.org/10.1186/2193-1801-2-265.

Kim, M. S., Daughtry, C. S. T., Chappelle, E. W., McMurtrey, J. E., & Walthall, C. L. (1994). *The use of high spectral resolution bands for estimating absorbed photosynthetically active radiation.* Proceedings of the 6th Symp. on Physical Measurements and Signatures in Remote Sensing, Jan. 17–21, 1994, Val D'Isere, France (1994), pp. 299-306.

Kladivko, E. J., Griffith, D. R., & Mannering, J. V. (1986). Conservation tillage effects on soil properties and yield of corn and soya beans in Indiana. *Soil and Tillage Research*, *8*, 277-287. https://doi.org/10.1016/0167-1987(86)90340-5.

Koohafkan, P., & Stewart, B. A. (2008). *Water and cereals in drylands*. chapter 2 - Cereal production in drylands. Earthscan. FAO, Rome (2008).

Koulouri, M., & Giourga, C. (2007). Land abandonment and slope gradient as key factors of soil erosion in Mediterranean terraced lands. *Catena*, *69*(3), 274-281. https://doi.org/10.1016/j.catena.2006.07.001.

Land management in Mexican sugarcane crop fields. *Land Use Policy*, *78*, 763-780. https://doi.org/10.1016/j.landusepol.2018.07.034.

Lobry de Bruyn, L. A., & Abbey, J. A. (2003). Characterisation of farmers' soil sense and the implications for on-farm monitoring of soil health. Australian Journal of Experimental Agriculture, 43, 285–305. https://doi.org/10.1071/EA00176.

Lobry de Bruyn, L., & Ingram, J. (2019). Soil information sharing and knowledge building for sustainable soil, use and management: Insights and implications for the 21st Century. Soil Use and Management, 35, 1–5. https://doi.org/10.1111/sum.12493 Mäder, P., Fliessbach, A., Dubois, D., Gunst, L., Fried, P., & Niggli, U. (2002). Soil fertility and biodiversity in organic farming. Science, 296, 1694–1697. https://doi.org/10.1126/science.1071148.

Malczewski, J. (2006). GIS-based multicriteria decision analysis: a survey of the literature. *International journal of geographical information science*, *20*(7), 703-726. https://doi.org/10.1080/13658810600661508 .

Mapanda, F., Mangwayana, E. N., Nyamangara, J., & Giller, K. E. (2005). The effect of long-term irrigation using wastewater on heavy metal contents of soils under vegetables in Harare, Zimbabwe. *Agriculture, Ecosystems & Environment*, *107*(2-3), 151-165. https://doi.org/10.1016/j.agee.2004.11.005.

Marklein, A., Elias, E., Nico, P., & Steenwerth, K. (2020). Projected temperature increases may require shifts in the growing season of cool-season crops and the growing locations of warm-season crops. *Science of The Total Environment*, *746*, 140918. https://doi.org/10.1016/j.scitotenv.2020.140918.

McCormick, J. I., Virgona, J. M., & Kirkegaard, J. A. (2012). Growth, recovery, and yield of dual-purpose canola (Brassica napus) in the medium-rainfall zone of south-eastern Australia. *Crop and Pasture Science*, *63*(7), 635-646. https://doi.org/10.1071/CP12078.

Melillos, G., Themistocleous, K., & Hadjimitsis, D. G. (2020, August). Detecting underground structures in vegetation indices: MSR, RDVI, OSAVI, IRG, time series using histograms. In *Eighth International Conference on Remote Sensing and Geoinformation of the Environment (RSCy2020)*(Vol. 11524, p. 115241P). International Society for Optics and Photonics. https://doi.org/10.1016/j.jag.2020.102198.

Meng, X. D., Ma, H., Wei, M., & Xing, Y. X. (1997, May). Breeding of vegetable crops for protected growing conditions. In *International Symposium on Growing Media and Hydroponics 481* (pp. 695-700). https://doi.org/10.17660/ActaHortic.1999.481.83.

Miller, P. R., McConkey, B. G., Clayton, G. W., Brandt, S. A., Staricka, J. A., Johnston, A. M., ... & Neill, K. E. (2002). Pulse crop adaptation in the northern Great Plains. *Agronomy journal*, *94*(2), 261-272. https://doi.org/10.2134/agronj2002.2610.

Ministry of Environment and Forests (MoEF). *Bangladesh Climate Change Strategy and Action Plan 2008*; Government of the People's Republic of Bangladesh: Dhaka, Bangladesh, 2008.

Mitchell, S., & Cohen, K. (2014, October). Fuzzy logic decision making for autonomous robotic applications. In *2014 IEEE 6th International Conference on Awareness Science and Technology (iCAST)* (pp. 1-6). IEEE. https://doi.org/10.1109/ICAwST.2014.6981843.

Mottaleb, K. A., Kruseman, G., & Erenstein, O. (2018). Determinants of maize cultivation in a land-scarce rice-based economy: The case of Bangladesh. *Journal of Crop Improvement*, *32*(4), 453-476. https://doi.org/10.1080/15427528.2018.1446375.

Mwinuka, P. R., Mbilinyi, B. P., Mbungu, W. B., Mourice, S. K., Mahoo, H. F., & Schmitter, P. (2020). The feasibility of hand-held thermal and UAV-based multispectral imaging for canopy water status assessment and yield prediction of irrigated African eggplant (Solanum aethopicum

L). *Agricultural Water Management*, 106584. https://doi.org/10.1016/j.agwat.2020.106584.

Nahar, Q., Choudhury, S., Faruque, M., Sultana, S., & Siddiquee, M. (2013). Desirable Dietary Pattern for Bangladesh. *Final Research Results*, 226.

Nahusenay, A., & Kibebew, K. (2015). Land suitability evaluation in Wadla Delanta Massif of north central highlands of Ethiopia for rainfed crop production. *African Journal of Agricultural Research*, *10*(13), 1595-1611. https://doi.org/10.5897/AJAR2014.9248.

Narasimhan B., and R. Srinivasan. (2005). Development and evaluation of soil moisture deficit index and evapotranspiration deficit index for agricultural drought monitoring, Agricultural and Forest Meteorology 133: 69-88.

Nasim, M., Shahidullah, S. M., Saha, A., Muttaleb, M. A., Aditya, T. L., Ali, M. A., & Kabir, M. S. (2017). Distribution of crops and cropping patterns in Bangladesh. *Bangladesh Rice Journal*, *21*(2), 1-55. https://doi.org/10.3329/brj.v21i2.38195

Nath, J. A., Lal, R., & Das, A. K. (2015). Ethnopedology and soil quality of bamboo (Bambusa sp.) based agroforestry system. Science of the Total Environment, 521, 372–379.

Ngoy, K. I., & Shebitz, D. (2020). Potential Impacts of Climate Change on Areas Suitable to Grow Some Key Crops in New Jersey, USA. *Environments*, *7*(10), 76. https://doi.org/10.3390/environments7100076.

Nguyen, T. T., Verdoodt, A., Van Y, T., Delbecque, N., Tran, T. C., & Van Ranst, E. (2015). Design of a GIS and multi-criteriabased land evaluation procedure for sustainable land-use planning at the regional level. *Agriculture, Ecosystems & Environment*, *200*, 1-11. https://doi.org/10.1016/j.agee.2014.10.015.

Niemeijer, D., & Mazzucato, V. (2003). Moving beyond indigenous soil taxonomies: Local theories of soils for sustainable development. Geoderma, 111, 403–424. https://doi.org/10.1016/ S0016-7061(02)00274-4.

Noorollahi, E., Fadai, D., Akbarpour Shirazi, M., & Ghodsipour, S. H. (2016). Land suitability analysis for solar farms exploitation using GIS and fuzzy analytic hierarchy process (FAHP)—a case study of Iran. *Energies*, *9*(8), 643. https://doi.org/10.3390/en9080643.

Novara, A., Gristina, L., Sala, G., Galati, A., Crescimanno, M., Cerdà, A., ... & La Mantia, T. (2017).

Agricultural land abandonment in Mediterranean environment provides ecosystem services via soil carbon sequestration. *Science of the Total Environment*, *576*, 420-429. https://doi.org/10.1016/j.scitotenv.2016.10.123.

Novara, A., Minacapilli, M., Santoro, A., Rodrigo-Comino, J., Carrubba, A., Sarno, M., ... & Gristina, L. (2019). Real cover crops contribution to soil organic carbon sequestration in sloping vineyard. *Science of The Total Environment*, *652*, 300-306. https://doi.org/10.1016/j.scitotenv.2018.10.247.

Olivero, J., Real, R., & Marquez, A. L. (2011). Fuzzy chorotypes as a conceptual tool to improve insight into biogeographic patterns. *Systematic Biology*, *60*(5), 645-660. https://doi.org/10.1093/sysbio/syr026.

Ostovari, Y., Honarbakhsh, A., Sangoony, H., Zolfaghari, F., Maleki, K., & Ingram, B. (2019). GIS and multi-criteria decision-making analysis assessment of land suitability for rapeseed farming in calcareous soils of semi-arid regions. *Ecological indicators*, *103*, 479-487. https://doi.org/10.1016/j.ecolind.2019.04.051

Pandey, V. L., Dev, S. M., & Jayachandran, U. (2016). Impact of agricultural interventions on the nutritional status in South Asia: A review. *Food policy*, *62*, 28-40. https://doi.org/10.1016/j.foodpol.2016.05.002

Paul, B.; Rashid, H. *Climatic Hazards in Coastal Bangladesh: Non-Structural and Structural Solution*; Butterworth-Heinemann: Oxford, UK, 2016; pp. 121–152.

Pelosi, C., Baudry, E. & Schmidt, O. Comparison of the mustard oil and electrical methods for sampling earthworm communities in rural and urban soils. *Urban Ecosyst* (2020). https://doi.org/10.1007/s11252-020-01023-0.

Pilevar, A. R., Matinfar, H. R., Sohrabi, A., & Sarmadian, F. (2020). Integrated fuzzy, AHP and GIS techniques for land suitability assessment in semi-arid regions for wheat and maize farming. *Ecological Indicators*, *110*, 105887. https://doi.org/10.1016/j.ecolind.2019.105887.

Pimentel, D., & Burgess, M. (2013). Soil erosion threatens food production. *Agriculture*, *3*(3), 443-463. https://doi.org/10.3390/agriculture3030443.

Purnamasari, R. A., Noguchi, R., & Ahamed, T. (2019). Land suitability assessments for yield prediction

of cassava using geospatial fuzzy expert systems and remote sensing. *Computers and Electronics in Agriculture*, *166*, 105018. https://doi.org/10.1016/j.compag.2019.105018.

Qin, S., Li, L., Wang, D., Zhang, J., & Pu, Y. (2013). Effects of limited supplemental irrigation with catchment rainfall on rain-fed potato in semi-arid areas on the Western Loess Plateau, China. *American journal of potato research*, *90*(1), 33-42. https://doi.org/10.1007/s12230-012-9267-y.

Ramanathan V.; Crutzen P.; Kiehl J.; Rosenfeld D. (2001). Aerosols, Climate, and the Hydrological Cycle. Science, 294, 2119–2124.

Redulla, C. A., Davenport, J. R., Evans, R. G., Hattendorf, M. J., Alva, A. K., & Boydston, R. A. (2002). Relating potato yield and quality to field scale variability in soil characteristics. *American Journal of Potato Research*, *79*(5), 317-323. https://doi.org/10.1007/BF02870168

Ren, H., & Feng, G. (2015). Are soil-adjusted vegetation indices better than soil-unadjusted vegetation indices for above-ground green biomass estimation in arid and semi-arid grasslands?. *Grass and Forage Science*, *70*(4), 611-619. https://doi.org/10.1111/gfs.12152.

Richards, J., Madramootoo, C. A., & Goyal, M. K. (2014). Determining irrigation requirements for vegetables and sugarcane in Jamaica. *Irrigation and Drainage*, *63*(3), 340-348. https://doi.org/10.1002/ird.1811.

Richardson A.J., Wiegand C.L. (1977) - Distinguishing vegetation from soil background information. Photogrammetric Engineering & Remote Sensing, 43 (2): 1541-1552.

Romano, G., Dal Sasso, P., Liuzzi, G. T., & Gentile, F. (2015). Multi-criteria decision analysis for land suitability mapping in a rural area of Southern Italy. *Land Use Policy*, *48*, 131-143. https://doi.org/10.1016/j.landusepol.2015.05.013.

Rondeaux, G., Steven, M., & Baret, F. (1996). Optimization of soil-adjusted vegetation indices. *Remote sensing of environment*, *55*(2), 95-107. https://doi.org/10.1016/0034-4257(95)00186-7.

Saini, G. R., & Grant, W. J. (1980). Long-term effects of intensive cultivation on soil quality in the potato-growing areas of New Brunswick (Canada) and Maine (USA). *Canadian Journal of Soil Science*, *60*(3), 421-428. https://doi.org/10.4141/cjss80-047.

Salman, S.M.; Mahul, O.; Bagazonzya, H.K. *Agricultural Insurance in Bangladesh: Promoting Access*

to Small and Marginal Farmers (No. 53081, pp. 1-146). The World Bank: Washington, DC, USA, 2010; Available online: http://documents.worldbank.org/curated/en/482331468013812662/Agricultural-insurance-in-Bangladesh-promoting-access-to-small-and-marginal-farmers (accessed on 1 October 2020).

Samanta, S.; Pal, B.; Pal, D.K. (2011). Land Suitability Analysis for Rice Cultivation Based on Multi-Criteria Decision Approach through GIS. *Data Base*, 12–20.

Sarker, R. A., Talukdar, S., & Haque, A. A. (1997). Determination of optimum crop mix for crop cultivation in Bangladesh. *Applied Mathematical Modelling*, *21*(10), 621-632. https://doi.org/10.1016/S0307-904X(97)00083-8.

Schutter, M., Sandeno, J., & Dick, R. (2001). Seasonal, soil type, and alternative management influences on microbial communities of vegetable cropping systems. *Biology and Fertility of Soils*, *34*(6), 397-410. https://doi.org/10.1007/s00374-001-0423-7.

Serio, F., Miglietta, P. P., Lamastra, L., Ficocelli, S., Intini, F., De Leo, F., & De Donno, A. (2018). Groundwater nitrate contamination and agricultural land use: A grey water footprint perspective in Southern Apulia Region (Italy). *Science of the Total Environment*, *645*, 1425-1431. https://doi.org/10.1016/j.scitotenv.2018.07.241.

Seyedmohammadi, J., Sarmadian, F., Jafarzadeh, A. A., & McDowell, R. W. (2019). Development of a model using matter element, AHP and GIS techniques to assess the suitability of land for agriculture. *Geoderma*, *352*, 80-95. https://doi.org/10.1016/j.geoderma.2019.05.046.

Shimoda, S., Kanno, H., & Hirota, T. (2018). Time series analysis of temperature and rainfall-based weather aggregation reveals significant correlations between climate turning points and potato (Solanum tuberosum L) yield trends in Japan. *Agricultural and Forest Meteorology*, *263*, 147-155. https://doi.org/10.1016/j.agrformet.2018.08.005.

Somvanshi, S. S., & Kumari, M. (2020). Comparative analysis of different vegetation indices with respect to atmospheric particulate pollution using sentinel data. *Applied Computing and Geosciences*, *7*, 100032. https://doi.org/10.1016/j.acags.2020.100032.

Sonobe, R., Yamaya, Y., Tani, H., Wang, X., Kobayashi, N., & Mochizuki, K. I. (2018). Crop classification from Sentinel-2-derived vegetation indices using ensemble learning. *Journal of*

Applied Remote Sensing, *12*(2), 026019. https://doi.org/10.1117/1.JRS.12.026019.

Stark, J. C., Thornton, M., & Nolte, P. (Eds.). (2020). *Potato production systems*. Springer Nature.Zadeh, L. A. (1965). Fuzzy sets. *Information and control*, *8*(3), 338-353. DOI：10.1016/S0019-9958(65)90241-X.

Sulaiman, A. A., Sulaeman, Y., Mustikasari, N., Nursyamsi, D., & Syakir, A. M. (2019). Increasing sugar production in Indonesia through land suitability analysis and sugar mill restructuring. *Land*, *8*(4), 61. https://doi.org/10.3390/land8040061.

Svinurai, W., Hassen, A., Tesfamariam, E., & Ramoelo, A. (2018). Performance of ratio-based, soil-adjusted and atmospherically corrected multispectral vegetation indices in predicting herbaceous aboveground biomass in a Colophospermum mopane tree–shrub savanna. *Grass and Forage Science*, *73*(3), 727-739. https://doi.org/10.1111/gfs.12367.

Tashayo, B., Honarbakhsh, A., Akbari, M., & Eftekhari, M. (2020). Land suitability assessment for maize farming using a GIS-AHP method for a semi-arid region, Iran. *Journal of the Saudi Society of Agricultural Sciences*, *19*(5), 332-338. https://doi.org/10.1016/j.jssas.2020.03.003.

Thaker, S., & Nagori, V. (2018). Analysis of fuzzification process in fuzzy expert system. *Procedia computer science*, *132*, 1308-1316. https://doi.org/10.1016/j.procs.2018.05.047.

Timsina, J., Wolf, J., Guilpart, N., Van Bussel, L. G. J., Grassini, P., Van Wart, J., ... & Van Ittersum, M. K. (2018). Can Bangladesh produce enough cereals to meet future demand?. *Agricultural systems*, *163*, 36-44. https://doi.org/10.1016/j.agsy.2016.11.003.

Todmal, R. S., Korade, M. S., Dhorde, A. G., & Zolekar, R. B. (2018). Hydro-meteorological and agricultural trends in water-scarce Karha Basin, western India: Current and future scenario. Arabian Journal of Geosciences. https://doi.org/10.1007/s12517-018-3655-7.

Tucker, C.J., 1979. Red and photographic infrared linear combinations for monitoring vegetation. Remote Sens. Environ. 8 (2), 127–150. https://doi.org/10.1016/0034-4257(79)90013-0.

United Nations Development Program (UNDP), 2004.*Reducing Disaster Risk: A Challenge for Development-A Global Report*; UNDP: New York, NY, USA.

Ustaoglu, E., & Aydınoglu, A. C. (2020). Suitability evaluation of urban construction land in Pendik

district of Istanbul, Turkey. *Land Use Policy*, *99*, 104783. https://doi.org/10.3390/rs12091463.

Venancio, L. P., Mantovani, E. C., do Amaral, C. H., Neale, C. M. U., Gonçalves, I. Z., Filgueiras, R., & Campos, I. (2019). Forecasting corn yield at the farm level in Brazil based on the FAO-66 approach and soil-adjusted vegetation index (SAVI). *Agricultural Water Management*, *225*, 105779. https://doi.org/10.1016/j.agwat.2019.105779.

Venancio, L. P., Mantovani, E. C., do Amaral, C. H., Neale, C. M. U., Gonçalves, I. Z., Filgueiras, R., & Campos, I. (2019). Forecasting corn yield at the farm level in Brazil based on the FAO-66 approach and soil-adjusted vegetation index (SAVI). *Agricultural Water Management*, *225*, 105779. https://doi.org/10.1016/j.agwat.2019.105779.

Wang, Y.H., and Li, J.Y. (2005). The plant architecture of rice (Oryza sativa). Plant Mol. Biol. 59: 75-84.

WDI, Washington, World Bank, DC (2014), Doi: 10.1596/978-1-4648-0163-1.

World Health Organization. (2019). *Healthy diet* (No. WHO-EM/NUT/282/E). World Health Organization. Regional Office for the Eastern Mediterranean. https://apps.who.int/iris/handle/10665/325828.

Xing, Z., Chow, L., W. Rees, H., Meng, F., Monteith, J., & Stevens, L. (2011). A comparison of effects of one-pass and conventional potato hilling on water runoff and soil erosion under simulated rainfall. *Canadian Journal of Soil Science*, *91*(2), 279-290. https://doi.org/10.4141/cjss10099.

Y.J. Kaufman, D. Tanre Atmospherically resistant vegetation index (ARVI). IEEE Trans. Geosci. Remote Sens., 30 (1992), pp. 261-270. Doi: 10.1109/36.134076.

Yalew, S. G., van Griensven, A., Mul, M. L., & van der Zaag, P. (2016). Land suitability analysis for agriculture in the Abbay basin using remote sensing, GIS and AHP techniques. *Modeling Earth Systems and Environment*, *2*(2), 101.101. https://doi.org/10.1007/s40808-016-0167-x.

Yalew, S. G., van Griensven, A., Mul, M. L., & van der Zaag, P. (2016). Land suitability analysis for agriculture in the Abbay basin using remote sensing, GIS and AHP techniques. *Modeling Earth Systems and Environment*, *2*(2), 101.101. https://doi.org/10.1007/s40808-016-0167-x.

Zadeh, L. A. (1965). Fuzzy sets. *Information and control*, *8*(3), 338-353. https://doi.org/10.1016/S0019-9958(65)90241-X.

Zhao, H., Xiong, Y. C., Li, F. M., Wang, R. Y., Qiang, S. C., Yao, T. F., & Mo, F. (2012). Plastic film mulch for half growing-season maximized WUE and yield of potato via moisture-temperature improvement in a semi-arid agroecosystem. *Agricultural Water Management*, *104*, 68-78. https://doi.org/10.1016/j.agwat.2011.11.016.

Zhu, K. W., Chen, Y. C., Zhang, S., Yang, Z. M., Huang, L., Li, L., ... & Li, Y. C. (2020). Output risk evolution analysis of agricultural non-point source pollution under different scenarios based on multi-model. *Global Ecology and Conservation*, e01144. https://doi.org/10.1016/j.gecco.2020.e01144.

Zinat, M.R.M., Salam, R., Badhan, M.A. *et al.* Appraising drought hazard during Boro rice growing period in western Bangladesh. *Int J Biometeorol* **64,** 1687–1697 (2020). https://doi.org/10.1007/s00484-020-01949-2.

Zolekar, R. B., & Bhagat, V. S. (2015). Multi-criteria land suitability analysis for agriculture in hilly zone: Remote sensing and GIS approach. *Computers and Electronics in Agriculture*, *118*, 300-321. https://doi.org/10.1016/j.compag.2015.09.016.

Zolekar, R. B., & Bhagat, V. S. (2018). Multi-criteria land suitability analysis for plantation in Upper Mula and Pravara basin: Remote sensing and GIS approach. Journal of Geographical Studies,2(1), 12-20.

Appendix A

Table A1: Crop diversification methods in Bangladesh's northern region

Category (Number)	No	Crop Name	Category (Number)	No	Crop Name	Category (Number)	No	Crop Name
Cereal (CL) ($n_1 = 5$)	1	Aus rice		22	Water Gourd	Fruits (FR) ($n_6 = 18$)	1	Mango
	2	Aman rice		23	Wax gourd		2	Banana
	3	Boro rice		24	Tomato		3	Pineapple
	4	Maize		25	Radish		4	Jack fruit
	5	Wheat		26	Bean		5	Papaya Ripe
Non-Carbohydrate Vegetables (VN) ($n_2 = 31$)	1	Pumking		27	Carrot		6	Watermelon
	2	Brinjal		28	Spinach		7	Litchi
	3	Patal		29	Bengal Spinach		8	Guava
	4	Okra		30	Red amaranth		9	Lime Lemon
	5	Ridge Gourd		31	Amaranth		10	Pomelo
	6	Bitter Gourd	Carb-Veg (VC) ($n_3 = 2$)	1	Potato		11	Melon
	7	Arum		2	Sweet potato		12	Star apple
	8	Ash Gourd	Pulses (PL) ($n_5 = 7$)	1	Lentil		13	Kirai
	9	Cucumber		2	Pea (Motor)		14	Black berry
	10	Long bean		3	Green gran		15	Carambola Apple
	11	Snake ground		4	Black gram		16	wood Apple (Bell)
	12	Amaranth		5	Arhar		17	Green coconut
	13	Cucurbitaceae		6	Khesari		18	Ripe-Palmyra
	14	Sponge gourd		7	Gram	Spices (SP) ($n_7 = 8$)	1	Chili
	15	Colocacia	Oilseed (OS) ($n_4 = 4$)	1	Sesame		2	Onion
	16	Green papaya		2	Mustard		3	Garlic
	17	Green banana		3	Groundnut		4	Turmeric
	18	Rabi brinjal		4	Coconut		5	Ginger
	19	Cauliflower	Molasses (MS) ($n_8 = 3$)	1	Sugarcane		6	Coriander seed
	20	Cabbage		2	Date-palm		7	Chili
	21	Cucurbita		3	Palmyra palm		8	Onion

Table A2: SAVI, ARVI, SARVI, MSAVI and OSAVI from 2017-2020 for 36 subunits.

Ground Points	SAVI				ARVI				SARVI				MASAVI				OSAVI			
	2017	2018	2019	2020	2017	2018	2019	2020	2017	2018	2019	2020	2017	2018	2019	2020	2017	2018	2019	2020
1	0.501	0.557	0.698	0.593	0.388	0.42	0.398	0.43	0.388	0.42	0.418	0.303	0.688	0.582	0.668	0.602	0.388	0.402	0.458	0.401
2	0.445	0.54	0.35	0.42	0.405	0.303	0.355	0.32	0.345	0.34	0.385	0.32	0.545	0.54	0.55	0.452	0.415	0.394	0.435	0.302
3	0.534	0.65	0.71	0.69	0.414	0.525	0.501	0.39	0.544	0.475	0.531	0.49	0.684	0.785	0.739	0.59	0.544	0.595	0.591	0.589
4	0.643	0.67	0.682	0.77	0.69	0.66	0.71	0.57	0.539	0.506	0.51	0.47	0.869	0.866	0.919	0.827	0.69	0.66	0.61	0.57
5	0.408	0.519	0.417	0.375	0.42	0.35	0.29	0.355	0.282	0.285	0.309	0.2655	0.442	0.475	0.4729	0.3949	0.292	0.295	0.329	0.195
6	0.321	0.401	0.315	0.227	0.251	0.201	0.224	0.19	0.221	0.21	0.235	0.2	0.31	0.41	0.501	0.4	0.631	0.621	0.6827	0.62
7	0.472	0.597	0.698	0.784	0.394	0.397	0.385	0.301	0.448	0.447	0.47	0.421	0.674	0.707	0.745	0.681	0.364	0.397	0.377	0.5501
8	0.595	0.671	0.772	0.689	0.681	0.661	0.5	0.59	0.4801	0.51	0.54	0.439	0.7981	0.7981	0.829	0.739	0.681	0.61	0.5	0.79
9	0.799	0.797	0.779	0.769	0.669	0.577	0.67	0.539	0.479	0.508	0.529	0.449	0.799	0.896	0.99	0.859	0.379	0.386	0.49	0.289
10	0.479	0.621	0.631	0.303	0.33	0.366	0.431	0.31	0.33	0.32	0.31	0.303	0.415	0.436	0.4831	0.423	0.5	0.436	0.431	0.383
11	0.748	0.699	0.692	0.598	0.48	0.487	0.49	0.44	0.48	0.39	0.42	0.404	0.68	0.747	0.842	0.724	0.608	0.547	0.642	0.474
12	0.584	0.394	0.733	0.4387	0.54	0.49	0.539	0.387	0.454	0.49	0.49	0.487	0.754	0.749	0.89	0.707	0.54	0.49	0.49	0.487
13	0.519	0.603	0.645	0.538	0.479	0.46	0.47	0.439	0.479	0.46	0.507	0.45	0.679	0.686	0.747	0.669	0.479	0.46	0.497	0.4069
14	0.688	0.789	0.667	0.582	0.38	0.439	0.41	0.312	0.408	0.415	0.478	0.37	0.718	0.739	0.741	0.702	0.358	0.309	0.371	0.252
15	0.484	0.411	0.583	0.292	0.312	0.301	0.391	0.282	0.22	0.291	0.23	0.212	0.44	0.31	0.623	0.52	0.24	0.31	0.33	0.182
16	0.419	0.372	0.44	0.36	0.35	0.312	0.34	0.30	0.29	0.22	0.254	0.22	0.39	0.32	0.24	0.5	0.39	0.432	0.424	0.405
17	0.45	0.562	0.685	0.541	0.43	0.502	0.425	0.341	0.35	0.373	0.385	0.31	0.655	0.642	0.635	0.5601	0.645	0.622	0.735	0.621
18	0.786	0.699	0.794	0.744	0.676	0.604	0.6144	0.544	0.56	0.504	0.5144	0.4944	0.976	0.904	0.991	0.904	0.476	0.404	0.4744	0.384
19	0.401	0.36	0.548	0.297	0.4	0.36	0.38	0.307	0.349	0.395	0.418	0.3279	0.74	0.736	0.858	0.77	0.34	0.426	0.434	0.377
20	0.487	0.601	0.751	0.475	0.387	0.397	0.441	0.25	0.487	0.37	0.431	0.375	0.787	0.797	0.794	0.695	0.587	0.607	0.641	0.595
21	0.788	0.692	0.789	0.774	0.696	0.652	0.66	0.501	0.531	0.502	0.53	0.464	0.761	0.862	0.85	0.824	0.661	0.692	0.695	0.584
22	0.787	0.793	0.8013	0.699	0.617	0.771	0.535	0.505	0.507	0.56	0.575	0.505	0.977	0.9161	0.8535	0.905	0.337	0.301	0.335	0.29
23	0.4027	0.212	0.45	0.222	0.127	0.102	0.165	0.102	0.2277	0.262	0.275	0.222	0.4377	0.432	0.425	0.382	0.477	0.462	0.5495	0.442
24	0.795	0.806	0.799	0.708	0.415	0.45	0.506	0.427	0.485	0.45	0.476	0.44	0.6725	0.65	0.816	0.697	0.385	0.385	0.346	0.27
25	0.65	0.393	0.693	0.492	0.35	0.343	0.33	0.302	0.325	0.33	0.373	0.302	0.35	0.533	0.493	0.342	0.55	0.733	0.783	0.642
26	0.79	0.762	0.818	0.799	0.69	0.662	0.68	0.598	0.479	0.469	0.498	0.4998	0.979	0.9662	0.998	0.998	0.609	0.622	0.648	0.591
27	0.75	0.54	0.77	0.55	0.45	0.54	0.67	0.52	0.475	0.488	0.479	0.4022	0.795	0.854	0.847	0.782	0.465	0.454	0.497	0.382
28	0.693	0.487	0.688	0.491	0.39	0.418	0.418	0.281	0.39	0.408	0.408	0.321	0.709	0.718	0.738	0.701	0.39	0.398	0.398	0.2971
29	0.512	0.605	0.586	0.36	0.491	0.425	0.56	0.35	0.32	0.35	0.36	0.395	0.45	0.52	0.603	0.495	0.52	0.55	0.66	0.5
30	0.701	0.503	0.629	0.635	0.51	0.523	0.619	0.485	0.497	0.453	0.509	0.4785	0.761	0.853	0.849	0.785	0.61	0.53	0.649	0.585
31	0.622	0.731	0.687	0.547	0.512	0.501	0.591	0.47	0.492	0.501	0.489	0.437	0.7652	0.751	0.848	0.697	0.552	0.591	0.648	0.547
32	0.339	0.44	0.486	0.295	0.27	0.224	0.256	0.235	0.249	0.247	0.299	0.225	0.439	0.474	0.486	0.385	0.37	0.324	0.326	0.295
33	0.568	0.647	0.704	0.503	0.48	0.47	0.49	0.43	0.46	0.44	0.44	0.43	0.6	0.747	0.844	0.73	0.56	0.47	0.644	0.43
34	0.392	0.45	0.44	0.23	0.28	0.235	0.314	0.193	0.28	0.205	0.294	0.213	0.438	0.445	0.424	0.403	0.32	0.35	0.324	0.33
35	0.791	0.59	0.787	0.686	0.57	0.59	0.607	0.586	0.471	0.593	0.457	0.389	0.871	0.859	0.947	0.786	0.51	0.79	0.6747	0.586
36	0.598	0.697	0.778	0.609	0.38	0.403	0.458	0.395	0.488	0.447	0.549	0.435	0.688	0.582	0.668	0.602	0.68	0.694	0.6948	0.575